Schweizerische Eidgenossenschaft
Confédération suisse
Confederazione Svizzera
Confederaziun svizra

Eidgenössisches Departement für Umwelt, Verkehr, Energie und Kommunikation UVEK
Département fédéral de l'environnement, des transports, de l'énergie et de la communication DETEC
Dipartimento federale dell'ambiente, dei trasporti, dell'energia e delle comunicazioni DATEC

Bundesamt für Strassen
Office fédéral des routes
Ufficio federale delle Strade

Development of a self-healing asphalt road via induction heating

Entwicklung einer selbsterneuernden Asphaltstrasse mittels induktiver Erwärmung

Développement d'une route d'asphalte auto-réparante par des moyens de chauffage par induction)

Empa, Road Engineering and Sealing Components
Prof. Dr. Manfred N. Partl
Dr. Moisés Bueno

Forschungsprojekt ASTRA 2011/012_OBF auf Antrag der Bundesamt für Strasse (ASTRA)

Dezember 2015 **1547**

Schweizerische Eidgenossenschaft
Confédération suisse
Confederazione Svizzera
Confederaziun svizra

Eidgenössisches Departement für Umwelt, Verkehr, Energie und Kommunikation UVEK
Département fédéral de l'environnement, des transports, de l'énergie et de la communication DETEC
Dipartimento federale dell'ambiente, dei trasporti, dell'energia e delle comunicazioni DATEC

Bundesamt für Strassen
Office fédéral des routes
Ufficio federale delle Strade

Development of a self-healing asphalt road via induction heating

Entwicklung einer selbsterneuernden Asphaltstrasse mittels induktiver Erwärmung

Développement d'une route d'asphalte auto-réparante par des moyens de chauffage par induction

Empa, Road Engineering and Sealing Components
Prof. Dr. Manfred N. Partl
Dr. Moisés Bueno

Forschungsprojekt ASTRA 2011/012_OBF auf Antrag der Bundesamt für Strasse (ASTRA)

Dezember 2015 **1547**

Impressum

Forschungsstelle und Projektteam
Projektleitung
Prof. Dr. Manfred N. Partl

Mitglieder
Dr. Moisés Bueno
Dr. Álvaro García
José Norambuena Contreras
Alessandro Menozzi
Josep Andrés

Begleitkommission
Präsident
Sandra Dünner, Walo Bertschinger AG

Mitglieder
Schmid Bernard, Laboroute SA
Rudolf Schluep, Kanton Solothurn
Luzia Seiler, Bundesamt für Strassen ASTRA
Pillip Truffer, Truffer Ingenieurberatung AG

Antragsteller
Bundesamt für Strasse (ASTRA)

Bezugsquelle
Das Dokument kann kostenlos von http://www.mobilityplatform.ch heruntergeladen werden.

Inhaltsverzeichnis

Zusammenfassung

Rissbildung kann bei Strassen in Asphaltbauweise zum Belagsversagen führen. Dieser Umstand wird durch Schwachstellen im Belag gefördert, welche während des Einbaus oder durch eine Kombination von Alterung, Verkehrsbelastung und thermisch induzierte Belastungen entstehen. An diesen Schwachstellen im Belag können Spannungskonzentrationen auftreten, welche die Bildung von Mikrorissen initiieren. Unter wiederholter Verkehrsbelastung können sich diese Mikrorisse ausbreiten und zu grösseren, sichtbaren Rissen quer oder längs zur Fahrtrichtung verbinden. Ungeachtet dessen ist bekannt, dass Asphaltmaterialien Eigenschaften zur natürlichen Erholung und sogenannte Selbstheilungseigenschaften besitzen. Diese Prozesse verlaufen unter Umgebungstemperaturen nur sehr langsam und würden, um in der Realität angewendet werden zu können, eine Sperrung der betroffenen Strasse mit sich bringen. Es wurde jedoch festgestellt, dass der Selbstheilungseffekt bei höheren Temperaturen schneller abläuft. Unter diesem Aspekt kann der Einsatz von induktiver Erwärmung zur Erhöhung der Lebensdauer einer Asphaltstrasse in Betracht gezogen werden. Dieses Versuchskonzept beinhaltet die Zugabe von elektrisch leitenden oder magnetischen Zuschlagsstoffe (z.B. metallische Fasern oder Partikel) im Herstellungsprozess des Mischguts. Um diese Additive danach erwärmen zu können, wird ein durch ein Induktions-Heizsystem erzeugtes elektromagnetisches Wechselfeld angelegt. Aufgrund von Wärmeleitungseffekten wird danach das die Zuschlagsstoffe umschliessende Bitumen erwärmt, was dessen Viskosität reduziert. Dies ermöglicht es, nahegelegene Mikrorisse zu verschliessen wie auch die Bindungen zwischen dem Bitumen und den Mineralstoffen wiederherzustellen.

Das Ziel dieses Forschungsprojektes war es, eine selbstheilende Asphaltstrasse mittels induktiver Erwärmung zu entwickeln. Zu diesem Zweck wurde der Einfluss verschiedener elektromagnetisch leitfähiger Zuschlagsstoffe auf die Eigenschaften des Asphaltbetons untersucht um die Vorteile und Grenzen dieses innovativen Ansatzes zu analysieren. Darüber hinaus wurde die Effizienz der Selbstheilung untersucht mit dem Ergebnis, dass diese sehr stark von den thermischen, rheologischen und chemischen Eigenschaften des Bitumens abhängig ist. Zum Schluss wurde durch gezieltes Aufbringen von realitätsnahen Verkehrslasten zwecks Schädigung eines Belages die Umsetzbarkeit des Selbstheilungskonzeptes in einem grösseren Massstab untersucht.

Von Anfang an zeigten sich Probleme bei der Verwendung von Stahlwollfasern als Zuschlagsstoffe. Die Beimischung dieser Fasern verbesserte wider Erwarten die mechanischen Eigenschaften des Mischgutes nicht. Genauer gesagt wurde festgestellt, dass sich beim Herstellungsprozess Klumpen aus Fasern bildeten. Diese Ansammlungen führten zu Veränderungen der internen Struktur und erhöhten den Hohlraumgehalt des Mischgutes. Als Konsequenz konnte nachgewiesen werden, dass der höhere Hohlraumgehaltes, einen negativen Einfluss auf die mechanischen Eigenschaften hat, vornehmlich auf die Widerstandsfähigkeit gegen Kornausbrüche. Des Weiteren wurde festgestellt, dass durch den aufgrund der Zugabe von Stahlwollfasern erhöhten Hohlraumgehalt eine verminderte Wärmeleitung im Mischgut stattfindet. Aus diesen Gründen wurde entschieden, anstatt der Fasern partikelförmige Zuschlagsstoffe zu verwenden, um die Klumpenbildung zu verhindern und somit die mechanischen Eigenschaften des Mischgutes zu verbessern.

Bei der Untersuchung des Potentials zur Selbstheilung eines Belags wurden die Bitumeneigenschaften als Schlüsselfaktoren identifiziert. Um Risse effektiv verschliessen zu können, muss das Bitumen fliessfähig im Sinne eines quasi Newton'schen Fluides sein. Um dies zu ermöglichen, muss die Temperatur des Mischguts über ein bestimmtes Limit (Heizphase) gebracht und danach für eine bestimmte Zeit konstant gehalten werden (Abkühlphase). Die zu wählende Temperatur hängt dabei vom Bitumentyp und dessen rheologischen Eigenschaften ab. Es konnte ausserdem gezeigt werden, dass die natürliche Heilung dabei auch eine signifikante Rolle spielt, insbesondere wenn ein hoher Anteil an weichem

Bitumen im Mischgut verwendet wird. Weiter konnte nachgewiesen werden, dass das vom Induktions-Heizgeräte erzeugte elektromagnetische Feld keinen Einfluss auf die chemische Struktur des Bitumens hat. Nichtdestotrotz sollte eine zu starke Erhitzung des Mischgutes im gesamten Prozess vermieden werden, da eine zu hohe Temperatur lokal zur Zersetzung des Bitumens führt. Deshalb ist es essentiell, die Heizleistung und somit die Temperatur zu regeln, um die Alterung des Bitumens aufgrund der Hitzeeinwirkung zu minimieren.

Experimentelle Untersuchungen zeigten, dass permanente Deformationen durch induktive Erwärmung nicht repariert werden können. Darüber hinaus wurde festgestellt, dass diese Technik nur Risse im Mikrometerbereich verschliessen kann und daher die Behandlung vor dem Beginn der irreversiblen Schädigung stattfinden muss. Nach der Skalierung der Untersuchungen auf einen realitätsnäheren Massstab unter Verwendung des mobilen Verkehrslastsimulators MMLS3 auf 1.8m langen Asphaltplatten konnte abschliessend gezeigt werden, dass je früher die induktive Erwärmung angewendet wurde, desto höher die totale Anzahl an Lastzyklen bis zum Auftreten des Belagsversagens war. Daraus kann geschlossen werden, dass diese Methode eine mögliche Unterhaltsmassnahme sein könnte um frühzeitiges Belagsversagen zu verhindern.

Die in diesem Projekt durchgeführten Versuche haben das Potential der induktiven Erwärmung als Massnahme zur Verlängerung der Lebensdauer eines Asphaltbelags klar aufgezeigt. Ausserdem ermöglichen die Resultate der mechanischen Leistungsfähigkeit und die Analyse der die eigentliche Heilung betreffenden Faktoren das Aufzeigen der Grenzen dieser innovativen Methode. Die nächsten Schritte sollten auf die Optimierung des mit leitungsfähigen Zuschlagsstoffen versehenen Mischgutes fokussiert sein, um spezifische Eigenschaften für den Einbau und den Gebrauch in der Praxis zu erreichen. Ebenfalls in diesem Zusammenhang sollte in einem weiteren Forschungsvorhaben eine angemessene Validierung dieser neuartigen Belagskonzepte vollzogen werden. Hierfür wäre es ideal eine Teststrecke im realen Massstab zu erstellen um Feldtests unter realistischen Klimabedingungen mit dem Verkehrslastsimulator MLS10 durchzuführen. Den eigentlichen Heilungsprozess betreffend sollte eine mobile Induktions-Heizanlage mit einstellbaren Parametern (Frequenz, Leistung und Form des Induktors) verwendet werden. Des Weiteren können die zentralen Aspekte dieser Forschungsarbeit für spezifische Anwendungen genutzt werden um die Qualität bestehender Strassen zu erhöhen. Auf diesem Weg sollten auch andere Anwendungsgebiete erschlossen werden. Dabei geht es nicht nur um den Einsatz der induktiven Erwärmung zu Erhaltungszwecken von Strassen (z.B. Reduktion von Reflexionsrissen mit Hilfe von leitfähigen Bewehrungen, welche induktiv aufgeheizt werden können), sondern auch um den Einsatz in anderen Baubereichen wie beispielsweise Belagsfugen oder Fahrbahnübergängen mit besserer Leistungsfähigkeit und Langlebigkeit aufgrund der Verbesserung der Hafteigenschaften.

Résumé

Dans les chaussées d'asphalte, les dommages causés par fissuration peuvent conduire à une défaillance irréversible. Cet effet est accentué par de nombreux défauts dans les structures des chaussées en raison de la construction ou d'une combinaison du vieillissement et de détériorations induites par la température et au trafic. C'est autour de ces imperfections que les contraintes se concentrent permettant l'initiation et la propagation de microfissures. Sous charges répétées, ces microfissures peuvent se développer et finir par fusionner pour former de grandes fissures transversales ou perpendiculaires à la direction principale. Néanmoins, il est bien connu que les matériaux bitumineux présentent des caractéristiques naturelles pour s'auto-réparer. Cet effet est très lent à température ambiante, ainsi il serait préférable de limiter la circulation afin de donner à la route le temps de s'auto–réparer. De même, il est déjà constaté que le taux de réparation naturelle augmente avec une augmentation de température. Dans ce contexte, l'utilisation d'un chauffage par induction commence à être considérée comme une technique de réparation pour augmenter la durée de vie d'une chaussée d'asphalte. Ce concept expérimental implique l'addition de matériaux électriquement conducteurs et/ou magnétiques (par exemple, des particules métalliques ou des fibres) comme additifs dans les mélanges bitumineux. Ensuite, un champ électromagnétique alternatif peut être généré en utilisant un dispositif de chauffage par induction pour chauffer les particules. Après, par conduction de chaleur, le bitume autour de ces additifs conducteurs est chauffé diminuant sa viscosité, entraînant son écoulement et la fermeture de fissures à proximité ainsi que le rétablissement des interfaces avec les granulats minéraux.

L'objectif initial de ce projet était de développer une route d'asphalte auto-réparante via l'utilisation d'un chauffage par induction. À cet effet, l'influence de différents additifs conducteurs sur les propriétés des mélanges bitumineux a été analysée afin de connaître les avantages et/ou les limites de cette nouvelle approche. De plus, la capacité à se réparer a été évaluée permettant d'obtenir des conclusions significatives liées à l'importance des propriétés thermiques, rhéologiques et chimiques du bitume. Enfin, la faisabilité du concept d'autoréparation pour les chaussées d'asphalte a été analysée à grande échelle en simulant l'effet du trafic réel sur la détérioration de la chaussée.

Dès le départ, les résultats expérimentaux ont montré les difficultés de l'utilisation de fibres de laine d'acier comme additifs conducteurs. L'incorporation de ces fibres n'a pas amélioré les propriétés mécaniques des mélanges bitumineux comme il avait été initialement prévu. En fait, des « pelotes » de fibres se sont formées au cours de la procédure de mélange. Ces « pelotes » ont mené à des changements significatifs dans la structure interne de la préparation en augmentant le taux de porosités. En conséquence, on a pu observer que de hauts taux de porosités ont montré un effet négatif sur les propriétés mécaniques des mélanges bitumineux, notamment sur la résistance à la perte de particules. De plus, la conductivité thermique était plus basse pour des mélanges bitumineux avec des plus hauts taux de porosité due à l'addition de fibres de laine d'acier. Après ces résultats, l'utilisation d'un matériau en forme de particules comme additifs conducteurs a été trouvé comme une alternative importante pour améliorer la performance mécanique des mélanges bitumineux en évitant la formation de pelotes de fibres.

En ce qui concerne la capacité à s'auto-réparer, les propriétés du bitume sont les éléments-clés qui permettent le contrôle du processus. Il a été remarqué que le bitume doit pouvoir s'écouler comme un fluide quasi-newtonien pour fermer les fissures. Pour cette raison, la température du matériau doit être augmentée au-dessus d'une certaine limite (phase de chauffage) et maintenue pendant un certain temps (phase de refroidissement). La température durant le processus de réparation dépend du type de bitume et de ses propriétés rhéologiques. Il a également été montré que la réparation dite naturelle a eu un rôle important dans le processus lorsqu'un pourcentage élevé de bitume mou est utilisé dans le mélange. En outre, il a été constaté que le champ électromagnétique nécessaire pour le processus de chauffage par induction n'a eu aucun effet sur la structure chimique du bitume. Cependant, l'excès de température pendant le

chauffage par induction peut dégrader localement le bitume en raison des températures extrêmes atteintes par les particules métalliques. Ainsi, il est fortement recommandé de contrôler la température de chauffage dans le but de minimiser le vieillissement du bitume causé par la surchauffe.

Les dernières études expérimentales ont conclu que la déformation permanente ne peut pas être réparée par chauffage par induction. Il a été d'abord expérimentalement vérifié que cette technique de réparation peut seulement fermer des fissures proches d'une certaine taille (à l'échelle du micromètre) et que le traitement de chauffage doit être effectué avant que des dommages irréversibles puissent s'initier. Enfin, lors de la mise à l'échelle du concept de réparation à des dimensions proches de la réalité en utilisant le modèle portable MMLS3 de simulation de charges sur des échantillons d'asphalte longs de 1,8 m, il a été montré que le nombre de cycles de chargement jusqu'à la rupture totale était plus long lorsque le processus de réparation était accompli plus tôt. Ainsi, il est possible de conclure que cette méthode pourrait être une option raisonnable d'entretien pour prévenir la détérioration prématurée des chaussées d'asphalte.

Les études expérimentales développées au cours de ce projet ont confirmé le potentiel de réparation par induction permettant de prolonger la durée de vie des chaussées d'asphalte. L'expérience acquise après l'analyse des principaux facteurs qui influent sur les performances mécaniques et de réparation va nous permettre de déterminer les limites de ce nouveau procédé. Les prochaines étapes devraient être axées sur l'optimisation des mélanges bitumineux par des particules conductrices qui répondent aux caractéristiques spécifiques nécessaires à la construction de la route. Dans ce contexte, la validation de ces modèles devrait être incluse dans tout futur projet de travail. Dans ce but, la construction de chaussées d'asphalte sur le terrain doit être effectuée. Le comportement de ces modèles en utilisant le modèle de simulation de charges répétées MLS10 ainsi que, l'influence des conditions climatiques pourraient être analysées. Concernant le processus de réparation, un dispositif de chauffage par induction mobile avec des caractéristiques appropriées (c'est-à-dire la fréquence à laquelle l'opération de réparation est effectuée, la puissance du générateur et la forme de la bobine d'induction) devrait être utilisé. Les principales conclusions de ce projet pourraient être utilisées pour d'autres applications spécifiques qui améliorent la qualité des chaussées d'asphalte actuelles. De cette façon, des alternatives doivent être adressées non seulement aux routes à des fins de maintenance (par exemple la réduction de fissures par réflexion en utilisant des renforts métalliques pouvant être chauffés par induction électromagnétique), mais aussi à des protocoles de construction (par exemple, nouvelles techniques de construction et des systèmes de joints d'asphalte avec de meilleures performances et durabilité dues à l'amélioration de l'adhérence entre chaque côté).

Summary

In asphalt roads, cracking damage can lead to failure. This effect is increased by numerous defects in pavements structures as a result of either construction or a combination of aging and traffic- and thermal-induced distresses. It is around, these imperfections that stress concentrates allowing micro-cracks initiation and propagation. Under repetitive loading, these micro-cracks can grow and eventually, combine to large cracks transverse or perpendicular to the driving direction. Nevertheless, it is known that asphalt materials show natural or self-healing characteristics. This effect is very slow at ambient temperature thus, it should be necessary to stop the traffic circulation in order to give the road time to heal. Likewise, it is reported that the rate of natural healing increases with an increase in temperature. In this context, the use of induction heating may be considered as a healing technique to increase the life of an asphalt concrete pavement. This experimental concept involves the addition of electrically conductive and/or magnetic materials (e.g. metallic particles or fibers) as additives into the asphalt mixture. Then, an alternating electromagnetic field can be generated by using an induction heating device for heating the particles. Afterwards, through heat conduction, the bitumen around these conductive additives will be heated decreasing its viscosity, eventually flowing and closing cracks nearby as well as recovering the adhesive bonds with the mineral aggregates.

The aim of this research project was to develop a self-healing asphalt road via induction heating. For that purpose, the influence of different conductive additives on the properties of the modified asphalt mixtures was analysed in order to know the advantages and/or limits of this innovative approach. Moreover, the healing performance was evaluated obtaining significant conclusions related to the importance of thermal, rheological and chemical properties of the bitumen. Finally, the feasibility of the healing concept for asphalt roads was analysed at large scale by simulating the effect of real traffic on the deterioration of a pavement.

From the beginning, experimental results showed the problems of using steel wool fibers as conductive additives. The incorporation of these fibers did not improve the mechanical properties of the modified asphalt mixtures as it was originally expected. In fact, clusters of fibers were formed during the mixing procedure. These clusters leaded to changes in the internal structure of the mixture by increasing the air void content. As a consequence, it could be observed that higher air void contents showed a negative effect on the mechanical properties of the modified asphalt mixtures, mainly on the particle loss resistance. Furthermore, the thermal conductivity was lower for asphalt mixture with higher air void contents due to the addition of steel wool fibers. After these results, the use of particle-shaped material as conductive additives was found as an important alternative to improve the mechanical performance of the modified asphalt mixtures by avoiding the formation of fibers clusters.

Concerning the healing capability, bitumen properties were found the key factor to control the process. It was observed that the bitumen must be able to flow as a near-Newtonian fluid in order to close the cracks. For this reason, the temperature of the material must be increased above certain limit (heating phase) and maintained during some time (cooling phase). The healing temperature depends on the type of bitumen and its rheological properties. It was also shown that natural healing had a significant role in the process when high percentage of soft bitumen is used in the mixture. In addition, it was found the electromagnetic field needed for the induction heating process had no effect on the chemical structure of the bitumen. Nevertheless, excess of temperature during induction heating might degrade the bitumen locally due to the extreme temperatures reached by the metallic particles. Thus, it is highly recommended to control the heating temperature in order to minimize the aging of the bitumen caused by overheating.

Last experimental studies concluded that permanent deformation cannot be repaired by induction heating. Moreover, it was experimentally checked that this healing technique can only close cracks of certain size (micrometre scale) and that the heating treatment

must be carried out before irreversible damage starts. Finally, during the upscaling of the healing concept to dimensions close to reality by using the model mobile load simulator MMLS3 over 1.8 m long asphalt test slabs, it was showed that the number of loading cycles until total failure was longer when the healing process was accomplished earlier. Thus, it could be concluded that this method could be a reasonable maintenance option to prevent premature deterioration of asphalt roads.

The experimental studies developed during the research project have confirmed the potential of the induction healing as technique to extend the life-span of the asphalt roads. Besides, the experience gained after the analysis of the main factors affecting the mechanical and healing performance will allow us to know the limits of this innovative procedure. Next steps should be focused on the optimization of asphalt mixtures modified by conductive particles that meet the specific characteristics required for the road construction. In this context, the validation of these designs should be included in any future working proposal. For this aim, the construction of test tracks in the field should be carried out. The behaviour of these final designs by using the Model Load Simulator MLS10 as well as, the influence climate conditions could be analysed. Concerning the healing process, a movable induction heating device with the suitable characteristics (i.e. working frequency, generator power and inductor shape) should be used. Furthermore, the main findings of this research project could be used for other specific applications that enhance the quality of the current asphalt roads. In this way, alternatives should be addressed not only to roads maintenance purposes (e.g. reduction of reflective cracking by using metallic reinforcement that could be heated by electromagnetic induction), but also to building protocols (e.g. new construction techniques and asphalt joint systems with better performance and durability due to the improvement of the adhesion between each side).

1 Introduction

Asphalt concrete is one of the most commonly used materials in pavements due to its excellent performance in comfort, durability and water resistance, but it usually exhibits distresses over time caused by repeated traffic loading and environmental conditions such as freeze-thaw cycles. In order to maintain its characteristics during its lifetime, asphalt concrete wearing courses should be constantly maintained and repaired before irreversible damage can happen.

Currently the only practical solution for building more durable roads is to make the asphalt layers thicker. Before the top layer of the pavement can be severely damaged without complete structural failure; this layer is usually milled and replaced for maintenance. Nevertheless, it is well known that asphalt is a material with some intrinsic self-healing properties which are directly linked to temperature [[1],[2]] and to the rest periods in the traffic regime [3]. When a crack opens in the pavement, it can close when the temperature is high enough and the crack is not too big. This healing can be positively influence by thermal dilatation and traffic action. Although healing in asphalt is known to occur and is empirically important in the formulation and performance of asphalt mixtures, limited work has been done to systematically understand its mechanisms. Different authors [[4]-[6]] proposed that two main types of healing exist in asphalt mixtures: adhesive healing at the asphalt aggregate interface, and cohesive healing within the viscoelastic asphalt binder. Additionally, Little and Basin [7] explain that when both faces of the crack are in contact this process is governed by the van der Waals forces [8] and the diffusion of molecules from one face to the other ensues. This will happen until the crack has completely disappeared and the repaired material reaches the original level of strength.

In practice, it is often problematic to stop traffic circulation in order to give the road time to heal. Earlier investigations [[9]-[14]] explored the induction heating as a method to accelerate the natural healing and to increase the lifetime of asphalt pavements. Induction heating is a process which is used to bond, harden or soften metals or other conductive materials. When an alternating electrical current is applied across a conductive coil, an alternating magnetic field with the same frequency as the alternating current is created [12]. According to Faraday’s effect, if a magnetically susceptible and electrically conductive material is located within the magnetic field, an electric current (eddy current) will be induced with the same frequency than the magnetic field. The idea applied to asphalt roads consists of incorporating conductive additives to the asphalt mixture. Heat is generated through the energy loss when eddy currents face the resistance of the material and, finally, bitumen is melted decreasing therefore its viscosity and allowing it to flow for closing cracks and recover bonding among the mineral aggregates. Moreover, important parameters for the optimization of the induction heating process are the total volume of conductive material in the mixture as well as its magnetic permeability and resistivity, the frequency and the intensity of the alternating current and the configuration of the inductor. For example, it was shown that the increase of temperature in asphalt concrete due to induction heating depends more on the radius of the fibers than on their volume in the mixture [15].

It has been shown that induction heating can be used for improving the self-healing properties of asphalt concrete; but in order to obtain a reasonable performance, it is necessary to mix electrically conductive additives, such as, steel wool fibers or cast iron particles, into the mixture [[15], [16]]. For example, beside other applications that involve the improvement of asphalt characteristics and its performance [[16]-[26]], fibers in asphalt concrete are used to enhance its electrical conductivity. For this application, different works dealt with the use of carbon fibers [[14],[27],[28]] and steel wool [29]. It is known that the electrical resistivity of asphalt concrete decreases with the amount of fibers. If an increasing mass of fibers is added to the aggregate-bitumen mixture, there is a point where these percolate, creating an electrically conductive path thought the material [[27],[29]]. Electrically conductive asphalt may be used for de-icing purposes. When an electrical current “meets” the resistance of the material, its temperature will increase, due to the Joule effect, transporting heat and helping the pavement to be at a higher temperature [[27], [28]]. Another application for electrically conductive asphalt is asphalt monitoring, because changes in the internal structure of the material will cause changes in its electrical conductivity [14].

Asphalt mixtures may increase its temperature very fast due to induction heating [30]: with the actual state of the technology, the temperature of asphalt concrete can change from 20°C to approximately 100°C in less than 1 minute. After the heating, the cooling process may take various hours. Hence, the healing performance of the material also depends on the cooling rate of the asphalt mixture, which is directly related to its porosity [31]. Asphalt concrete can heal because bitumen behaves as a Newtonian fluid when its temperature is above a certain threshold, between 30°C and 70°C, depending of the type of bitumen [[32]-[34]]. Above this temperature, bitumen will flow through any possible crack in the pavement, in a sort of capillary flow. Healing will happen while the temperature is higher than the temperature threshold. The healing rates of asphalt concrete increase with temperature following the Arrhenius equation [35]. Furthermore, it has been hypothesized that the viscosity of bitumen may be critical for the healing process, as bitumen with lower viscosity seems to heal faster; but it is not yet clear how it may affect it. Additionally, it has to be proven if the healing process can be repeated several times [35].

The objective of this research project was to put light into the induction-healing properties of asphalt mixtures modified with electrically conductive additives. For this reason, different types of electrically conductive steel wool fibers as well as cast iron and cast steel particles were mixed into reference dense asphalt mixtures. The addition of such fibers would probably influence the mechanical properties of the pavement material. However, it was not clear which was the optimum amount, length and diameter of fibers needed for not having a negative impact in the mixture. The dispersion of steel wool fibers in the mixture, the mechanical resistance of asphalt concrete and the resistance of asphalt mixture to environmental factors, such as salt water, were also evaluated. Additionally, the thermal and induction heating properties of the dense asphalt mixtures modified with steel wool fibers were evaluated. The resulting healing properties were analysed and compared to those of a porous asphalt mixture obtained from an experimental track in the Dutch motorway A58 concerning the properties of the corresponding bitumen. In order to find the limits of this application, the influence of induction heating on the ageing of bitumen was analysed by rheological and chemical characterisations. Moreover, the performance recovering after fatigue damage and longitudinal cracking were investigated. Finally, the feasibility of the experimental concept at larger scale was studied by means of healing process of test slabs previously damaged by the Model Mobile Load Simulator MMLS3.

This report collects the main findings obtained in connection with the research project. Some of the work was done as independent research but thematically liked to the project, such as the master thesis by Alessandro Menozzi (University of Parma), but, in the interest of providing a comprehensive picture, they are referenced to in this report. Some of that work has already been published. The document is divided into different sections. First, the materials and test sample types used for the different experimental tests are presented by explaining the details of the asphalt mixtures as well as the additives incorporated in order to get the induction heating properties required for the healing application (Section 2). Then, the results obtained from the tests carried out for the characterization of the additives and the modified asphalt mixtures are detailed and discussed (Section 3). In the Section 4, the theoretical approach of the healing concept by inductive heating for asphalt mixtures is developed. Furthermore, analysis of the healing performance in dense and porous asphalt mixtures modified with different types of steel wool fibers is presented (Section 5). In the same way, experimental results from the fatigue behaviour and cracking strength of asphalt mixtures modified with cast iron particles before and after healing processes are shown in Section 6. Afterwards, the analysis of the upscaling study is shown where the model load simulator is used to damage asphalt slabs in order to simulate a scenario closer to a real pavement. Finally, the most important conclusions are summarized.

2 Materials

A number of asphalt mixtures modified with electrically conductive additives has been used in this research project. Dense asphalt mixtures with different types of additives (i.e. steel wool fibers, cast steel and cast iron particles) were prepared for compacting specimens varying shapes and sizes in order to be evaluated by different experimental tests. For the sake of comparison, porous asphalt cores from an experimental track in The Netherlands were also assessed. In this section, the different modified asphalt mixtures are detailed.

2.1 Asphalt mixtures modified with steel wool fibers

Dense asphalt mixtures modified with different of types steel wool fibers (diameter and length) were prepared for the first stage of the experimental part. The dense aggregate size gradation is shown in Table 2.1. The mineral aggregates consisted of crushed basaltic material (grain size between 2 and 11 mm and specific density 2770 kg/m^3), crushed sand (grain size between 0.063 and 2 mm and specific density 2688 kg/m^3) and filler (size <0.063mm and density 2638 kg/m^3). The virgin bitumen used was B70/100, with density 1032 kg/m^3.

***Table 2.1** Composition of the dense asphalt mixture with fibers*

Sieve size (mm)	Aggregate weight (% retained)	Cumulative aggregate weight (% retained)	Weight (g)
11.2-8.0	15	15	2325
8.0-5.6	15	30	2325
5.6-4.0	10	40	1550
4.0-2.8	10	50	1550
2.8-2.0	10	60	1550
2.0-1.4	7	67	1085
1.4-1.0	6	73	930
1.0-0.5	9	82	1395
0.5-0.25	6	88	930
0.25-0.09	5	93	775
<0.063	7	100	1085
Bitumen 70/100	**(% of Weight of Mixture)**	5.6	868
Steel Wool Fibers Diameter (mm)	**Length (mm)**	**% volume of bitumen**	
0.02855 (Type 0000) 0.03642 (Type 00) 0.08389 (Type 1) 0.15498 (Type 3)	2.5 and 7	2% 4% 6%	132 264 396

Moreover, steel wool fibers were added to the mixture. The material used in the steel wool was low-carbon steel, with density 7180 kg/m^3. These fibers had 4 different diameters: 0.02855 mm (Type 0000), 0.03642 mm (Type 00), 0.08389 mm (Type 1) and 0.15498 mm (Type 3) and two different initial lengths: short fibers, with approximately 2.5 mm average length and long fibers, with roughly 7 mm average length. Finally, 4 different amounts of fibers were used: 0%, 2%, 4% and 6%, by total volume of bitumen in the mixture (see *Table 2.1*). In total, 25 different types of mixtures were prepared: 24 with different original sizes, types and volumes of fibers and 1 without steel fibers (reference mixture), always maintaining the same mass of aggregates and bitumen, but changing the mass of fibers.

The materials were mixed in a laboratory planetary mixer at a mixing speed of 312 rpm. Two mixture batches were prepared for each of the 25 asphalt mixtures studied. The amount of material in each mixture was something more than 16 kg. Materials were heated to 160ºC before mixing. The raw materials were added to the bowl in the following order: first the bitumen and the fibers, then the coarse aggregates, then the sand and finally, the filler. Thus, all the materials were mixed during approximately 5 minutes.

The first 16 kg batch was used for preparing asphalt mixture slabs (Fig. 2.1). These slabs were compacted by using a pneumatic laboratory wheel compactor [36]. Before the compaction started, the specimen was subjected to a pre-compaction with a low tire pressure (0.1 MPa) and a low maximum wheel load (1 kN). The effective compaction of the rolling-wheel specimen was performed at higher tire pressure (0.6 MPa) and a constant wheel load (5 kN). After compaction, both faces of the samples were polished until they reached a height of 5 cm. From this, the samples were sawn into blocks of $25 \times 25\ cm^2$. The slabs were used for measuring physical properties of the modified asphalt mixtures such as thermal conductivity and electrical resistivity. Additionally, from these blocks, prismatic specimens of 12 cm x 5 cm x 5 cm were cut for the analysis of the flexural properties by bending test and their healing performances. For this study, a 3 mm wide and 8 mm deep notch was also created in the prismatic test samples; the notch was cut at the mid-point in the direction of the loading from the central axis of the sample.

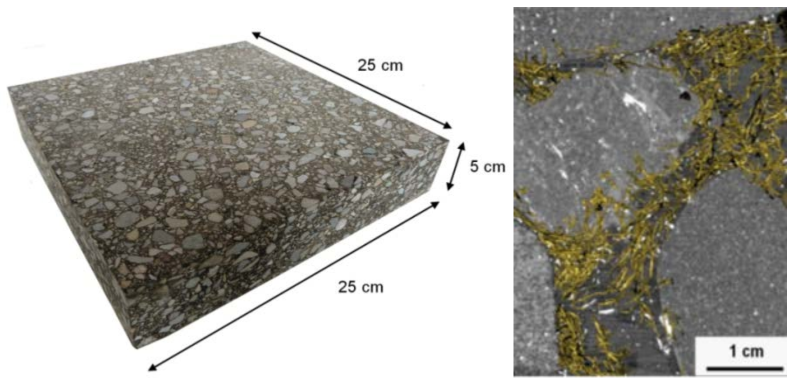

(a) (b)

Fig. 2.1 *Asphalt mixture slab (a) and detail of steel wool fibers type 00 distributions in asphalt concrete (b)*.

The second 16 kg batch was used to make Marshall specimens of 10 cm diameter, approximately 6 cm in height and exactly 1190 g of mass. Immediately after placing the mixture into the mould, they were heated to 140ºC and compacted with a Marshall hammer, applying 50 blows on each face of the specimens. Afterwards, semi-circular test samples were cut from the cylindrical specimens in order to evaluate their flexural strength by means of semi-circular bending tests (SCB-T) as well as their healing behaviour. 50 Marshall test samples were used for building semi-circular test samples. Furthermore, a notch in the test samples was cut with a thickness of about 2 mm and a depth of about 10 mm; the notch was cut at the mid-point in the direction of the loading from the central axis of the sample.

In addition, cylindrical porous asphalt cores were wet-drilled from an induction-healing porous asphalt trial section in the Dutch motorway A58 built in December 2010 [37]. This porous asphalt mixture with Bitumen 70/100 pen (5.2% weight of aggregate) and an air void content of 17.2 % was produced in an asphalt plant. Besides, steel wool fiber (1.5%

weight of mixture) with 10 mm length and diameters ranging from 8.89 to 12.79 μm were used in the modified mixture. For comparison purposes, drilled cores of 10 cm diameter and 5 cm height were cut to semi-circular test samples with a 2 mm thick notch and a depth of about 10 mm the mid-point of the sample. These specimens were used for studying the healing performance.

2.2 Asphalt mixtures modified with steel and iron particles

Results obtained from the first experimental part of the project showed that the use of fibers lead to the formation of clusters during the mixing procedure. As it will be presented in Section 3, the existence of clusters had a significant influence on the mechanical performance of the modified asphalt mixture. Hence, at that point, it was decided to start using particle shape additives as electrically conductive material in order to avoid this fiber related problem. In the last experimental stages, cast steel as well as cast iron particles were used as additive in dense asphalt mixtures for giving the properties required to be healed by induction heating.

In order to evaluate the induction healing after fatigue damage as well as the effect of the heating on the ageing of the bitumen, 10 cm diameter Marshall test specimens were prepared. These specimens were compacted following the procedure explained above from a dense asphalt mixture with maximum aggregate size of 8 mm, 6 % of bitumen 70/100 pen and 19.4% by weight of mixture of cast steel particles (7600 kg/m3). The sizes of the steel particles added to the mixture were between 0.6 mm and 1.4 mm.

Additionally, two different asphalt mixtures modified with 20% by weight of mixture with cast iron particles (0.6-1.0 mm) were prepared to assess the induction healing of prismatic slabs after longitudinal cracking by double torsion tests. The two asphalt mixtures had 4 mm of maximum aggregate size and 8% of bitumen 70/100 pen and 6% of bitumen 35/50 pen, respectively. To get the specimen geometry for double-torsion fracture tests, specimens were cut from asphalt slabs compacted by the so-called French roller compactor developed for wheel tracking tests. The thickness of 20 mm was chosen because the double-torsion fracture test concept was based on the thin plat theory where specimens should have enough thickness, more than three times than the maximum aggregate size (in this case 4 mm), to reduce the aggregate dependency on test results. A beam length of 300 mm, twice the width (150 mm) and more six times the thickness, was chosen to produce reasonable bending conditions within the size limitation of the temperature chamber. Moreover, a notch 30 mm length and 3 mm width was used as stress concentration point for the crack initiation and a rectangular guide groove was made on the bottom surface of the specimen in order to control the propagation path of the crack. Details of the specimen geometry can be observed in *Fig. 2.2*.

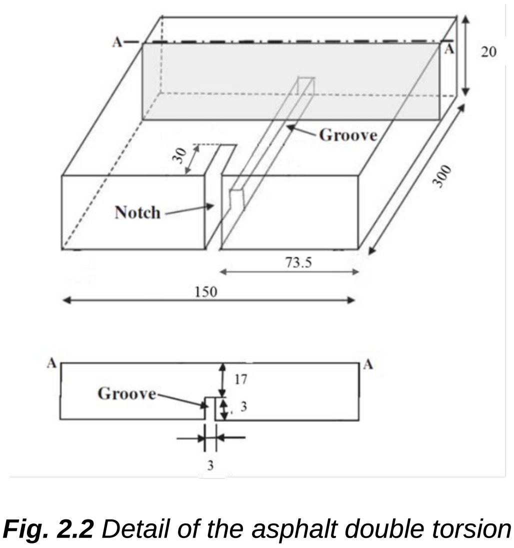

Fig. 2.2 *Detail of the asphalt double torsion test specimen (dimensions in mm).*

Finally, the last step of this research project was focused on the analysis of 1.8 m long test slabs damaged by the Model Mobile Load Simulator MMLS3 in order to prove the feasibility of the healing concept at larger scale. For this aim, four slabs (1800 mm x 435 mm x 40 mm) were compacted from a reference dense asphalt mixture with 5.9%wt. of bitumen 50/70 and a maximum mineral aggregate size of 8 mm. Moreover, cast iron particles (7400 kg/m^3) of 0.6-1 mm diameter were added (14% wt.) to the mixture in order to ease the heating process via induced electromagnetic fields. In addition, two rectangular 10 mm deep and 5 mm wide grooves were cut along the bottom surface of each slab. These grooves were used as stress concentration points for crack initiation during the test and in order to control the propagation path of the cracks. Details of the specimen geometry can be observed in Fig. 2.3.

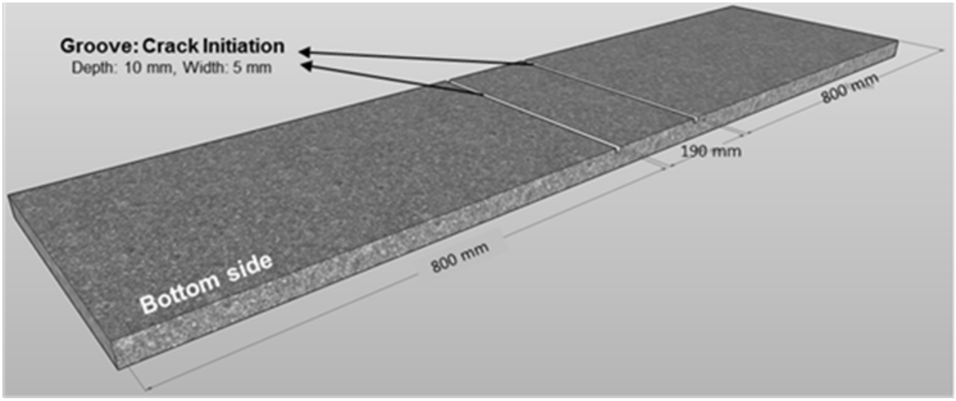

Fig. 2.3 *Detail of the asphalt test slab.*

3 Effect of the steel wool fibers as additive in asphalt mixtures

In this section, experimental results about individual characteristics of the steel wool fibers as well as the effect of its incorporation as additive to asphalt mixtures are presented and discussed. The influence of steel fibers on the mechanical, electrical and thermal properties of the modified asphalt mixtures is analysed.

3.1 Analysis of the properties of steel wool fibers

3.1.1 Tensile strength

Tensile strength of individual fibers was measured by using an electromechanical screw-driven universal testing machine with computer control and equipped with a 10 kN load cell (*Fig. 3.1*). After measuring their diameter, each individual fiber was glued at each end into a paper form with approximately 50 mm diameter and tested until failure. The force resisted by the fibers was defined as the average value obtained from 12 fibers samples.

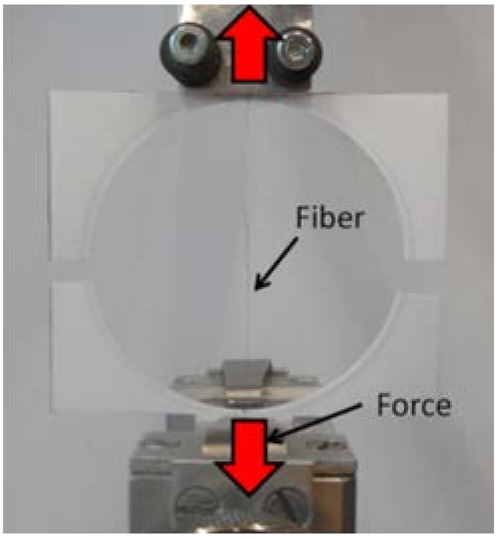

Fig. 3.1 *Fiber tensile strength test by using a screw-driven universal testing machine.*

The tensile strength of the fibers (*Pa*) can be calculated as:

$$Tensile\ strength = \frac{F}{A} \qquad (3.1)$$

where *A* is the area of the fibers in m^2, which was assumed circular and *F* is the average force resisted by the fibers, measured in ***N*.**

The average force resisted by the fibers and its average tensile strength is shown in Fig. 3.2. It can be seen that the force resisted by the fibers increased with their diameter even considering that this value can vary along their length due to the existence of microdefects Additionally, it can be observed that the strength was reduced with increasing diameter.

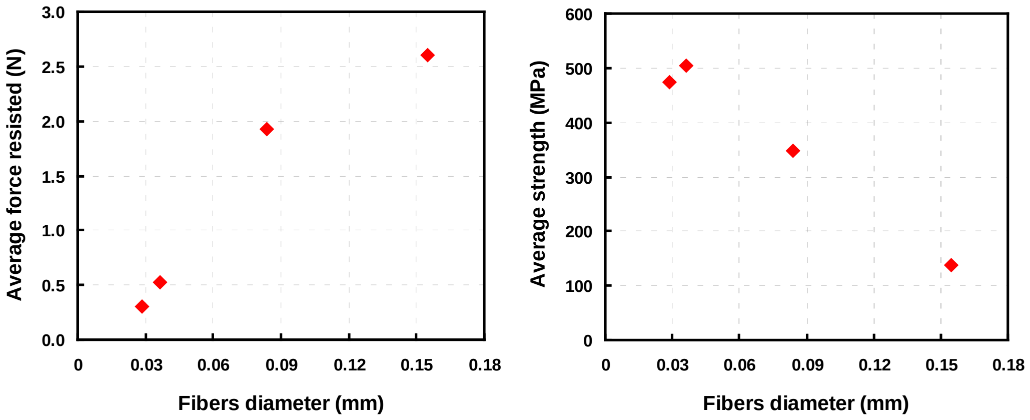

(a) (b)

Fig. 3.2 *Influence of the fiber diameter on (a) the force resisted by the fibers and (b) the tensile strength of the fibers [38].*

This behaviour could be mainly explained by physical changes in the fibers during manufacturing process. For this reason, microscopy images of the fibers were taken. The surface aspect of the fibers was studied by using an Environmental Scanning Electron Microscope (ESEM XL30, FEG) available at the Empa facilities. Each batch of fibers was examined before mixing. As an example, different images of a fiber type 0000 and a fiber type 1 are presented in Fig. 3.3. From these images, it can be observed that fibers with large diameter have more surface defects than fibers with small diameter. The reason for this is that steel wool fibers are originally cut from bigger diameter steel wires (≈2mm). The knives used for this purpose are subjected to different kind of vibrations, which create flaws in the fibers surface (see Fig. 3.3(b)). The smaller the fibers are, the more uniform they appear, which makes the fibers less likely to failure when submitted to tensile force.

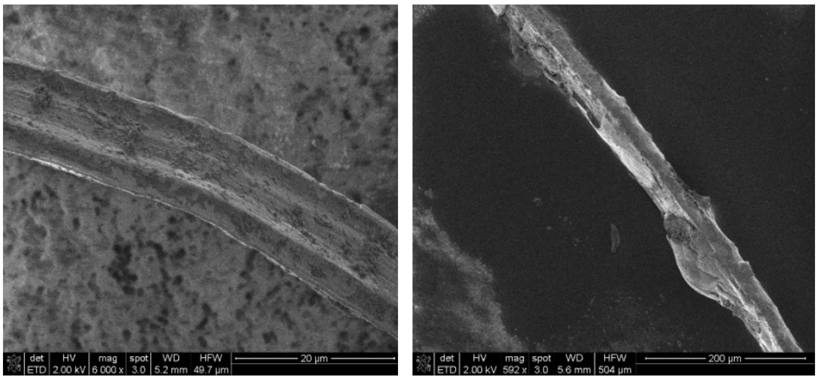

(a) (b)

Fig. 3.3 *ESEM images of steel wool fibers type 0000 (a) and a fiber type 1 (b) before mixing [38].*

3.1.2 Influence of the mixing procedure on the steel wool fibers (Length reduction and morphology)

In order to guarantee a good distribution of the fibers in the mixture, they must have an optimum length and diameter. The average length of 50 single fibers of different type, before the mixing process and retrieved from each mixture containing fibers, was measured by taking photographs under an optical microscope and by measuring the individual fiber length with an image processing program (ImageJ®). Fibers were obtained by solving the bitumen in toluene and by extracting them with a magnet.

In Fig. 3.4, the length of the fibers before and after mixing is shown. It can be observed that in the case of the long fibers, there is a reduction of more than 6 times in their original length. In the case of long and short fibers type 3. This is especially remarkable, where the average original length was 7.75 mm and 2.44 mm. But after mixing and Marshall compaction, the average length of the fibers was 1.98 mm for the long ones and 1.89 mm for the short ones. Hence, it seems that, after compaction the fibers incorporated into the mixture presented similar lengths, regardless their initial length before mixing.

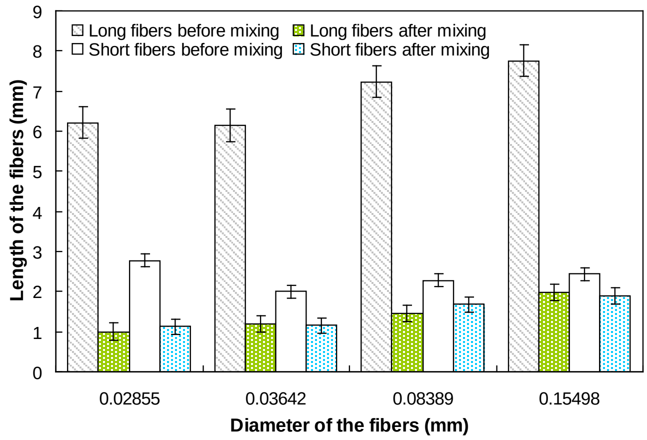

Fig. 3.4 *Average length of the long and short fibers before and after mixing and compacting [38].*

Moreover, to analyse if the fibers end up with the same length after mixing and Marshall compaction, the cumulative distribution function for the length of the four types of fibers studied is shown in Fig. 3.5. Based on this distribution, the cumulative probability for getting a certain fiber length after mixing and compacting, has been calculated as:

$$p_c = \frac{i - 0.5}{n} \qquad (3.2)$$

where p_c is the cumulative probability of obtaining a certain fiber length, n is the number of fibers being measured, and i is the rank length of a certain fiber. It can be seen that the accumulative probability can be fitted as a Weibull probability distribution function. This was proved for the four types of fibers studied, which means that the fibers of each type end up with the same length after mixing and Marshall compaction (see Fig. 3.4), and that there is a mixing process (312 rpm at 160°C) that makes uniform fibers length. This result is similar to what it has been reported in previous studies about fibers in composites [39].

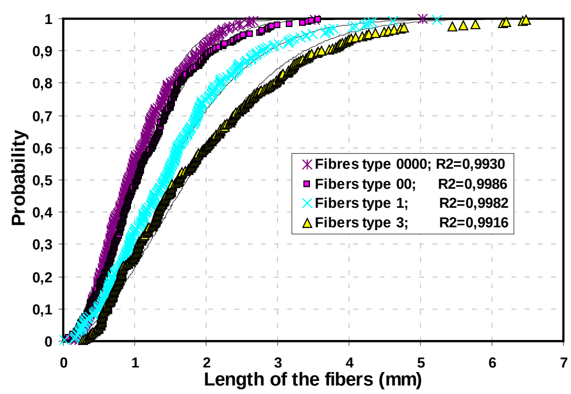

Fig. 3.5 *Probability distribution functions of the length of the fibers after mixing and compacting [38].*

In addition, a significant number SEM images was taken to analyse the effect of the mixing procedure on the fibers. Details of the morphology and surface damage of two types of steel wool fibers after mixing are shown in Fig. 3.6. It can be observed that the fiber with big diameter (type 1) suffers higher damage than the fiber with smaller diameter (type 0000). This happens because when the diameter is reduced, fibers can easily move during the mixing and compaction process. In the case of fibers type 0000, their surface was just scratched (see Fig 3.6(a)), while in the case of fibers type 1 the fibers presented a high number of impacts and damages (see Fig. 3.6(b)).

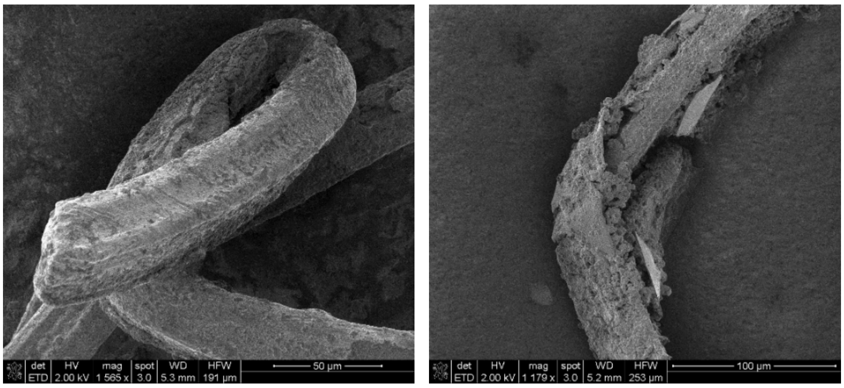

(a) (b)

Fig. 3.6 *SEM images of steel wool fibers type 0000 (a) and type 1 (b) after mixing procedure [38].*

3.1.3 Fiber distribution and effect on air void content

The air void content of the asphalt concrete mixtures was calculated in a geometrical way. For this, the exact height and weight of 4 cylindrical test specimens for each mixture were measured in order to calculate the bulk density of each specimen. Additionally, as the exact percentage of materials and their density for each mixture were known, the theoretical density without voids for each mixture was found. From this, the air void percentage was calculated as:

$$Air\ void\ content = \left(1 - \frac{\rho_b}{\rho_t}\right) \cdot 100 \qquad (3.3)$$

where ρ_b is the bulk density of the asphalt mixture, measured in kg/m^3, and ρ_t is the theoretical density without voids of the mixture, measured in kg/m^3.

The air void content of all mixtures with long and short fibers is depicted in Fig. 3.7. It can be seen that the lowest air voids content is obtained for the reference mixture, without fibers (1.5% air void content). This happened because, in this case, the total specific surface was lower than in the cases where steel wool fibers were used. The second remarkable point is the data from the evaluation of mixtures with 2% long fibers. It is significant that mixtures with 2% long fibers with 0.15498 mm diameter have a much lower air void content than the rest of the mixtures and 2% long fibers. As discussed later, the existence of more fiber clusters with long fibers than with short fibers was found as a possible reason. Additionally, in the cases where 4% long fibers type 0000 and type 00 are used, the air void content is very similar to the corresponding cases where 2% of fibers were used.

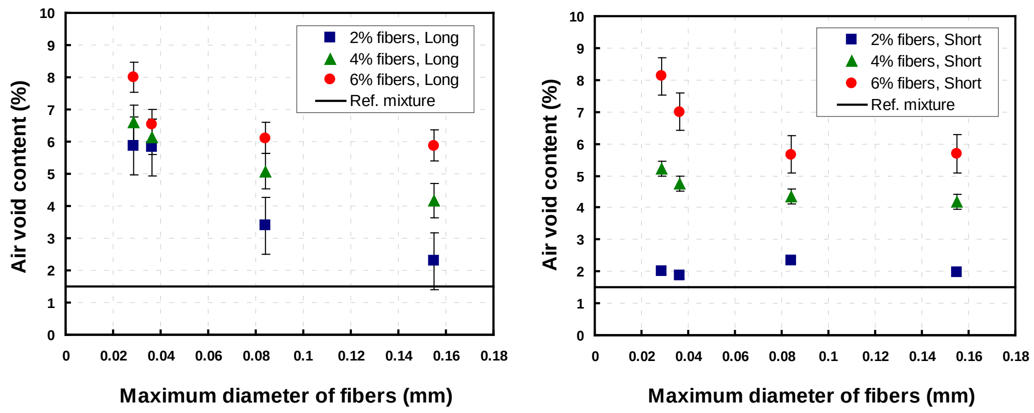

(a) (b)

***Fig. 3.7** Effect of fiber percentage and diameter on air voids content in (a) mixtures with long fibers and (b) mixtures with short fibers [38].*

Furthermore, the air voids content in all mixtures with 6% fibers was higher than the air voids content in the rest of the mixtures. The number of fibers in these mixtures was very high, which means that their specific surface was also quite high. It can also be noticed that the air void content in case of 6% fibers remained nearly the same regardless of the length of fibers and did not change for fibers with maximum diameter above 0.08389 mm. However, it was observed that for smaller diameters of fibers, the obtained air void contents were higher.

In addition, in order to have an insight of the microstructure of the dense asphalt mixture, X-ray micro-tomography on different samples was performed. Hence, representative beams of 10×2×2 mm^3 were extracted from test samples with 2% of long fibers type 00 (0.03642 mm diameter), with 2% of short fibers type 00 (0.03642 mm diameter), with 6% of long fibers type 00 (0.03642 mm diameter), with 6% of short fibers type 00 (0.03642mm diameter), with 2% of long fibers type 3 (0.15498mm diameter) and with 2% of short fibers type 3 (0.15498 mm diameter). The reconstructions of the fibers were prepared by segmenting the materials found in a specific volume, based in a simple algorithm of thresholding [40]. With this simple method, aggregates, bitumen and air voids could be readily separated. Finally, the softwares used for these reconstructions were ImageJ®, DeVIDE® and Meshlab®.

In Fig. 3.8, the fibers distributions in six different types of mixtures after mixing and Marshall compaction are shown. The objective of this set of CT Scan images is to show a qualitative representation of the distribution of fibers into an asphalt mixture. It can be observed that the fibers distribution was very different in all different types of mixtures, even when the same type of fibers was used. The first surprising finding is the difference between Fig. 3.8(a) and Fig. 3.8(b), which represent mixtures that have 2% by mass of fibers, with the same diameter (0.03642 mm), but of different lengths. It can be observed that in case of using long fibers, their density in the mixture was much lower, which could be an indication of a higher air void content in the case of mixtures with long fibers (see Fig. 3.7). Hence, the effective number of fibers in the mixture was lower, and their possible beneficial effects were minimized.

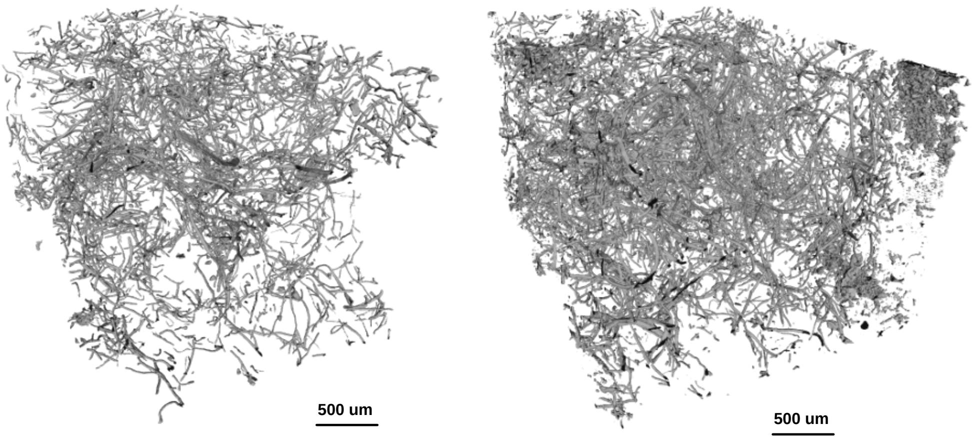

(a) (b)

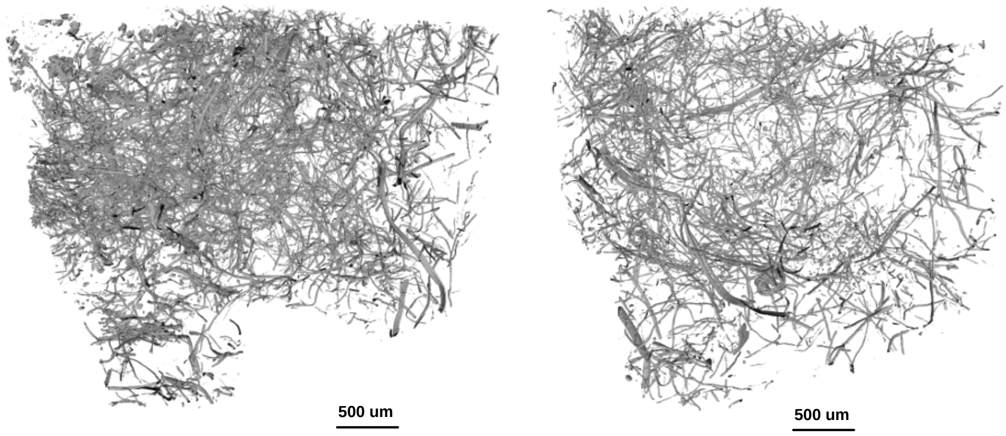

(b) (c)

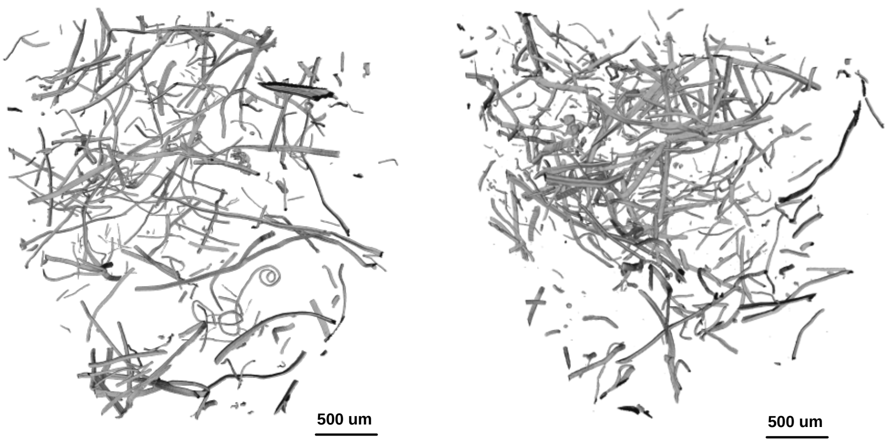

(d) (e)

Fig. 3.8 *Micro-CT Scan images: (a) 2% of long fibers type 00 (0.03642 mm diameter) (b) 2% of short fibers type 00 (0.03642 mm diameter) (c) 6% of long fibers type 00 (0.03642 mm diameter) (d) 6% of short fibers type 00 (0.03642 mm diameter) (e) 2% of long fibers type 3 (0.15498 mm diameter), and (f) 2% of short fibers type 3 (0.15498 mm diameter) [38].*

In the cases presented in Fig. 3.8(c) and Fig. 3.8(d), which represent mixtures that have 6% by mass of fibers with the same diameter (0.03642 mm) but of different lengths, the percentage of fibers in the mixture seems to be very similar, but lower than in samples from mixtures with 2% fibers. As it was shown in the previous analysis, these mixtures with 6% steel fibers presented a very similar air void content. Finally, Fig. 3.8(e) and Fig. 3.8 (f) show mixtures that have 2% fibers type 3, with the same diameter (0.15498 mm) but with different lengths. As in the cases of samples from mixtures with steel fibers type 00, the mixture with long fibers (Fig. 3.8(e)) presents a higher air void content, and as a result of this the distribution, density of fibers was lower. Additionally, as the diameter of fibers type 3 is bigger than the diameter of fibers type 00, in the cases where fibers type 3 were used the total number of fibers was lower for the same volume of fibers in the mixture than in the cases where fibers type 00 were used. As a conclusion, it can be established that a short initial length of fibers seems to provide a lower air void content and a better distribution of fibers in the mixture.

As every fiber-composite, the primary requirement to obtain a high performance is good dispersions of the fibers in the matrix [41] and good anchoring. When the fibers are not dispersed, clusters (entangled fibers) and agglomerations of fibers appear which can have a negative effect on the mechanical properties of an asphalt mixture (Fig. 3.9). Research in concrete materials has shown that cracks initiate and advance from the zones that have large fiber-free matrix regions and fiber self-adhesion or clumping [42]. This can be taken as an indication that clusters would be weak points also in asphalt concrete mixture. Additionally, as steel fibers clusters have a very high specific area, they could behave as “sponges” for bitumen [37].

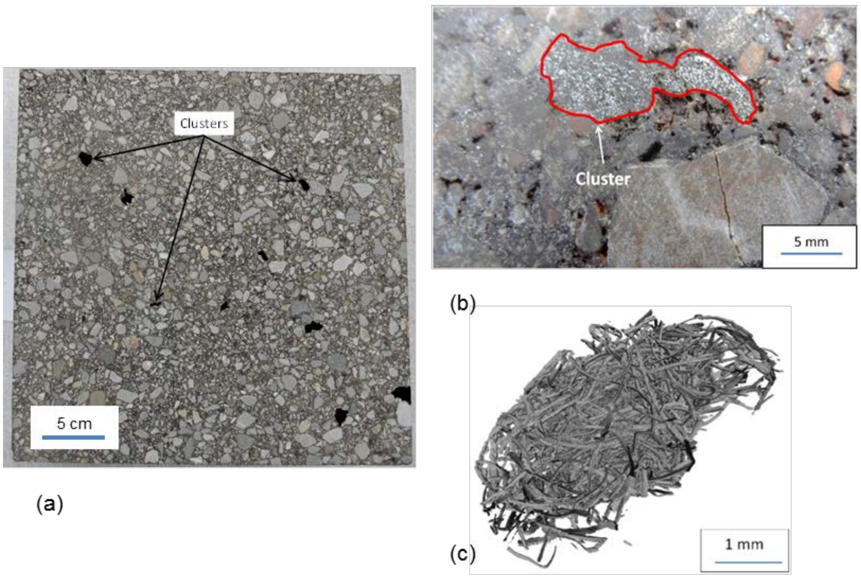

Fig. 3.9 *Fiber cluster distribution on one of the asphalt mixture slab (a), detail of a cluster (b) and its CT Scan reconstruction (c).*

Hence, fiber clusters in the mixtures were detected and measured by taking photographs of both faces from the 25×25×5 cm^3 slabs and by analysing the fiber clusters with ImageJ®. An example of one of the analysed pictures is represented in Fig 3.9. The percentage of clusters in the mixture was calculated as:

$$\text{Percentage of clusters} = \frac{1}{2}\left(\frac{A_{c1}}{A_{p1}} + \frac{A_{c2}}{A_{p2}}\right) \tag{3.4}$$

where A_{c1} and A_{c2} are the area of clusters in the upper and the lower faces of the slab respectively, and A_{p1} and A_{p2} are the areas of the upper and the lower faces of the slab.

In Fig. 3.10, the area percentage of clusters of fibers according to the equation (3.4) in some of the tested mixtures, after mixing and compacting is shown. When the fibers are initially long (Fig. 3.10(a)), the final amount of clusters formed is slightly higher than when fibers are initially short (Fig. 3.10(b)). The average percentage of clusters in the mixture for short fibers is 0.35% calculated by eq. (3.4), while the average percentage of clusters for long fibers is 0.41%. Thus, it seems that the initial length does not influence the cluster formation of fibers since they decreases their length during the mixing procedure as it has been explained in the previous section. Nevertheless, it is clear that the amount of clusters formed increases with the percentage of fibers. It is remarkable that the highest amount of clusters appeared for fibers type 0000 with 0.02855 mm diameter, while the minimum was for fibers type 3 with 0.15498 mm diameter. This fact was influenced by the total number of fibers in the mixture and was higher for the fibers with short diameter. In case of too many fibers in the mixture the probability of entangled and forming clusters is very high. This happens also in case of having very long and flexible fibers [43].

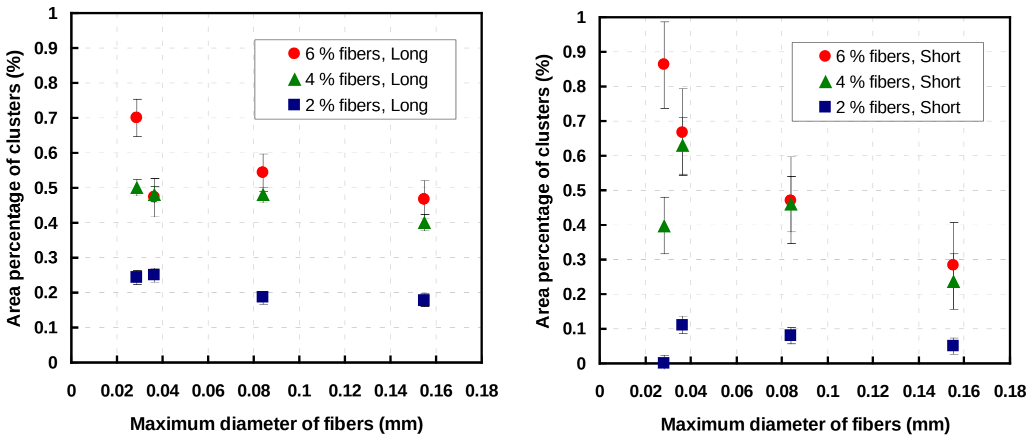

(a) (b)

Fig. 3.10 *Area percentage of clusters in the mixture versus the maximum diameter of fibers in: mixtures with long fibers (a) and with short fibers (b).*

It is important to remark that during this study sometimes it was observed that clusters of fibers appeared during the first moments of mixing and that the mixing process can serve for dissolving them. Thus, a solution to improve the dispersion of the fibers in the mixture could be to increase the shear rate during the mixing process. Another solution could be reducing the diameters of the fibers added into the mixture. During this research, it could be observed that fibers get more easily dispersed at a high shear rate than at a low shear rate, although it was decided to leave aside this variable in this study.

Finally, the effect of the percentage of clusters in the mixture on the air void content, for all 24 mixtures with fibers is shown in Fig. 3.11. It can be observed that the air void content in dense asphalt mixture increases with the number of clusters, taking as a reference 1.52% which is the air void content for the mixtures with no addition of steel fibers. It can also be seen that the percentage of clusters, as well as the air void content, are highly dependent of the percentage of fibers in the mixture. This means that the formation of clusters in asphalt mixture depends firstly, on the volume of fibers in the mixture, since there are fewer clusters with a smaller number of fibers. Secondly, it depends on the fiber diameter: the bigger it is, the stiffer the fibers are and the probability of forming clusters is reduced.

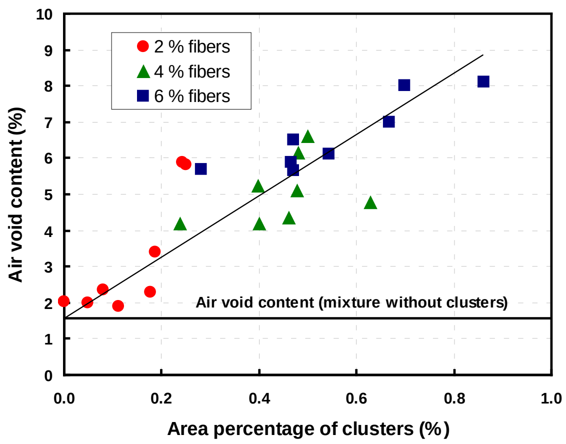

Fig. 3.11 *Air voids content versus area percentage of clusters into dense mixture [38].*

3.2 Study of the effect of steel wool fibers on asphalt mixture properties

3.2.1 Particle loss resistance

One the main purposes of fibers in dense asphalt mixture is to prevent damage in road pavements, especially ravelling or potholes. For this reason, particle loss resistance tests were chosen to assess the effect of steel wool fibers on the particle loss properties of the mixture.

In addition, before testing, Marshall specimens were preconditioned in three different ways, according to the following configuration:

- Dry test: Samples were conditioned in a temperature-controlled room at a temperature of 20ºC during 24 hours.
- Water: Firstly, test samples were vacuum-saturated. Secondly, they were submerged in a 40ºC water bath for 120 hours.
- Salt water: Firstly, test samples were vacuum-saturated. Secondly, they were submerged in a 40ºC salt-water bath for 120 hours. The salt content (sodium chloride) was 30% by weight of water.

After these treatments, Marshall test samples were conditioned at a temperature of 20ºC during 24 hours, in the same temperature-controlled room where the test setup was installed. Then, each sample was subjected to 300 cycles at 30 rpm in the steel drum without steel balls. The mass of the specimen before (w_1) and after (w_2) the test was recorded, and the particle loss (PL) was calculated using the equation (3.5):

$$PL = \frac{w_1 - w_2}{w_1} \times 100 \tag{3.5}$$

The relationship between the particle loss resistance of dense asphalt mixture with steel fibers after different pre-treatments and the air void content of the asphalt mixtures is presented in Fig. 3.12. It could be concluded that the particle loss behaviour of dense asphalt mixture with fibers changed depending on the type of environmental damage that the pavement material has suffered. In Fig. 3.12(a), test samples under dry conditions showed a relatively higher particle loss resistance than the rest of the test samples, pre-treated under different aggressive environments. For example, dense asphalt mixture, with 2% fibers and 2% air void content, under dry conditions, shows 3% particle loss, while the particle loss is approximately 5.5%, 3% and 3.5% for water damage, salt water damage and ageing pre-treatments, respectively. On the other hand, dense asphalt mixtures, with 2% fibers and 6% air void content, shows 10% of particle loss, while the particle loss is approximately 11.5%, 13% and 11.5%, for water damage, salt water damage and ageing pre-treatments, respectively.

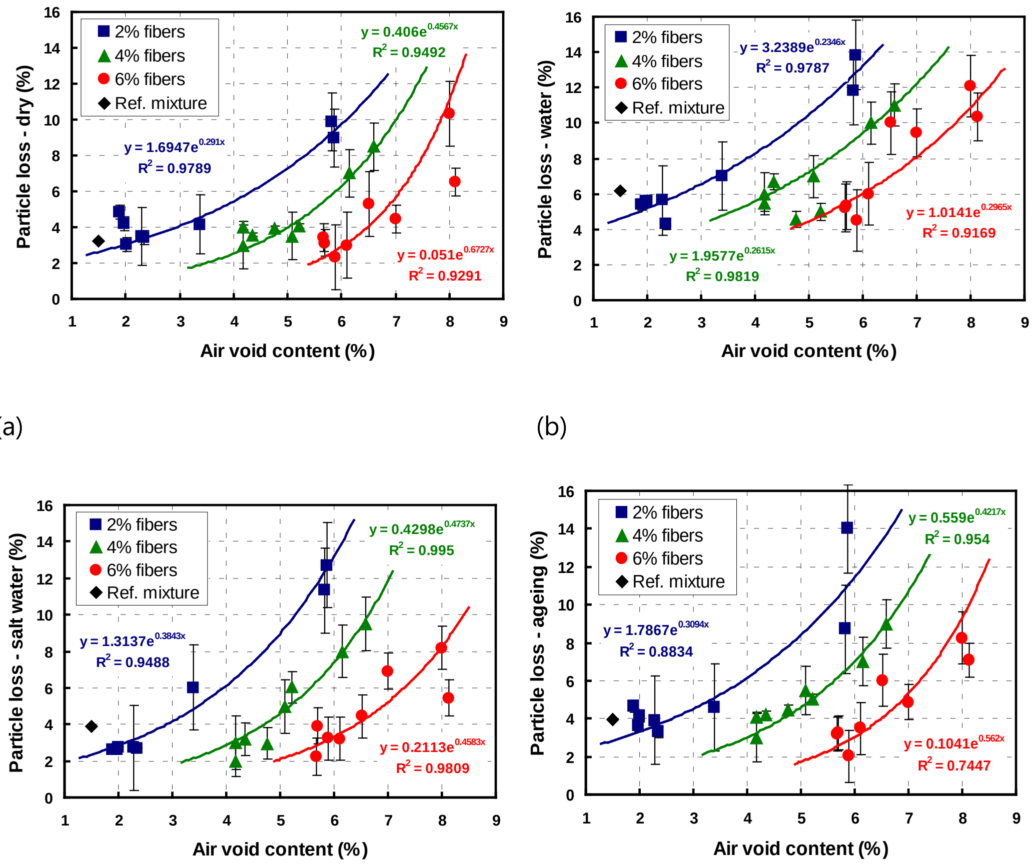

(a) (b)

(c) (d)

***Fig. 3.12** Particle loss percentage of test samples versus their air void content for: (a) dry conditions, (b) water damage, (c) salt water damage, and (d) ageing* [44].

Finally, in order to identify the type of pre-treatment that affected more the particle loss resistance of dense asphalt mixture, a Damage Increase Factor (DIF) has been defined as the relationships between the particle loss of pre-treated (PLtreated) and non-pre-treated (PLnon-treated) specimens with equivalent air void content (eq. (3.6)) [44]:

$$DIF = \frac{PL(\%)_{treated}}{PL(\%)_{non-treated}} \tag{3.6}$$

To assess the damage increase caused by the pre-treatments, an average of the DIF values for all the mixtures has been calculated. The values obtained can be observed in Table 3.1. From these values it can be seen that there is no significant difference in the damage levels found for mixtures with long fibers or short fibers. This happens because mixtures with long fibers presented a higher porosity: as it is well known, particle loss increases with the air void content in the mixtures (see Fig. 3.12).

Additionally, it seems that water was the factor that causes more damages on asphalt mixtures with fibers (Average DIF 1.578). This happens because the contact angle between water and bitumen is relatively small and water can penetrate the interface between the binder and the aggregates, reducing the adhesion properties of asphalt mixture [45]. Moreover, in case of the salt water pre-treatment, the final damage levels were lower than in case of water pre-treatment (Average DIF 1.149). Although it is known that salt in water can decrease the contact angle between bitumen and aggregates [46], increasing the damage levels, in this case the high concentration of salt (30%), served to decrease the oil-water viscosity ratio reducing damage penetration [45]. Finally, ageing was the pre-treatment that showed a lower damage increase factor (Average DIF 1.090). During the ageing process, dense asphalt mixture stiffness increased due to the oxidation of bitumen [47] and the binder showed more likely brittle fracture.

***Table 3.1** Results of the damage increase factor.*

Damage type ratio	**Short fibers**	**Long fibers**	**Average DFI (short + long fibers)**
Water damage	1.508	1.647	1.578
Salt water damage	1.167	1.131	1.149
Ageing	1.074	1.105	1.090

However, from these data, it is still unclear if steel wool fibers in dense asphalt mixture can reduce the particle loss levels caused by environmental damage. For this reason, in Fig.3.13, the Weibull probability of all the calculated DIFs has been calculated and presented against the data percentiles. The Weibull probability distribution function was used in this study considering that particle loss in dense asphalt mixture occurs due to the many small cracks that happen during each loading cycle. Accordingly, when impacts are repeated during the tests and due to the accumulated damage, cracks that separate the aggregates from the matrix can appear. Thus, the particle loss data can be modelled as a fracture process of aggregate of the mixture, adjusted to a probability distribution of Weibull type.

In Fig. 3.13 the P-P plots for short fibers and for long fibers are presented. In both figures, it can be observed that the relationship between the Weibull probability and the data percentiles is linear, for every pre-treatment applied. This means that the DIFs for each pre-treatment can be represented by a single Weibull distribution function, and that the variability of this function happens due to the scatter, not to the amount or type of fibers in the mixture. For this reason, it can be confirmed that steel wool fibers do not contribute to improve the damage resistance of dense asphalt mixture to water, water with salt and ageing of dense asphalt mixture.

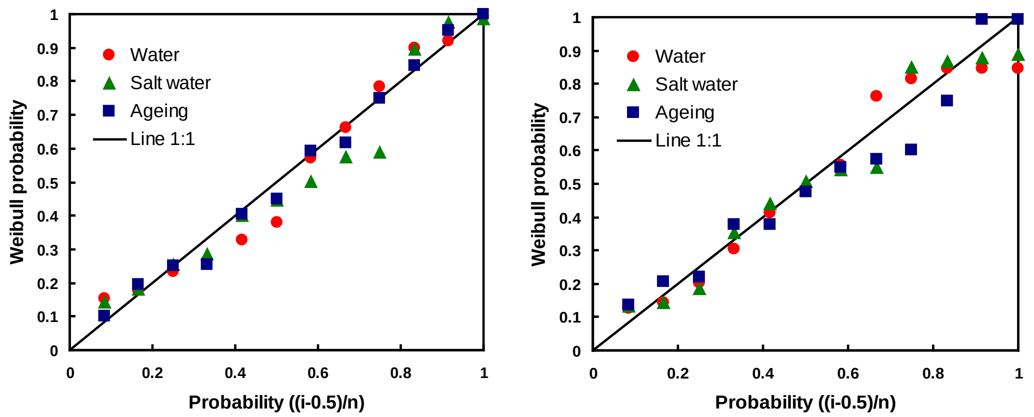

(a) (b)

***Fig. 3.13** Probability-probability plot of the relationship between the particle loss of pre-treated specimens and non-pretreated specimens for: (a) mixtures with short fibers and (b) mixtures with long fibers [44].*

3.2.2 Flexural strength

The flexural strength of dense asphalt mixture specimens modified with steel wool fibers was measured by means of semi-circular bending tests (SCB-T) (Fig. 3.14). Semi-circular test samples with 10 cm of diameter and 2 cm of thickness were cut from Marshall test specimens. Additionally, a notch in the test samples was cut with a thickness of about 2 mm and a depth of about 10 mm; the notch was cut at the mid-point in the direction of the loading from the central axis of the sample.

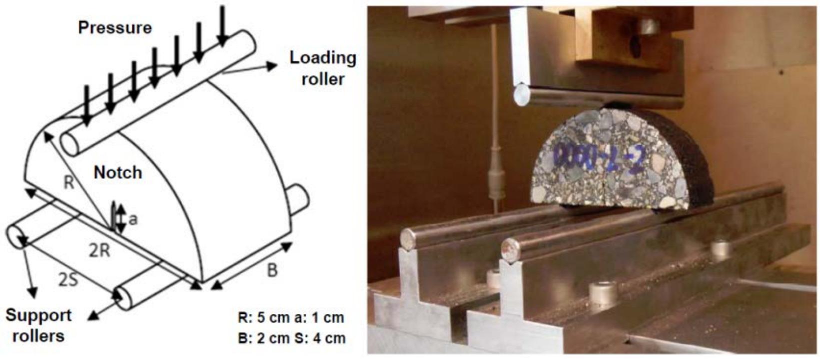

(a) (b)

Fig. 3.14 *Semi-circular bending test used to measure flexural strength.*

All tests were performed inside a temperature-controlled chamber at four different temperatures: -20ºC, -7ºC, 7ºC and 20ºC. Prior to testing, test specimens were kept in the temperature-controlled chamber at the test temperature for 2 hours, to prevent any temperature gradient within the samples. The test setup for the semi-circular tests samples consisted of two support rollers at the straight (bottom) edge and one loading roller at the mid-point of the semi-circular arch (Fig. 3.14). The spacing between the two support rollers was 8 cm. The equipment used for testing was a universal servo-hydraulic Dynasphalt machine with capacity of 10 kN. The test load of 1 kN was applied at a loading rate of 0.5 mm/min. Approximately 200 semi-circular test samples were tested.

The influence of the incorporation of steel fibers on the flexural strength at different temperatures is shown in Fig. 3.15. It can be observed that the addition of steel fibers reduced the maximum load resisted in comparison to the reference asphalt mixture without modification. This reduction of strength was found for short and long fibers regardless the amount of incorporated material. Nevertheless, this effect was less significant at higher temperatures. As expected, it can be seen that the maximum load resisted by dense mixture reduced with the increase of the temperature. The reason for this is the loss of viscosity that bitumen suffers when the temperature is raised, which results in a decrease in the adhesion properties of the asphalt mixture.

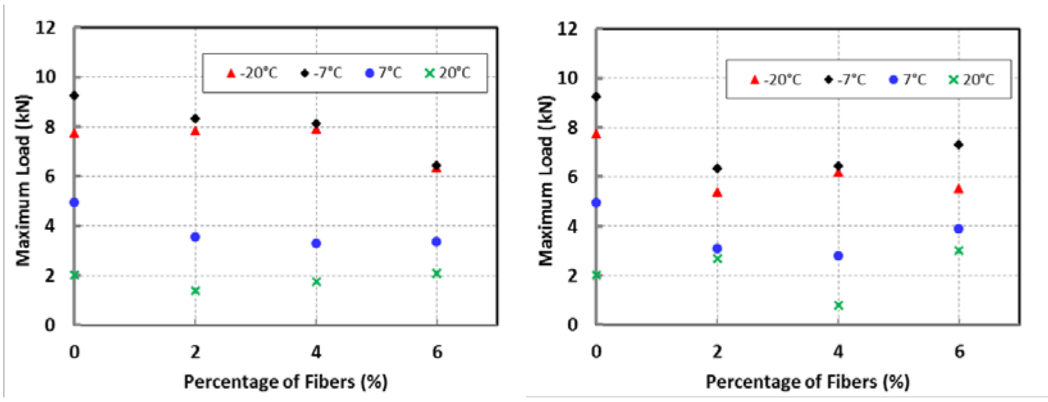

(a) (b)

Fig. 3.15 *Maximum flexural load resisted by semi-circular samples at different temperatures in: (a) mixtures with short fibers and (b) mixtures with long fibers.*

The effect of the diameter and percentage of fibers on the ultimate flexural load resisted by the dense asphalt mixture at 20 °C was evaluated by statistical analysis. In Fig. 3.16, the P-P plot of the samples subjected to flexural strength, using a normal distribution function, for all the mixtures studied is represented. In this figure, it can be observed that all the results can be aligned in a 1:1 straight line, which indicates that the fiber amount or diameter does not have a significant effect on the semi-circular flexural strength of dense asphalt mixture.

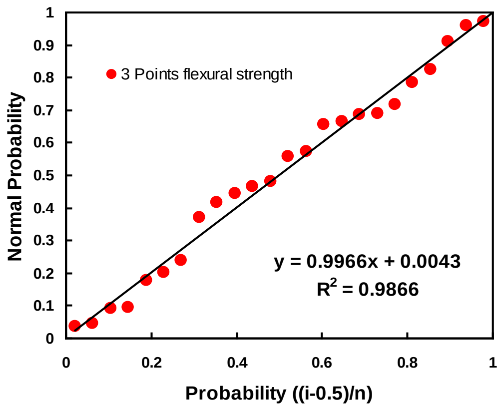

Fig. 3.16 *Probability-probability plot of semi-circular flexural strength of dense asphalt mixtures modified with steel wool fibers.*

3.2.3 Electrical resistivity

The electrical resistivity measurements were done in asphalt slabs at room temperature 20ºC. The electrodes were made of nickel, measured 25 x 25 cm^2 and were placed in the wide side of the prismatic specimens to measure the electrical volumetric resistance, without applying any extra pressure than the own weight of the test specimen. A resistance tester was used to measure the resistance. From the resistance data, the electrical resistivity was obtained from the second Ohm-law:

$$\rho = \frac{RS}{L} \tag{3.7}$$

where ρ is the electrical resistance, L is the internal electrode distance, S is the electrode conductive area and R is the measured resistance. The electric field was assumed constant and the end-effects considered negligible.

It is known that if enough fibers are added to the mixture, they may form a conductive path, which would imply a sudden drop on the electrical resistivity of asphalt concrete [14]. The volumetric electrical resistivity of dense asphalt concrete versus the diameter of the fibers in the mixture is shown in Fig. 3.17. It can be observed that the amount of fibers added was not enough to reach the percolation threshold in asphalt concrete. In this study, 6 % was the maximum amount of fibers used, because, with a higher volume, it would have been very difficult to obtain a good dispersion. Moreover, it can be stated that the percentage of fibers has a clear influence on the electrical resistivity of dense asphalt concrete: the electrical resistivity decreases with the increase of the percentage of fibers. For example, mixtures with 2 % short fibers of 0.1549 mm diameter (Type 3), show a resistivity of 10.27 Ω·m, while mixtures with 6 % short fibers of 0.1549 mm diameter show a resistivity of 8.87 Ω·m. It can be also seen that mixtures with fibers with smaller diameters had lower electrical resistivity. This happened because, for a fixed volume of fibers in the mixture, their number was higher when their diameter was reduced. Finally, it can be observed that there is not a clear difference in the electrical resistivity between long and short fibers.

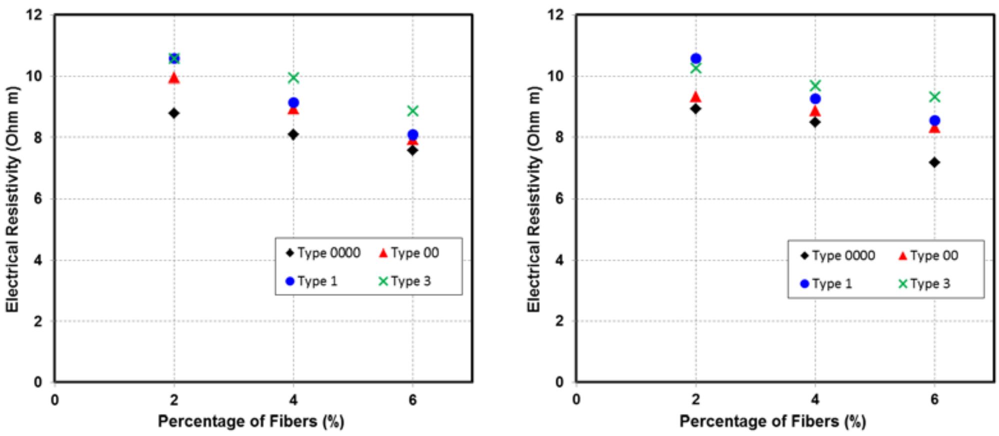

(a) (b)

Fig. 3.17 *Influence of the diameter of the steel wool fibers on the volumetric electrical resistivity.*

Nevertheless, it must be taken into account that the percentage of steel fibers showed a direct effect on the air voids content. In order to analyse this influence, the volume electrical resistivity of dense asphalt concrete is shown versus the air void content in Fig. 3.18. It can be observed that the electrical resistivity of dense asphalt concrete has a clear tendency to decrease with the air void content. As it has been explained, the highest air void content and the lowest electrical resistivity happen in mixtures with 6 % fibers. In the same way, the lowest air void content and the highest electrical resistivity happen in mixtures with 2 % fibers. This happens independently of the diameter, volume or original length of the steel wool fibers.

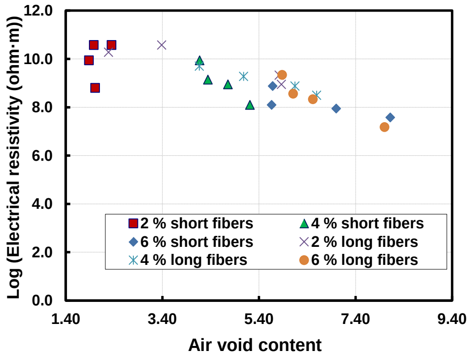

Fig. 3.18 *Effect of the air voids content on the volumetric electrical resistivity.*

3.2.4 Thermal conductivity

Thermodynamic properties are related to the equilibrium state of the system which involves specific heat capacity, i.e. the amount of heat energy required to raise the temperature, and thermal conductivity, or, in other words the ability of a material to conduct heat. The thermal conductivity of a pavement at a certain temperature generally depends on the type of mixture, the binder type, the aggregates type and size, the level of compaction and overall density. For example, porous asphalt pavements show lower temperatures compared to other materials with similar or higher albedo because of the insulating properties created by a high air void content and less particle contact [48]. Thickness also plays an important role in the thermal behaviour of the road. However, surface temperatures become unaffected above a certain pavement thickness [49].

Thermal conductivity measurements were done through the hot plate method (Fig. 3.19). It consisted of a flat, heated metering plate and a cooled plate in between which the test specimen is placed. All the system was surrounded on all lateral sides by an isolating layer, which provided adiabatic conditions. In this case, the lower plate was at a constant temperature of 5°C and the upper plate at a constant temperature of 50°C. These conditions were maintained during 24 hours, to assure a stable temperature flux through the specimen.

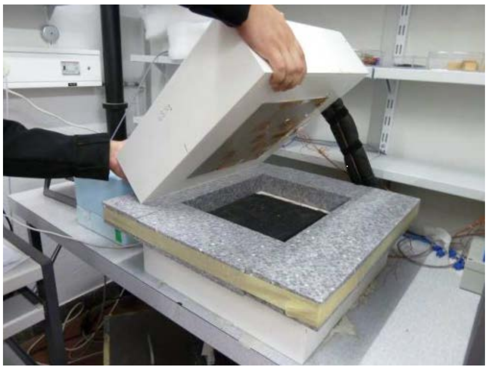

Fig. 3.19 *Guarded hot-plate apparatus.*

The results from the measurements of thermal conductivity for all the mixtures analysed are shown in Fig. 3.20, where the thermal conductivity is presented versus the air void content of asphalt concrete. It can be observed that, in the mixtures without steel wool fibers the thermal conductivity reduces with the increase in the air void content, from 1.6 $W \cdot m^{-1} \cdot K^{-1}$ to 1.2 $W \cdot m^{-1} \cdot K^{-1}$ when the porosity is 2.91% and 11.90%, respectively. These results agree with previously ones reported in the literature [50]. The reason for this reduction is that above a certain percentage of air voids, the pores start being connected and the total asphalt concrete surface exposed to the air is much higher.

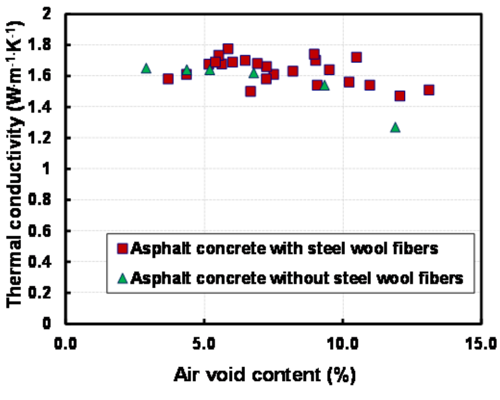

Fig. 3.20 *Influence of the air void content on the thermal conductivity of asphalt concrete with steel wool fibers.*

Moreover, it is well known that the thermal conductivity of steel is much higher than the thermal conductivity of asphalt concrete [51]. As a result the analysis of the influence on the thermal conductivity of the steel fibers incorporated into the asphalt mixtures was carried out. As detailed in Fig. 3.20, the thermal conductivity of asphalt concrete mixtures with steel wool fibers was slightly higher than the thermal conductivity of asphalt concrete mixtures without steel fibers, even with the same air void content. In Fig. 3.21, it is shown that the influence of the amount and type of fibers on the thermal conductivity is not clear and can be considered insignificant. As explained above, a parameter like the air voids content associated to the percentage of fibers can be the main factor affecting the thermal conductivity in this case.

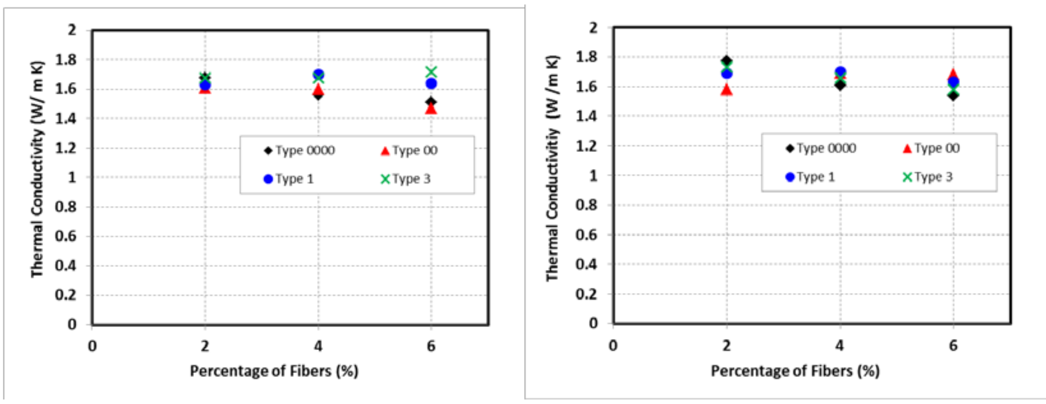

(a) (b)

Fig. 3.21 *Influence of the percentage and diameter of short (a) and long (b) steel fibers on the thermal conductivity of modified asphalt mixtures.*

Moreover, the volume electrical resistivity is related to the thermal conductivity in dense asphalt concrete. For this reason, these two parameters have been plotted in Fig. 3.22. In this Figure it can be observed that the electrical resistivity increases with the thermal conductivity of dense asphalt concrete. Additionally, the lowest electrical resistivity happens in the mixture with 6 % short fibers, while the lowest thermal conductivity happens in the mixture with 6 % long fibers. Furthermore, mixtures with 2 % short and long fibers show very high electrical resistivity and thermal conductivity. As it was explained above, steel wool fibers have a limited influence on the thermal conductivity of asphalt concrete, while they change the air void content to a very high percentage (from almost 3 % in the case where no fibers were added to more than 10 % in the case where 6 % fibers, with 0.02855 mm diameter were added). As a result, an increase of the volume of fibers in the mixture implies a decrease in the electrical resistivity of dense asphalt concrete and a decrease in the thermal conductivity of the mixture. For example, in the case of mixtures with 6 % short fibers type 00 of 0.03642 mm diameter, the electrical resistivity is 7.94 $\Omega \cdot m$, while the thermal conductivity is 1.47 $W.m^{-1}.K^{-1}$. But in the case of mixtures with 2 % short fibers type 3 of 0.15498 mm diameter, the electrical resistivity is 10.57 $\Omega \cdot m$, while the thermal conductivity is 1.68 $W.m^{-1}.K^{-1}$. The last mixture has less fibers and a lower air void content than the first one.

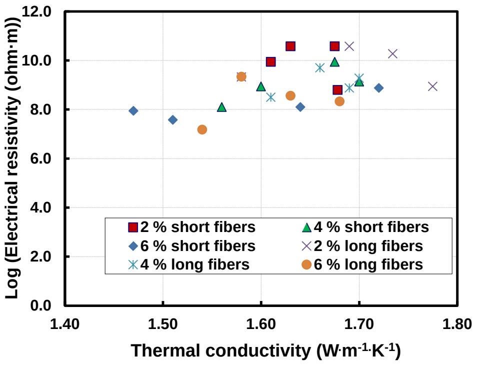

Fig. 3.22 *Relationship between the volumetric electrical resistivity and the thermal conductivity.*

3.2.5 Inductive heating and cooling properties

In this research, the induction heating processes which was used for thermal analysis as well as healing purposes, were performed by using a 30 kW induction heating generator able to generate a maximum frequency of 80 kHz due to the capacitors configuration and the shape and dimensions of the inductor (Fig. 3.23).

Fig. 3.23 *Induction heating source with matching box and coil inductor (left) and detail of shape of the coil inductor (right).*

In order to analyse the thermal behaviour by induction heating of the asphalt mixtures modified with different types and percentages of steel wool fibers, a number of asphalt slabs were heated during 1 minute. In this study, the temperature evolutions were measured with a 640 x 480 pixels, full colour infrared camera (Fig. 3.24).

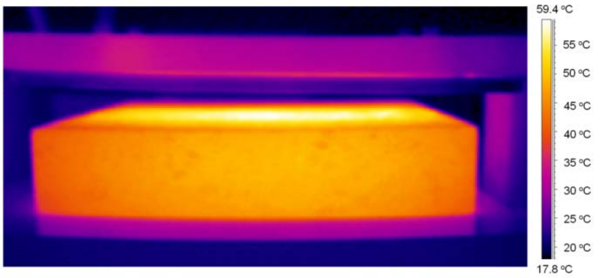

Fig. 3.24 *Example of the distribution of the temperature in a thermograph image of one test sample.*

A number of test slabs were randomly selected from the mixtures modified with different type and percentages of steel fibers in order to analyse the induction heating performance as well as their cooling evolution. The temperatures obtained on the surface and on the bottom of the prismatic specimens used for asphalt self-healing are presented in Fig. 3.25. These temperatures were measured from the lateral side of the test specimens. As explained in reference [15], the intensity of the magnetic field decreases with the square of the distance to the coil. In Fig. 3.25(a), it can be observed that after the time of induction heating, the temperature on the bottom of the specimen is approximately half of the temperature on the surface of the asphalt concrete. Moreover, the average temperature of the test samples, measured on one lateral side of the test specimen is also presented. It can be observed that the average temperature ranges from 30°C to more than 130°C. Although, in general, the top and bottom temperature follow the same trend, in this figure a very high dispersion in the temperatures at the bottom of the test samples can be observed. This may be due to the different thermal conductivities of the asphalt concrete test samples and, therefore, to the different air void contents of the material [30].

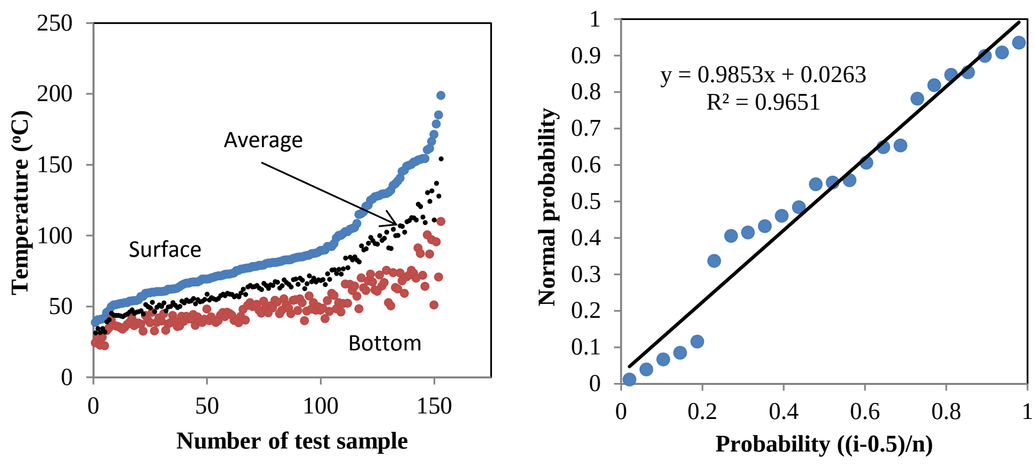

(a) (b)

***Fig. 3.25** (a) Range of temperatures at which the healing was measured. (b) Probability-probability plot of the Newtonian cooling constant (ξ) for all the test samples studied [52].*

Moreover, the Newtonian cooling constants (ξ) of test specimens were calculated by observing their cooling rates during 20 minutes and using these values for calculating the healing rates. The cooling phenomenon will be explained in detail in Section 4. The average value of the cooling constants (ξ) for all the mixtures studied was 0.0055 $m^{-2}\cdot s^{-1}$ with a standard deviation of 0.0012 $m^{-2}\cdot s^{-1}$. In order to clarify the influence of the fibers on the cooling rate of asphalt concrete, the probability-probability plot of the Newtonian cooling constants, from all the mixtures studied, is shown in Fig. 3.25(b). It shows that all the data align in a 45° line. This means that the difference between them is just a statistical error.

It seems clear that the effect of the air void content usually has a direct effect on the thermal performance. However, some works [53] found that differences in the air void content do not have an impact on the cooling rates of dense asphalt mixtures because the air voids of the dense asphalt concrete test specimens were not connected. Therefore convective air currents could not flow through the material, cooling down the asphalt mixture. In case of connected pores, for example in porous asphalt concrete, convective air flowing through the open pores would help in reducing the temperature of the mixture and as a result, asphalt concrete could cool down faster [31]. For this study, porous asphalt specimens taken from an experimental asphalt road with steel fibers were also evaluated [37]. It was found that the average value of the ξ constants for dense asphalt concrete during the heating cycle was 0.042 $m^{-2}\cdot s^{-1}$, while the average value of the ξ constants for porous asphalt concrete was 0.050 $m^{-2}\cdot s^{-1}$ which confirmed that porous asphalt mixture cools down faster than dense asphalt mixture.

Finally, the influence of type of steel fiber was also analysed by measuring the temperature peaks during the induction heating. Maximum temperatures reached in the dense asphalt specimens modified with steel fibers after heating during 1 minute are represented in Fig. 3.26. It can be observed that the maximum temperature depended on the diameter of fibers in the mixture. For example, it can be observed that the temperature reached in mixtures with 6% fibers of 0.02855 mm diameter is approximately 60°C, while the temperature in mixtures with fibers of 0.15498 mm diameter is approximately 90°C. Moreover, the amount of fibers has a higher impact on the maximum temperature reached. For example, in mixtures with fibers of 0.08389 mm diameter, the maximum temperature after 1 minute heating reached approximately 38°C, 55°C and 71°C for mixtures with 2%, 4% and 6%, respectively. However, the initial length of the fiber was reduced during the mixing procedure. Hence, this parameter does not seem to have a significant effect on the heating performance.

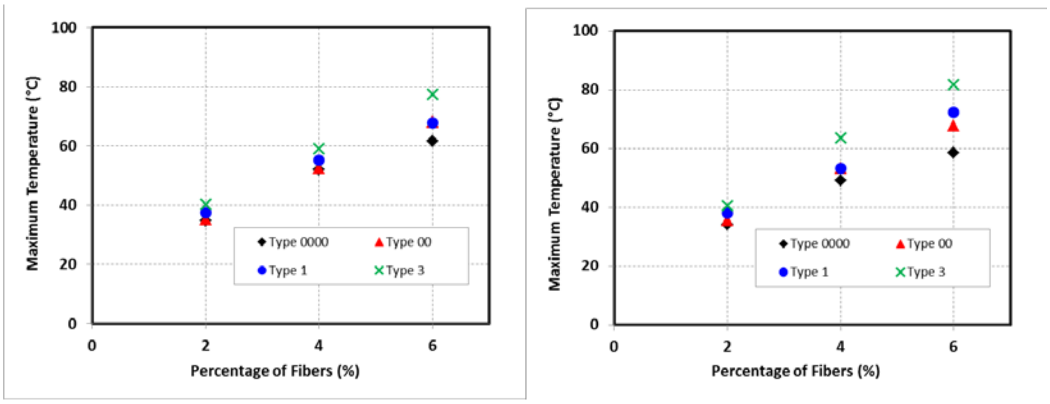

(a) (b)

***Fig. 3.26** Influence of the type and percentage of short (a) and long (b) steel fibers on the maximum surface temperature reached after 1 minute heating.*

In reference [15] it is explained that the temperature reached by asphalt concrete will increase linearly with the volume of fibers in the mixture, while the temperature will increase by a factor 4 with the diameter of the fibers. Although in the cases where the mass of fibers is fixed and the diameter of the fibers increases, the number of fibers in the mixture will decrease. In this way, the influence of the diameter of fibers on the increase of temperature is limited, especially in the cases where a small percentage of fibers was added to the mixture. Additionally, in reference [12] it was shown that the increase of the volume of conductive material in the mixture will increase the temperature only until a certain amount of particles is reached that corresponded to approximately 6%. The reason why more fibers do not increase the surface temperature of the mixture is because asphalt concrete reaches a saturation point when more fibers are introduced and there is not enough bitumen to cover them. For this reason, heat is dissipated in the air.

3.2.6 Parametric study on the influence of steel wool fibers in dense asphalt concrete

In order to have a clear view of the influence of the addition of different types and percentages of steel wool fibers, a study combining all the evaluated parameters was carried out. Abbreviations for the variables included in this study are presented in Table 3.2. In total, twelve variables were analysed:

- 3 concerning the characteristics of the fibers: diameter, initial length and final length of the fibers.
- 3 related to the volumetric properties of the mixtures: percentages of fibers in the mixture, air void content and percentage of clusters.
- 3 in relation to the mechanical properties of the mixtures: particle loss, semi-circular flexural strength and maximum deformation.
- 3 related to the physical properties: electrical resistivity, thermal conductivity and temperature after 1 minute of induction heating.

Table 3.2 *Variables included in the parametric study.*

Classification	Name	Abbreviation	Unit
Characteristics of the fibers	Diameter of fibers	DF	mm
	Initial length of the fibers	IL	mm
	Final length of the fibers	FL	mm
Volumetric properties of the mixtures	Percentage of fibers	PF	%
	Air void content	AVC	%
	Percentage of clusters	PC	%
Mechanical properties of the mixtures	Particle loss	PL	%
	Semi-circular flexural strength	FS	kN
	Semi-circular max. deformation	MD	mm
Physical properties of the mixtures	Electrical resistivity	ER	ohm·m
	Thermal conductivity	TC	$W \cdot m^{-1} \cdot K^{-1}$
	Induction heating temperature	IHT	^oC

The characteristics of the fibers and the physical and mechanical properties for all the mixtures analysed are summarized in Table 3.3. Values are averages of a number of test samples with the same properties.

***Table 3.3** Characteristics of the fibers and properties of the mixtures studied.*

Fibers type	Characteristics of the fibers			Volumetric properties of the mixture			Mechanical properties of the mixture		
	DF (mm)	**IL (mm)**	**FL (mm)**	**PF (%)**	**AVC (%)**	**PC (%)**	**PL (%)**	**FS (kN)**	**MD (mm)**
Short	0.02855	2.777	1.129	2	2.010	0.000	3.049	1.394	1.462
				4	5.213	0.398	4.061	1.747	1.071
				6	8.120	0.862	8.659	2.101	0.769
	0.03642	1.999	1.155	2	1.881	0.112	4.830	2.192	2.147
				4	4.758	0.629	3.929	1.782	1.116
				6	7.212	0.668	4.432	2.083	0.819
	0.08389	2.275	1.679	2	2.347	0.081	3.416	1.705	1.279
				4	4.345	0.461	3.565	1.264	1.135
				6	5.665	0.471	3.427	1.926	1.256
	0.15498	2.435	1.894	2	1.980	0.050	4.209	2.139	1.660
				4	4.174	0.237	3.998	2.412	1.263
				6	5.685	0.282	3.129	1.631	1.352
Long	0.02855	6.211	1.001	2	5.866	0.243	8.966	2.672	0.738
				4	6.594	0.500	8.492	0.786	1.424
				6	8.003	0.700	10.327	3.008	0.596
	0.03642	6.146	1.198	2	5.818	0.250	9.868	2.908	0.642
				4	6.146	0.480	7.213	1.022	2.110
				6	6.519	0.472	5.289	2.136	1.261
	0.08389	7.233	1.456	2	3.386	0.186	4.161	1.007	1.959
				4	5.083	0.479	3.493	0.718	2.062
				6	6.110	0.543	3.023	1.950	1.431
	0.15498	7.753	1.981	2	2.287	0.178	3.499	1.804	1.533
				4	4.168	0.412	2.993	2.322	1.189
				6	5.883	0.467	2.302	1.319	2.166
Reference mixture				-	1.511	-	3.221	2.032	1.656

For a parametric study, the Pearson's correlation coefficients between all the variables analyzed in the parametric study must be calculated in order to know the importance of each variable in relation to the other variables. This correlation coefficient has values between 0 and 1; 0 being no correlation at all and 1 a perfect correlation. When the Pearson's correlation coefficient ranges from 0 to 0.4 there is a low or very low correlation; from 0.4 to 0.7, there is a moderate correlation and from 0.7 to 1 there is a high or very high correlation. The relationships between all the variables measured in this chapter are shown in Table 3.4 and Table 3.5.

Table 3.4 *Pearson coefficients for the relationship between the variables studied in dense asphalt concrete (I).*

		Characteristics of the fibers			Volumetric properties of the mixtures			Mechanical properties of the mixtures		
		DF	**IL**	**FL**	**PF**	**AVC**	**PC**	**PL**	**FS**	**MD**
Characteristics of the fibers	**DF**	--								
	IL	0.14	--							
	FL	0.97	0.07	--						
Volumetric properties of the mixtures	**PF**	0.00	0.00	0.00	--					
	AVC	0.38	0.20	0.42	0.77	--				
	PC	0.33	0.09	0.33	0.79	0.86	--			
Mechanical properties of the mixtures	**PL**	0.59	0.17	0.66	0.03	0.54	0.30	--		
	FS	0.07	0.11	0.10	0.03	0.16	0.03	0.41	--	
	MD	0.34	0.23	0.33	0.19	0.46	0.35	0.49	0.67	--

In Table 3.3, the average length of the fibers before and after mixing is shown. Besides, in Table 3.4 it is statistically confirmed that the final length of the fibers is strongly influenced by their diameter. Moreover, in this study it was observed that clusters of fibers appeared during the mixing process. The percentage of clusters of fibers in the mixtures, after mixing and compacting is also shown in Table 3.3 where it can be observed that the air void content in the mixture increases with the number of clusters and that the percentage of clusters is highly dependent of the percentage of fibers in the mixture. However, the type of fibers presented less influence on the percentage of fiber clusters and, therefore, on the air void content. Furthermore, it is remarkable that the lowest air voids content is obtained for the reference mixture, without fibers (1.51% air void content). Additionally, mixtures with 2% long fibers, with 0.15498 mm diameter (type 3) have a much lower air void content than the rest of the mixtures with 2% of long fibers. This happened because, in the specific case when 2% of fibers were used, there were more clusters in mixtures with long fibers than in mixtures with short fibers. Additionally, in the cases where 4% long fibers with 0.02855 mm diameter (type 0000) and 0.03642 mm diameter (type 00) were used, the air void content was very similar to the corresponding cases with 2% of fibers.

Besides, the air void content in all the mixtures with 6% fibers was much higher than the air void content in the rest of the mixtures. This happened because the number of fibers in the mixture was very high and, therefore, their specific surface was also quite high. In Table 3.3, it can be also noticed that the air void content in case of 6% fibers remained the same regardless of the length of fibers and did not change for fibers with maximum diameter above 0.08389 mm (type 1). As a conclusion, it can be observed that the air void content in the mixture depends mainly on the percentage of clusters in the mixture.

Regarding the effect of the different variables on the mechanical properties of the modified asphalt mixtures characterized in this study, it seems that the length and diameter of the steel wool fibers slightly influence the particle loss resistance. Nevertheless, it can be observed that the different characteristics of the fibers and the volumetric properties of the modified asphalt mixtures have no direct influence on the flexural strength of the semi-circular samples analysed by bending tests.

The relationships for the physical properties of the evaluated asphalt mixtures are presented in Table 3.5. It can be observed that the thermal conductivity of modified asphalt concrete has low correlation with the length of the fibers and with their diameter. It can also be remarked that the percentage of the fibers does not show a significant influence on the thermal conductivity. In the case of the mixtures without fibers, the air void content in the mixture seems to have a more clear effect on the thermal conductivity, although more tests are needed to confirm this point. Regarding the electrical properties of the mixture, it can be confirmed that, the diameter and length of the fibers have an important influence on the electrical resistivity of the mixture as well as percentage of fibers and air voids content. Furthermore, a clear relation between the electrical resistivity and the thermal conductivity can be observed.

***Table 3.5** Pearson coefficients for the relationship between the variables studied in dense asphalt concrete (II).*

		Characteristics of the fibers			Volumetric properties of the mixtures		Physical properties of the mixtures		
		DF	**IL**	**FL**	**PF**	**AVC**	**ER**	**TC**	**IHT**
Characteristics of the fibers	**DF**	--							
	IL	0.14	--						
	FL	0.97	0.07	--					
Volumetric properties of the mixtures	**PF**	0.00	0.00	0.00	--				
	AVC	0.38	0.20	0.42	0.77	--			
Physical properties of the mixtures	**ER**	0.59	0.12	0.62	0.72	0.61	--		
	TC	0.41	0.48	0.47	0.26	0.39	0.61	--	
	IHT	0.32	0.21	0.98	0.89	0.59	0.42	0.23	--

Regarding the maximum temperature reached by dense asphalt concrete, it is important to remark that the length and percentage of fibers in the mixture are key parameters. It was observed that the relationship between the thermal conductivity or the electrical resistivity and the temperature reached is not as clear as the relationship between the type and volume of fibers with the maximum temperature reached. However, the air void content showed a secondary effect. For this reason, it can be concluded that the assessed physical parameters did not really show a strong influence on the induction heating temperature reached by asphalt concrete.

As main conclusion, it seems important to minimize the influence of the fibers on the air void content for optimizing the mechanical and thermal performance. Besides, to increase the thermal conductivity of asphalt concrete, the diameter and percentage of the electrically conductive fibers should be as high as possible, while the mechanical properties of the mixture are not reduced.

4 Asphalt healing by inductive heating. Theoretical background

In this section, the self-healing level is obtained by theoretical approach. The thermal evolution focused on the Newton's law of cooling as well as the capillary phenomena are taken into account as main factors throughout the mathematical development.

4.1 Thermal evolution of the asphalt materials

When an alternating current is applied across a conductive coil, an alternating magnetic field is created with the same frequency as the alternating current causing the field [37]. According to Faraday's law, if a magnetically susceptible and electrically conductive material, like steel wool fibers, is located within a magnetic field, an electric current will be induced with the same frequency than the magnetic field and the intensity circulating through the coil [12]. When the electrical current meets the electrical resistance of the electrically conductive additives embedded into the asphalt concrete, they will heat due to the Joule principle, and the mixture will increase its temperature. As is explained in reference [35], an appropriate healing level is reached when bitumen is heated for a sufficient time above the temperature at which it behaves as a Newtonian fluid (T_{newt}).

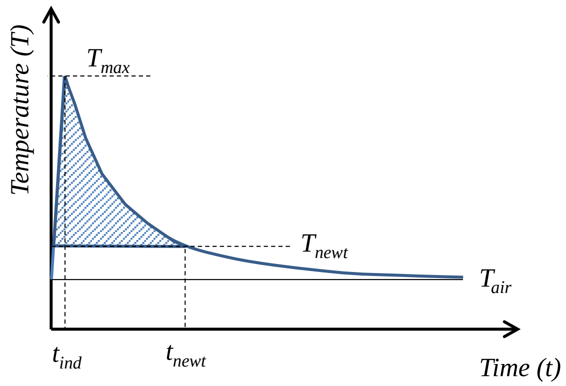

Fig. 4.1 *Temperature evolution in dense asphalt concrete due to induction heating.*

Healing does not happen only during the time induction heating, but also during the cooling time, as long as the temperature of asphalt concrete is still above T_{newt} (see coloured area in Fig. 4.1). With this in mind, it is well known that the cooling of a hot body will follow an approximate exponential function [37], which is described by the Newton's law of cooling:

$$\frac{dQ}{dt} = \alpha A\left(T_{air} - T\right) \tag{4.1}$$

where Q is the thermal energy, α is a heat transfer coefficient, taken constant for simplification, A is the surface area across which the heat is being transferred, T is the temperature of the asphalt surface and T_{air} is the temperature of the environment.

If the temperature of the asphalt concrete surface T is higher than the environmental temperature T_{air}, asphalt concrete will lose an amount of heat dQ in a time interval between t and $t + dt$, reducing its temperature T by dT following:

$$dQ = -mcdT \tag{4.2}$$

where m is the mass of asphalt concrete and c is its specific heat.

The equation that shows the change in temperature as a function of time is

$$-mc\frac{dT}{dt} = \alpha A\left(T_{air} - T\right) \tag{4.3}$$

Integrating this equation and knowing that at time t = 0s and the temperature of asphalt concrete will be T_{max} as well as introducing ξ for α/mc ($m^{-2}s^{-1}$), it is obtained:

$$\int_{T_{\max}}^{T} \frac{dT}{T_{air} - T} = -\xi A \int_0^t dt \tag{4.4}$$

and therefore

$$\ln\left(T - T_{air}\right) = -\xi A \cdot t + \ln\left(T_{\max} - T_{air}\right) \tag{4.5}$$

Hence, the time (t_{newt}) until the temperature of the test sample equals T_{newt}, i.e. when healing will be stopped is

$$t_{newt} = \frac{\ln\left(T_{\max} - T_{air}\right) - \ln\left(T_{newt} - T_{air}\right)}{\xi A} \tag{4.6}$$

With this in mind, the total time when the temperature of the test sample is above the environment temperature reads

$$t = t_{ind} + t_{newt} \tag{4.7}$$

where t_{ind} is the time of induction heating and t_{newt} is the time until the test sample comes back to T_{newt}.

As the time of induction heating is very small (less than 2.5 minutes) compared to the total time when the temperature of the sample is above T_{newt} (can be more than 500 minutes), it can be eliminated from the equation, and the healing time can be approximated with Eq. (4.6) alone.

Finally, by solving T in Eq. (4.5),

$$T = T_{air} + \left(T_{\max} - T_{air}\right)e^{\left(-\xi A \cdot t\right)} \tag{4.8}$$

the area below the cooling curve (coloured area in Fig. 4.1), between t_{ind}= t= 0 and t = t_{newt}, can be calculated:

$$\tau = (T_{newt}t_{newt})t_{newt} - \frac{\left(T_{\max} - T_{air}\right)}{\xi A}\left(e^{\left(-\xi A t_{newt}\right)}\right) \tag{4.9}$$

The parameter tau (τ) with units $K{\cdot}s$ quantifies the total amount of heat in asphalt concrete during the healing process.

4.2 Capillary phenomena

In reference [35] it is explained that healing of open cracks in asphalt concrete will happen when some of the points in both faces of a crack are in contact. Capillary phenomena will start from these contact points and it will extend through the crack if the temperature of asphalt concrete is high enough for bitumen to behave as a Newtonian fluid. Healing will happen faster in cracks deeply buried in the pavement.

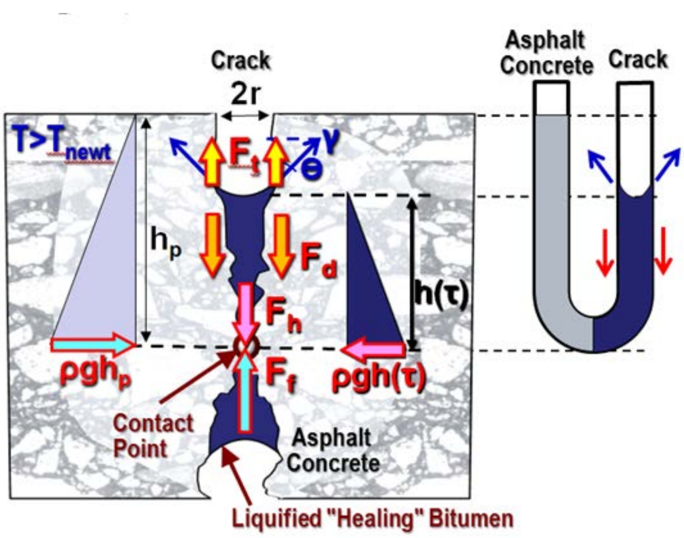

Fig. 4.2 *Scheme of the forces acting in an asphalt concrete crack during the healing process.*

The capillary phenomena can be studied through a modification of the Lucas-Washburn equation (see Fig. 4.2). As a simplification, in this research the crack has been assumed circular and vertical. The main forces that act in the crack are due to the surface tension (F_t),

$$F_t = 2\pi r \gamma \cos(\theta) \tag{4.10}$$

where r is the capillary radius or half the crack width in this case; γ is the surface tension of the liquid and θ the contact angle in the wetting front. The contact angle is not constant, but will vary with the healing rate and with the different materials in the composite. To simplify the model, the contact angle has been assumed constant, and $cos(\theta)$ equal to 1 in the calculations. Additionally, the force exerted by gravity (F_g) is considered in this model as the hydrostatic force in the zone where the binder is flowing into the crack (F_f) minus the force exerted by the weight of the healing material in the crack (F_h):

$$F_g = F_f - F_h = \rho g \pi r^2 \left(h_p - h(\tau)\right) \tag{4.11}$$

where $\rho g \pi r^2 h_p$ is the positive hydrostatic force in the crack, being ρ the density of the binder, g the gravity and h_p the distance from the beam surface to the bottom of the healed zone being considered and $\rho g \pi r^2 h(\tau)$ the weight of the healed zone, which depends on the τ parameter. In this case, h_p is an artificial reference point which represents the distance of the crack to the surface. It is variable in time for each healed zone, but constant and equal to the height of the specimen (H) (see Fig. 4.2) when the whole length of the crack is being considered.

Moreover, a dissipation parameter β can be introduced in order to take into account possible sources of energy dissipation during healing, for example the force of friction by the movement bitumen against the crack faces (F_d):

$$F_d = 2\pi r \beta \frac{dh(\tau)}{d\tau} \tag{4.12}$$

With this in mind, the equation obtained by balancing the surface tension force, the gravity force and the energy dissipation force is:

$$2\pi r\left(\gamma-\beta\cdot\frac{dh(\tau)}{d\tau}\right)=\rho g\pi r^{2}\left(h(\tau)-h_{p}\right) \tag{4.13}$$

And the analytical solution for Eq. (4.13) is given by

$$h(\tau)=\left(h_{p}+\frac{2\gamma}{\rho gr}\right)\left(1-e^{-\frac{\rho gr\tau}{2\beta}}\right) \tag{4.14}$$

4.3 Healing level

In previous works [[35], [52]], the theoretical healing index was obtained by considering the effective area ($A_E(\tau)$) in a broken beam after some time heating. This approach assumed that a certain number of contact points from where the healing process might happen. This complex development took into account parameters associated to bending tests as the maximum momentum in the test beam, the moment of inertia and force resisted by the specimen. Despite obtaining significant correlation values between the experimental results and the theoretical model, a simplified model was developed in order to avoid the use of many assumptions.

In this new approach, the type of test was not considered and a characteristic parameter more general was used. The healing level ($H(\tau)$) of asphalt mixtures is based on the filling height as a measure of the healing (Fig. 4.2) and is defined as the relationship:

$$H(\tau)=\frac{h(\tau)}{h_{p}} \tag{4.15}$$

Healing occurs locally according to the exponential function:

$$H(\tau)=C_{H}\left(1-e^{-D_{h}\cdot\tau}\right) \tag{4.16}$$

Where C_H and D_h are taken as constants, being:

$$C_{H}=\pi n\left(h_{p}+\frac{2\gamma}{\rho gr}\right)^{2} \tag{4.17}$$

and

$$D_{h}=\frac{\rho gr}{\beta} \tag{4.18}$$

5 Inductive healing of asphalt mixtures modified with steel wool fibers

In this section, the experimental results from different studies performed in connection with this project are analysed. The behaviour of dense asphalt mixtures with steel wool fibers was assessed in order to understand the most significant factors for the healing process. Moreover, the analysis of porous asphalt specimen taken from an experimental road in The Netherlands will be useful to define the influence of the type of bitumen as well as the consequences of multiple heating treatments. Finally, the effect of the induction heating by electromagnetic fields on the ageing properties of the bitumen was also studied.

5.1 Dense asphalt mixtures

First, the healing performance was studied by analysing the mechanical performance of a number of specimens compacted from asphalt mixtures modified with steel wool fibers. Prismatic test samples were tested by three-point bending tests at 20 °C before and after induction heating in order to evaluate the efficiency of the healing process. Inductive healing of this set of samples was done as follows: first the tests specimens were numbered; then, groups of test samples were randomly selected for heating times between 2 minutes and 3.5 minutes at intervals of 0.5 minutes. Later, they were tested under three-point bending configuration at -20 °C at a deformation rate of 0.5 mm/min, stopping the tests when the force in the discharging curve reached 20 N after the maximum load of the beams. This load was enough to produce a crack of approximately 200 µm width reaching from the tip of the notch to the load application point. Once cracks were created, the test specimens were let to rest during 2 hours at 20°C and subjected to a healing process by heating during the time selected. Finally, the test samples were tested again under three-point bending in order to validate the healing performance.

The experimental healing level ($S(\tau)$) was defined in this part of the study as the relationship between the ultimate force of the test specimens during a three point bending test, F_i, and the ultimate force measured in the specimens after the healing process $F_b(\tau)$, where τ is a parameter, as explained in the previous Section, that gives an idea of the amount of energy applied to the asphalt concrete test sample during the healing process:

$$S(\tau) = \frac{F_b(\tau)}{F_i} \tag{5.1}$$

The healing level ($S(\tau)$) of the prismatic test specimens at different average surface temperatures of the test samples is shown in Fig. 5.1. All results obtained from different test samples, with different percentages and diameters of steel wool are shown. One of the most remarkable points is that all results for the different materials align in one single curve. It can be observed that the healing, so as the point dispersion, starts at approximately 50°C, when bitumen has a near-Newtonian behaviour as will be later confirmed in the analysis of the rheological properties of the bitumen (Section 5.3). From this point, the healing levels increase with the temperature in the test samples until approximately 0.6, which happened at around 100°C.

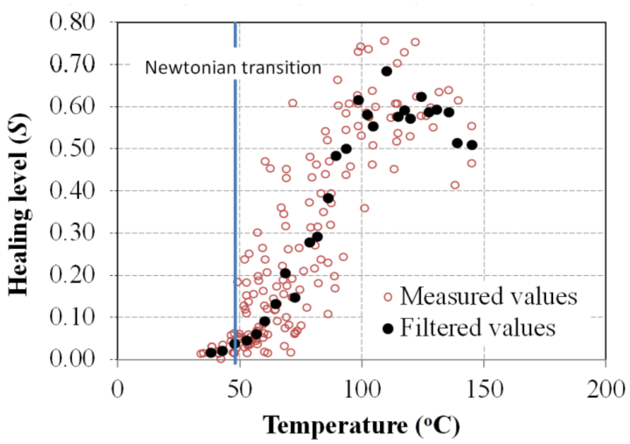

Fig. 5.1 *Healing data versus average temperature in the test samples.*

Additionally, to improve the understanding of the data, the healing results have been filtered by using a moving average filter (see solid points in Fig. 5.1).

Moreover, in order to take into account the cooling phase after induction heating, in Fig. 5.2, the healing levels versus the τ parameter and the fitting corresponding to Eq. (4.16) are shown. For the fitting, only data at a temperature higher than near-viscoelastic threshold have been considered. The fitting by the model is relatively good, with an R^2 coefficient of 0.966, a maximum error of 0.1167 and an average error of 0.037. The results obtained with the simplified theoretical model are similar to those found with the previous model that taken into account the type of test by introducing parameters such as the maximum momentum and the moment of inertia in the test beam during bending as well as the effective area for the healing process [52]. Hence, the new model could reasonably simulate the healing from a simpler approach.

From these data, and after comparing them with those presented in reference [35] it can be concluded that the most appropriate way for healing asphalt concrete is to increase and maintain the temperature above the Newtonian transition (see Fig. 5.1) for a certain amount of time. This cannot be done just by induction heating, because of the temperature history which shows a temperature peak followed by Newtonian cooling. If the temperature is very high during a long time, healing levels can be reduced, and if the temperature is too low, healing will not occur. For this reason, an optimum asphalt concrete material for self-healing applications should have a thermal conductivity as low as possible, such that the energy is not easily dissipated in the environment. With this, healing may happen at lower temperatures and the global efficiency of the system will be increased.

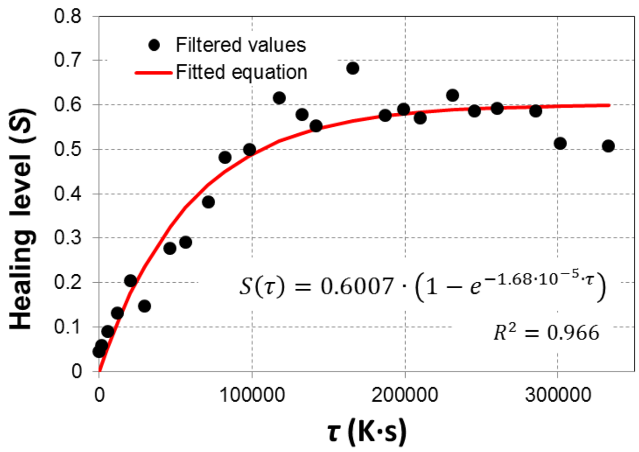

Fig. 5.2 *Healing level versus τ parameter and fitted equation.*

5.2 Comparison between dense and porous asphalt mixtures

In order to compare different self-healing performances, dense asphalt samples modified with steel fibers and porous asphalt specimens taken from an experimental road track built in the Netherlands [53] for healing purposes were tested following the experimental method described before. However, it is important to note that in this analysis semi-circular samples were used and tested by three-point bending tests.

The healing levels (eq. (5.1)) versus the surface temperature of dense and porous asphalt mixtures are shown in Fig. 5.3(a). In this Figure, it can be observed that the porous asphalt mixture heals faster than the dense mixture. Additionally, it can be observed that the maximum healing level of dense asphalt mixtures is lower than the maximum healing level of porous asphalt concrete, and that the healing of dense asphalt mixtures starts at a higher temperature than the healing of porous asphalt mixtures. The maximum healing level reached by porous and dense asphalt concrete was 78% and 51%, respectively.

Nevertheless, by only analysing the maximum temperature after the healing process, it is difficult to compare the healing performance of both porous and dense asphalt concrete mixtures. The reason for this is the different cooling rates of both mixtures. In order to solve this, the healing levels versus the τ parameters for dense and porous asphalt concrete are presented in Fig. 5.3(b). In this way, the effect of different air void contents in the cooling levels of asphalt concrete mixtures, as well as the temperature threshold of various types of bitumen can be neglected. Additionally, it is shown the fitting of the data to eq. (4.16). Furthermore the parameters for the fittings of porous and dense asphalt mixtures are given in Table 5.1.

Table 5.1 *Parameters for the porous and dense asphalt concrete fitting curves (eq. (4.16)).*

	C_H	D_h
Dense asphalt mixtures	0.521	$1.66\ 10^{-5}$
Porous asphalt mixtures	0.742	$1.62\ 10^{-5}$

Specimens from porous asphalt mixtures need less energy for healing than samples from dense mixtures. The reason for this is that higher energy is needed for reaching the healing temperature of bitumen in dense mixtures. In Table 5.1 suggests that the *D* parameters are constant for each type of asphalt mixture used. The reason of this is that the crack width was the same for both types of asphaltic materials. Moreover, the C_1 parameter is higher in the case of porous asphalt mixture, meaning that the maximum healing level in this case is approximately 50% higher than the maximum healing level in a dense asphalt mixture. Hence, the most critical parameter to obtain an asphalt concrete material with good self-healing properties is to use bitumen with a low healing temperature threshold.

In addition, the effect of a repetitive number of healing procedures after different crack formation has been analysed by multiple-healing tests. In Fig. 5.4 the percentage of test specimens that reach a certain healing level after a fixed heating time is shown. The same test specimens were broken and healed up to five times using the same healing time. The first remarkable fact is that the asphalt mixtures can be healed multiple times thanks to induction heating. Moreover, in the Figure it can be observed that the most frequent healing level obtained is between 0.2 and 0.4 in the case of dense asphalt concrete (Fig. 5.4(a)) and between 0.4 and 0.6 in the case of porous asphalt concrete (Fig. 5.4(b)). These values holds only for the range of temperatures analysed (see Fig. 5.3(a)) and would have increased if the heating times would have been longer.

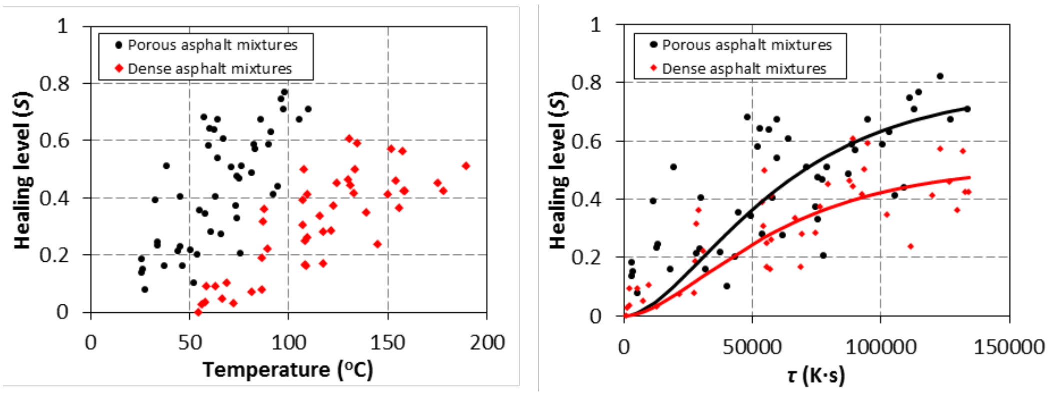

(a) (b)

***Fig. 5.3** (a) Healing levels versus the surface temperature of dense and porous asphalt mixtures, after the first healing treatment. (b) Healing levels versus the τ parameter, after the first healing treatment.*

Fig. 5.4 shows that the healing levels decreased gradually after each healing cycle. This is true for dense and porous asphalt concrete. In case of the dense asphalt concrete specimens, there is a clear reduction of the test specimens with a healing level between 0.4 and 1 and an increase in the number of specimens with healing levels between 0 and 0.4. In the case of porous asphalt concrete, it is very remarkable that after the fourth cycle, almost 50% of the test samples had a healing level between 0 and 0.2 and that there was also a gradual reduction of the specimens with healing level higher than 0.4.

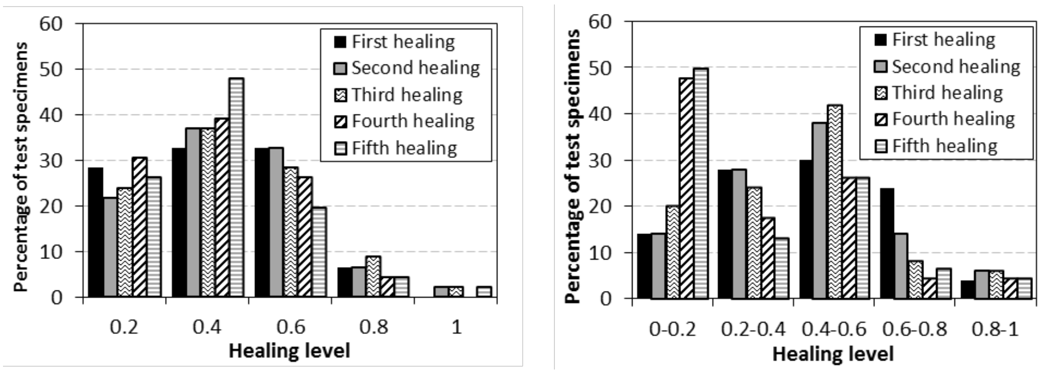

(a) (b)

Fig. 5.4 *Evolution of the healing levels with the number of healing cycles for (a) dense asphalt concrete test samples (b) porous asphalt concrete test samples [54].*

5.3 Effect of the bitumen properties. Rheological analysis

In the previous section, it was shown that different asphalt mixtures need different temperatures to be capable of self-healing. This phenomenon is directed related to the type of bitumen used in the mixture and its properties. It is widely known that bitumen can act like a Newtonian fluid at high temperatures. Nevertheless, it behaves viscoelastic and depends on temperature and time of loading [[55],[56]]. For this reason, the determination of the dynamic flow properties of the recovered bitumen was conducted by oscillatory frequency sweeps at constant strain in order to find out when the tested binder reaches a near-Newtonian flow behaviour.

Asphalt binder was recovered from the dense and porous mixtures by rotary evaporator in order to determine the temperature when Newtonian behaviour occurs. The rheological properties of bitumen were measured with a Physica MCR 301 dynamic shear rheometer in a configuration with 25 mm diameter parallel plates, with a 1 mm gap. Oscillatory frequency sweeps were carried out over a range of 0.001 Hz to 0.1Hz at temperatures from 30°C to 70°C under a constant strain of 0.1% within the linear viscoelastic region. The complex viscosity (η*) as a function of frequency (ω) at different temperatures was recorded automatically during the tests.

The effect of different frequency sweeps at various temperatures on the complex viscosity (η*) of the extracted bitumen from dense and porous asphalt mixtures is shown in Fig. 5.5(a) and Fig. 5.5(b), respectively. It can be seen that at the higher testing temperatures these bitumen present a near-Newtonian behaviour, where the complex viscosity is relativity independent of the applied shear frequency. In contrast, at lower temperatures, the complex viscosity decreases with increasing frequency, exhibiting shear-thinning behaviour (pseudoplasticity).

Additionally, in order to analyse the deviation of the bitumen behaviour from Newtonian, the rheological data were fitted through the following power law relationship [57]:

$$\eta^* = m \cdot |\omega|^{n-1} \tag{5.2}$$

where ω is the frequency and η* is the complex viscosity, with m and n denoting the fitting parameters. The dimensionless parameter n is also called the flow behaviour index. n = 1 corresponds to a Newtonian fluid and n < 1 reflects a higher degree of pseudoplastic properties of the fluid. As the transition from pseudoplastic to Newtonian behaviour is not clearly defined for bitumen in literature, in this study the bitumen properties were considered Newtonian when the flow behaviour index was higher than 0.9. The transition from 0.9 < n <1 is also known as near-Newtonian behaviour.

The flow behaviour indexes (n) obtained at different temperatures, for dense and porous asphalt mixtures, are plotted in Fig. 5.5(c) and Fig. 5.5(d), respectively. It follows that for both bitumen types studied, the flow behaviour index increased with increasing temperature, getting close to 1 (ideal Newtonian behaviour). Hence, it can be concluded that, the bitumen used in dense asphalt mixtures behaves like a near-Newtonian fluid at temperatures above 50°C, while the bitumen used in porous asphalt mixtures behaves like a near-Newtonian fluid at temperatures above 23°C. This means that porous asphalt concrete test samples will start healing at a lower temperature. These results verify the healing behaviour found in the previous section where dense mixtures needed higher temperatures to initiate the healing process as compared to the porous mixture.

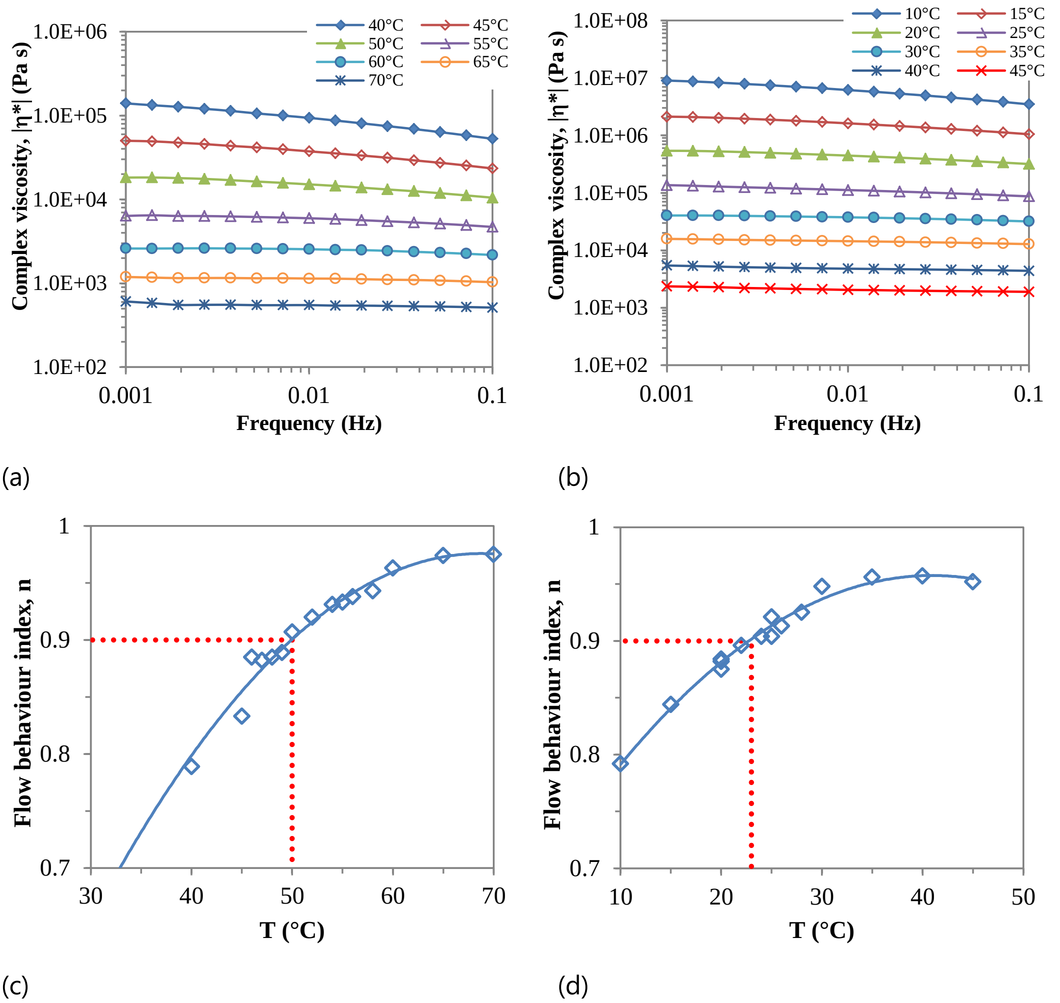

Fig. 5.5 (a) Complex viscosity (η^*) of recovered bitumen from dense asphalt mixture (test samples made in the laboratory) as a function of shear frequency; (b) Complex viscosity (η^*) of bitumen recovered from porous asphalt mixture (test samples obtained from the road) as a function of shear frequency; (c) flow behavior index (n) of bitumen from dense asphalt mixture at different temperatures; (d) flow behavior index (n) of bitumen from porous asphalt mixture at different temperatures.

5.4 Influence of the inductive heating in the aging state. Bituminous binder oxidation

In reference [58] it is stated that the properties of bitumen and its surface microstructure depend on the maximum temperature used and on the thermal history at which the binder is subjected. It is known that the maximum temperature reached by the binder and the total time at that temperature, plays a role on the ageing properties of bitumen [59]. This may have a strong influence on the macroscopic behaviour of bitumen [[60], [61]], which may see its healing properties reduced [62].

To analyse the effect of induction heating by electromagnetic fields on the ageing of bitumen, 10 g of bitumen 70/100 pen were distributed on steel plates of 10 x 20 cm^2 (Fig. 5.6(a)). The thickness of the bitumen film on the plates was about 200 µm. The test samples were divided in three sets of specimens: Set A, 10 specimens; Set B, 2 specimens and Set C, 5 specimens (see Table 5.2). Additionally, approximately 50 g of cast steel particles were spread over the bitumen film of the Set C test samples (*Fig. 5.6*(b)).

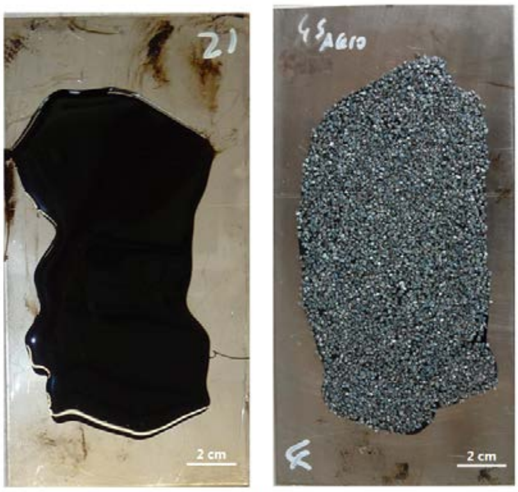

(a) (b)

Fig. 5.6 *(a) Steel plate with virgin bitumen 70/100 pen (b) Steel plate with virgin bitumen 70/100 pen and cast iron particles.*

To show the effect of induction heating on the ageing of bitumen, plates from Set A were heated under induction during 1s, 1.5s, 2s, 2.5s, 3s, 3.5s, 4s, 4.5s and 5s. The coil of the induction heating machine was at a distance of 5 cm from the plates. Additionally, one plate was not heated, as a reference.

Table 5.2 *Treatments of the test samples used for examining the ageing properties of bitumen under induction heating*

Type	Reference name	Number of test specimens	Temperature treatment
Bitumen on steel plates	Set A	10	Induction heating
	Set B	2	Induction heating
	Set C	5	Oven heating
Asphalt mixture	Set D	6	Oven heating
	Set E	5	Induction heating

The effect of cast steel particles under induction heating on the ageing of bitumen was evaluated by heating plates from Set B under induction during 2 and 4.5 s. The coil of the induction heating machine was at a distance of 5 cm from the plates. Moreover, plates from the Set C were heated in an air convection oven, at temperatures 60°C, 75°C, 95°C, 115°C and 150°C, during 90 minutes in order to study the influence of temperature on the ageing of bitumen.

After the different heating treatments, each analysed material was cooled down to room temperature (20 °C). In this way, the average value of the ξ constants for the steel plates was 0.00126 $m^{-2}s^{-1}$. Moreover, the average surface temperatures reached by the steel plates and by the surface of bitumen from Set A and B are shown in Table 5.3. An induction time of more than 5 s increased the temperature of the steel plate and bitumen above 200 °C and 60 °C, respectively. This phenomenon could damage the bitumen. Furthermore, the temperatures after 2 s and 4.5 s reached by the samples with steel particles (Set B) and bitumen samples (Set A) were similar. The average temperatures reached by the steel in the plates was 35 °C and 86 °C for the plates heated during 2 s and 4.5 s respectively. The average temperatures reached by the surface of bitumen was 31°C and 37°C for the plates heated during 2 and 4.5 s respectively. In this sense, it is difficult to determine the influence of the conductive material on the thermal history.

***Table 5.3** Average temperature reached by the bitumen and by the steel of the plates in the Set A and Set B.*

	Set A								Set B	
Time heating (s)	1.5	2	2.5	3	3.5	4	4.5	5	2	4.5
Temperature of the steel plate (°C)	39	36	43	40	54	55	88	210	35	86
Temperature of the bitumen surface (°C)	29	28	30	31	34	33	38	63	31	37

To determine the influence of induction heating on the ageing of bitumen, the bitumens were evaluated by analysing their flow behaviour at constant temperature. For this, the rheological properties were measured with a Physica MCR 301 dynamic shear rheometer in an 8 mm diameter parallel plate configuration with a 2 mm gap. Oscillatory frequency sweeps were carried out over a range of 0.001 Hz to 0.1 Hz at a reference temperature of 20°C under strain amplitude of 0.1% within the linear viscoelastic region. The complex viscosity (η^*) as a function of frequency (ω) was recorded automatically during the tests. Flow behaviour indexes were obtained from eq. (5.1).

In Fig. 5.7, the flow behaviour indexes (*n*) of the reference bitumen and of the bitumen in the test samples from set A, set B and set C are shown. Moreover, in order to normalize the indexes to a same scale, the τ parameter was selected as quantification of the energy involved in the heating and cooling phases. It can be observed that the *n* indexes from Set A were very similar to those of the reference bitumen. The average *n* index value of bitumen in the plates from Set A was 0.768, with standard deviation 0.0057, while the *n* index of the reference bitumen was 0.772. The average *n* index value of bitumen in the plates of Set B was 0.763.

The flow behaviour indexes of the bitumen in the test samples from Set C after the treatment are also shown. This figure shows that the *n* indexes of bitumen were constant until a certain value of τ in the range of 2.2 10^6 K·s to 2.6 10^6 K·s was reached. Until that moment, they had an average value of 0.756 and a standard deviation of 0.0011. These τ values correspond to maximum temperatures between 60 °C and 115 °C. Above these values, the *n* parameter decreased until its value was 0.689 at a τ level 2.8 10^6 K·s. This means that the flow capacity of bitumen as a Newtonian fluid was reduced during the long term treatment in the oven.

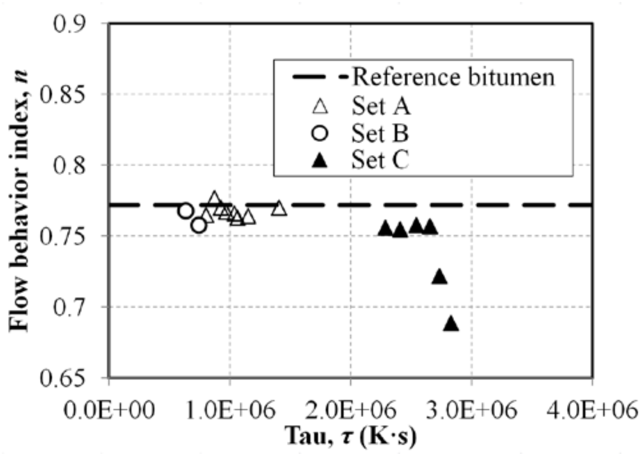

***Fig. 5.7** Flow behavior index for Set A, Set B and Set C.*

Furthermore, in order to characterize chemical changes in the bitumen as a result of oxidation one of the mechanisms associated to its ageing, Attenuated Total Reflectance Fourier Transform Infrared (ATR-FTIR) Spectroscopy was used. The measurements were performed at 23 °C in a Nicolet iS5 Fourier Transform Infrared Spectrometer in the Attenuated Total Reflectance (ATR) mode with a diamond crystal. ATR-FTIR measurements allow the identification of certain functional groups in bitumen. In the case of oxidation in bitumen, changes in the intensity of the spectral bands corresponding to carbonyl (C=O) and sulfoxide functional (S=O) groups are relevant. The carbonyl functional groups of different compounds such as carboxylic acids, esters, anhydrides, ketones and aldehydes are generally located in the region of the spectrum from 1650-1800 cm^{-1}. The sulfoxide functional group locates around 1030 cm^{-1}. The indexes $I_{C=O}$ and $I_{S=O}$ for carbonyl and sulfoxide functional groups, respectively, were considered using eq. (5.3) and eq. (5.4):

$$I_{C=O} = \frac{A_{C=O}}{A_{CH_2} + A_{CH_3}} \tag{5.3}$$

$$I_{S=O} = \frac{A_{S=O}}{A_{CH_2} + A_{CH_3}} \tag{5.4}$$

where A is the integrate band areas of the functional groups; in particular, of the peak corresponding to the carbonyl stretching vibration (peak centered around 1700 cm^{-1}), $A_{C=O}$, the sulfoxide stretching vibration (centered around 1030 cm^{-1}), $A_{S=O}$, and the peaks related to the asymmetric deformation vibration of CH_2 and CH_3 (around 1455 cm^{-1}) and to the symmetric deformation vibration (bending vibration) of CH_3 (around 1376 cm^{-1}), A_{CH2} and A_{CH3}. The limits of integration for the calculation of the areas under the bands were taken as the inflexion points of each side of the band. A_{CH2} and A_{CH3} were calculated together, i. e. the integration limits were 1500 cm^{-1} and 1325 cm^{-1}.

In this study, ATR-FTIR measurements were performed for the virgin bitumen used as reference, for bitumen placed on the steel plate under induction for 5 s from Set A, and for bitumen with steel particles under induction for 2 s and 4.5 s from Set B. The results are shown in Fig. 5.8. It can be seen that no significant difference between the virgin bitumen and the other two bitumen types was detected. The bands at 1577 cm^{-1} and 1540 cm^{-1} appearing for set B are coming from the cast steel particles.

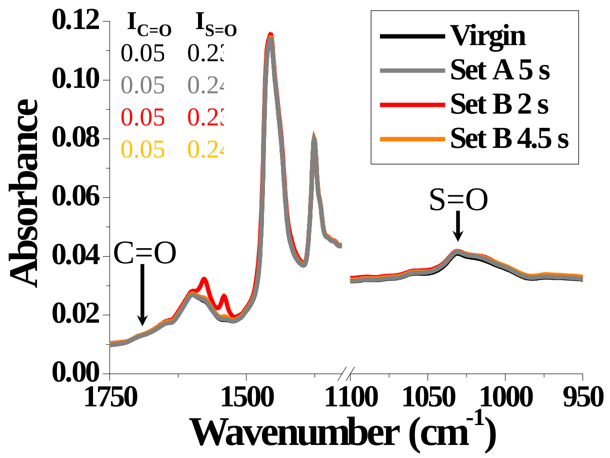

Fig. 5.8 *ATR-FTIR spectra for virgin bitumen, for bitumen placed on the steel plate under induction for 5 s from Set A, and for bitumen with steel particles under induction for 2 s and 4.5 s from Set B. The inset table shows the values calculated for $I_{C=O}$ and $I_{S=O}$.*

Additionally, ATR-FTIR measurements were performed in the bitumen exposed to the highest temperature from Set C to study its effect on the oxidation state. The ATR-FTIR spectra showed an increase of the $I_{C=O}$ (0.065) and $I_{S=O}$ (0.245) in comparison with the virgin bitumen ($I_{C=O}$ = 0.054 and $I_{S=O}$ = 0.237).

From the results from the ATR-FTIR measurements and from the rheological characterization, it can be stated that above a certain time at a high temperature, bitumen ages by oxidation. In addition, data obtained from bitumen from Set A and Set B showed that bitumen is not affected by the electromagnetic field during induction heating. Based on these results, it can be concluded that the only factors that may affect bitumen ageing during the induction heating process are the high temperatures reached by the bitumen.

Furthermore, a parallel study was focused on the analysis of the ageing of bitumen in dense asphalt mixtures and the effect of induction heating. For that, 11 cylindrical Marshall test specimens were compacted from an asphalt mixture containing 6% by volume of cast steel particles. The specimens were divided in two sets: Set D, 6 specimens and Set E, 5 specimens (see Table 5.2).

To analyse the effect of oven heating on dense asphalt concrete, the Marshall test specimens from Set D were heated in the forced air convection oven at 200 °C, during 5 min, 10 min, 15 min, 20 min, 25 min and 30 min. Moreover, to evaluate the induction heating effect on the properties of bitumen in a real mixture, the Marshall test specimens from Set E were heated under induction in a temperature controlled mode until they reached 80 °C, 120°C, 160 °C, 180 °C and 200 °C, respectively. The coil was placed at 3 cm from the surface of the test specimens. Again, one test specimen was not heated, as a reference.

In this study, the average value of the ξ constants for the mixtures studied (Set D and Set E) was 0.000436 $m^{-2}s^{-1}$. Besides, the average surface temperatures reached by the test specimens in the oven (Set D) during 5 min, 10 min, 15 min, 20 min, 25 min and 75.0°C, 95.2 °C, 112.3 °C, 126.5 °C, 136.5 °C, 140.8 °C, respectively. These temperatures were similar to those reached after induction heating (Set E).

With the purpose of examining the effect of high oven temperatures on the ageing behaviour of bitumen in asphalt concrete, Fig. 5.9 shows the flow behaviour indexes of the bitumen extracted from the reference Marshall test specimens and from the Marshall test specimens from Set D and E. The *n* index value of bitumen extracted from the Marshall test specimen without heating (reference extracted bitumen) was 0.845. This value is higher than the values shown in Fig. 5.7 for Set A, B and C due to the presence of toluene from the extraction procedure in the bitumen (detected in the ATR-FTIR measurements). The average *n* index value of bitumen extracted from test samples from Set D was 0.844 with a standard deviation 0.0068.

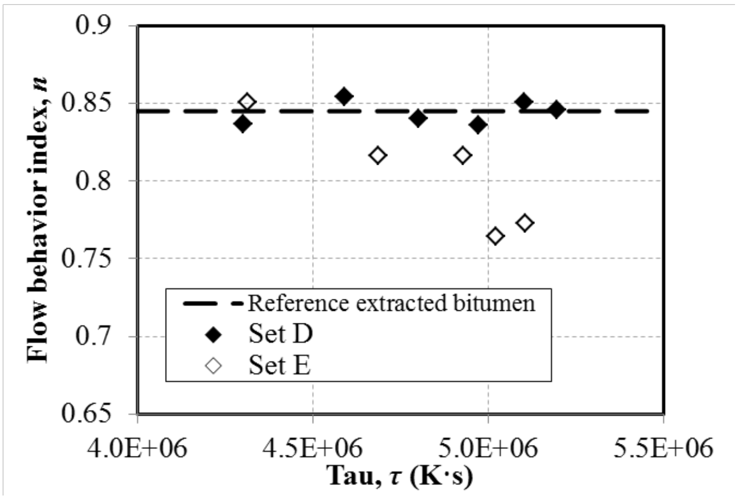

Fig. 5.9 *Flow behavior index for Set D and Set E.*

It can be also observed that the bitumen flow capacity was clearly affected by induction heating. While at low values of the τ parameter, the *n* index was very similar to that of the reference extracted bitumen (0.845), when the τ parameter increases to more than 5.0

10^6 K·s, the *n* index decreased down to 0.765. In addition, in the case of test specimens heated in the oven, for the same range of τ values, they did not show any change in the flow properties. This is a clear indication of the existence of some kind of damage to bitumen during induction heating when reaching a certain temperature or heat energy.

Following the same procedure previously explained, ATR-FTIR measurements were also performed on samples from the bitumen extracted from set D heated at 160 °C, from Set E heated during 30 min as well as from a test specimen without any heating treatment. The bitumen extracted without any treatment ($I_{C=O}$ = 0.050 and $I_{S=O}$ = 0.254) and the extracted bitumen from Set D ($I_{C=O}$ = 0.047 and $I_{S=O}$ = 0.240) did not show any significant difference in comparison to the virgin bitumen ($I_{C=O}$ = 0.054 and $I_{S=O}$ = 0.237). Nevertheless, the spectra for bitumen extracted from the Marshall test specimen exposed to induction until it reached 160 °C (Set E) showed that this bitumen presented the highest values for $I_{C=O}$ (0.082) and $I_{S=O}$ (0.288) in comparison to all the other measured bitumen samples. This fact corroborates the behaviour observed in the analysis of the flow behaviour.

Finally, to normalize the results a comparison between the τ values and the maximum temperatures reached by all the test samples and specimens is shown in Fig. 5.10. A clear difference can be observed between the asphalt mixture specimens (Set D and Set E) and the bitumen samples (Set A, Set B and Set C) due to their different sizes and compositions. It is important to remark that higher values of τ could not be reached during induction heating of the test samples in Set A, Set B and Set C, because of the high temperatures reached in the steel plates.

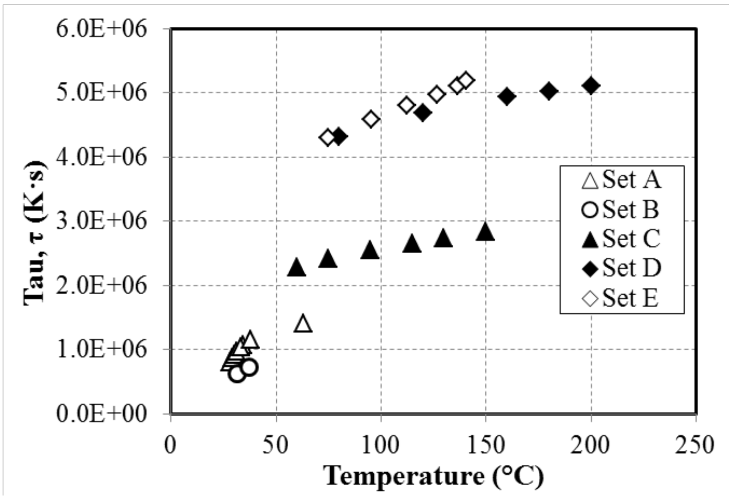

Fig. 5.10 *Maximum temperature reached by the test samples versus τ parameter.*

From the results presented in the previous analyses, it can be stated that the ageing level of bitumen was not affected by the alternating electromagnetic field applied during induction heating or by the eddy currents in the steel particles or in the steel plates. Nevertheless, some level of ageing was observed mainly due to the high temperatures reached during the heating processes.

In order to discern the effect of hot metallic particles in contact with bitumen, steel spherical particles (diameter = 10 mm) were embedded in a sample of bitumen in a glass plate were carefully heated by induction. The temperature evolution was monitored locally with the infrared camera to show the heat diffusion phenomenon after induction heating from a conductive material to the bitumen (Fig. 5.11). Obviously, when bitumen containing electrically conductive particles was subjected to induction heating, the particles increased their temperature very fast, while bitumen was not heated (Fig. 5.11(a)). The particles reached more than 200 °C in 20 s. After and during induction heating, the heat was transmitted by conduction from the particles to the bitumen (Fig. 5.11(b)); thus the temperature of bitumen increased and the temperature of the particles decreased. In previous studies, it has been found that the temperature of bitumen is homogenous in the surface of the Marshall test specimens when they are subjected to induction heating, but the fact is that aggregates, bitumen and steel particles increase their temperature at different rates [12]. For this reason, bitumen around the steel particles can be aged if the time induction heating is prolonged and, consequently, high temperatures are reached leading to an overheating effect.

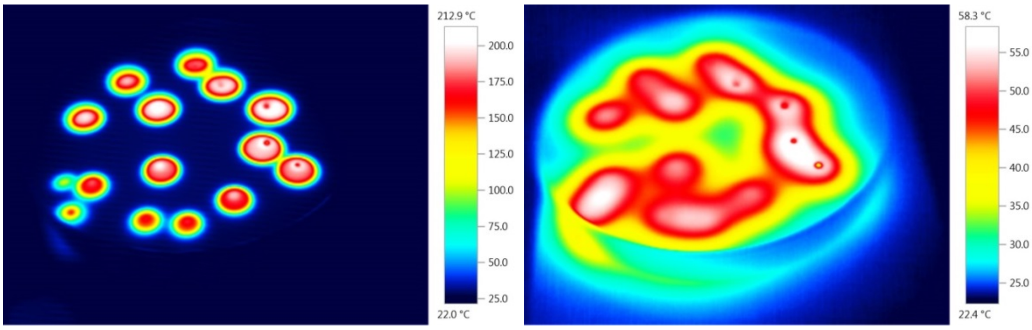

(a) (b)

Fig. 5.11 *Thermographic images of steel particles in bitumen, exposed during 20 s to induction heating, (a) 5 seconds cooling after induction heating. (b) 215 seconds cooling after induction heating.*

6 Inductive healing of asphalt mixtures modified with steel and iron particles

The practical limitations of the induction heating for healing asphalt concrete concerning type of damage are studied in this section. Hence, asphalt mixtures modified with cast steel or cast iron particles were prepared in order to evaluate the influence of fatigue damage and longitudinal cracking on the healing behaviour. In addition, the feasibility of the healing process at a larger scale by reproducing the effect of real traffic on the deterioration of a pavement is shown. For this last phase, the model mobile load simulator (MMLS3) was used to assess the mechanical performance of asphalt slabs as well as the recovery of their properties after healing process by induction heating.

6.1 Inductive healing of fatigue damage

The aim of this analysis was to have a first insight of when and for how long asphalt mixtures under fatigue damage have to be induction-heated to recover part of their original properties. With this purpose, indirect tensile fatigue tests were used for damaging the test specimens. Then, damaged test samples were healed by induction heating during different times. The healing recovery was defined as the relationship between the increase of the number of cycles resisted by the test samples after healing and the number of cycles resisted by unheated test samples. Finally, damage and healing recovery were observed by means of computed tomography scans.

For this study, Marshall test samples were compacted from an asphalt mixture AC8 with 6% weight of mixture of bitumen 70/100 and modified with 19.4 %wt. of mixture of cast steel particles (size between 0.6 mm and 1.4 mm).

To define the maximum load and temperature to be applied in the Indirect Tensile Fatigue (ITF) tests, different test temperatures (5 °C, 10 °C, 15 °C and 20 °C) were checked. The measurements were taken from 12 test specimens, 3 for each temperature analysed. The equipment used to measure the resistance was a Universal Testing Machine (UVP) of maximum load 150 kN. The indirect tensile strength of the specimen was determined by applying a load at a rate of 10 mm/min. The ultimate tensile strength of the test samples was 23.25 kN, 19.43 kN, 13.15 kN and 10.32 kN, respectively, for each one of the temperatures studied. Based on these results, the temperature of the ITF tests was defined as 10 °C and the maximum load applied at each cycle was 7 kN, which is approximately 35% of the ultimate tensile strength of the test samples. In addition, the minimum load was 0.32 kN. The equipment used was a Wille uniaxial compression/tension testing machine, with a maximum load application of 10 kN. The test frequency was 10 Hz. The breaking of the test samples was defined as the moment when the cylinder displacement was 2 cm.

To evaluate asphalt mixture self-healing, 8 groups of 10 test specimens were first damaged by means of ITF tests which were stopped after 1000, 1600, 2826, 3090, 3355, 3619, 3884 and 5838 cycles for each group of specimens. Later, each test sample was introduced in a box filled with sand (Fig. 6.1), and they were let to rest for 1 h at 20 °C. This was done to avoid deformations during induction heating. After this, every group of test specimens was induction heated during 20 s, which corresponds to a surface temperature of 80 °C, and then, they were let to rest during 3 h at room temperature, each test sample in one sandbox. Finally, the test specimens were extracted from the sandbox and introduced in a climatic chamber at 10 °C during 3 h prior to testing until failure.

Fig. 6.1 *Sample in a sandbox for induction healing.*

In this study, the healing level of Marshall test specimens (Healing index: HI) after a number of cycles (N_P) was defined as the relationship between the increase of the number of cycles after healing and the number of cycles for having a 50% probability of breaking the test samples before healing ($N_{0.5}$) [63]:

$$HI = \frac{N_p - N_{0.5}}{N_{0.5}} \tag{6.1}$$

In Fig. 6.2, the average values of healing index of asphalt test samples after heating process versus the number of fatigue cycles is shown. It can be observed that there is a certain number of cycles when the damage level is so high that the test samples cannot be healed any more. In this study, with these test parameters and for this modified asphalt mixture, the number of cycles is 2826 (critical moment for healing) reaching a maximum healing level of 31%. When this number of cycles is surpassed, induction-heating does not repair the mixture and it can even damage the material further.

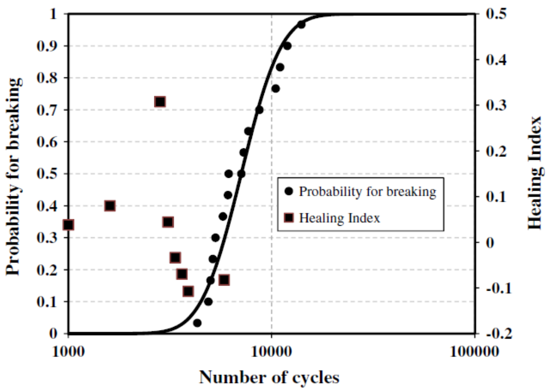

Fig. 6.2 *Number of cycles versus healing recovery and probability for breaking versus number of cycles [63].*

It can be said that every time a loading of an asphalt mixture is repeated, small defects appear. These can be permanent deformations, caused, for example, by the development of microcracks [64]. These grow with applied load cycles, until they percolate and the test specimen breaks [65]. This means that a minimum number of load cycles has to be applied before the probability of the test specimens for breaking reaches a significant value. As an example, in Fig. 6.2, the probability distribution for breaking a test specimen has been presented versus the healing levels of an asphalt mixture. The distribution has been done using a lognormal distribution. In this figure, it can be seen that at 3941 fatigue cycles the probability for the specimens to break is 5%. At 7092 fatigue cycles the probability for the specimens to break is 50% and at 12780 fatigue cycles the test specimens have 95% probability to break. In addition, the number of cycles at which the healing recovery is a maximum corresponds to a probability for breaking of 0.5%.

In previous works [52], it is explained that the self-healing of cracks in asphalt mixtures can occur only when the crack width is below a certain size. It can be argued that there is a critical point when the cracks width increase very fast and induction-healing cannot be applied any more, as it can clearly be seen in Fig. 6.2. On the other hand, every crack has a different width. This means that at the optimum moment for healing there may be cracks which are too wide for healing. Note also that the probability for breaking the test sample at this moment is only 0.5%, which means that asphalt mixture test specimens may still survive during a significant number of cycles after the catastrophic failure. Besides, the use of induction heating to repair asphalt mixtures after the critical moment for healing leads to further damage of the test specimens. This phenomenon has been observed before in [35], where it is explained that bitumen above the healing temperature starts flowing through the cracks even after the healing, which reduces the structural performance of the mixture.

Additionally, following the same fatigue damage processes, 9 groups of 10 specimens each were tested under ITF until 2826 cycles and heated during 0 s, 5 s, 7.5 s, 10 s, 15 s, 17.5 s, 20 s, 22.5 s and 25 s in order to evaluate the influence of the heating time and temperature on the healing performance. After this, each test sample was let to cool down during 3 h at room temperature. Finally, the test specimens were extracted from the sandbox, introduced in a climatic chamber at 10 °C during 3 h and tested until failure.

In Fig. 6.3, the healing index of asphalt test specimens, after 2826 loading cycles and applying induction heating for fixed periods of time is shown. In this figure it can be seen that without induction heating, the natural healing of asphalt mixture test samples reaches 11%. Additionally, after 8 s heating, equivalent to 55 °C, approximately 30% of healing recovery is reached. This is the maximum level of healing that can be reached in these mixtures. If induction heating is applied longer, the healing level of asphalt test specimens decreases. However, the reason for this behaviour is unclear. As a conclusion, it can be said that, for the type of mixture and damage studied, there is an optimum heating temperature, 55 °C, above which asphalt mixture should not be heated.

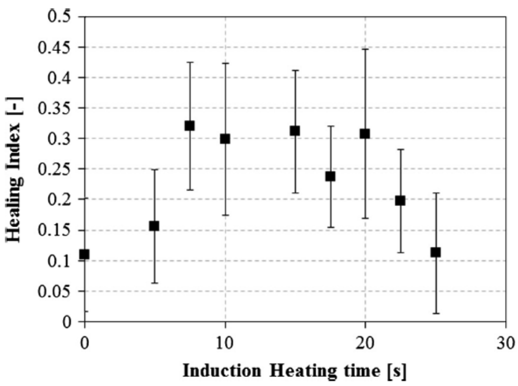

Fig. 6.3 *Influence of the time on the healing level.*

The study of the accumulated and recovered damage before and after healing was also conducted by analysing the energy loss during the fatigue tests. Energy loss is defined as the dissipated energy per load cycle in any repeated or dynamic tests. The dissipated or loss energy approach is a technique that provides a consistent indication of the level of deterioration in the specimen in terms of behaviour or remaining life. For its calculation, the hysteresis loop of the repeated loading cycles is considered by using the obtained force and displacement values. The area between the loading and the unloading part of curve represent the energy lost during a cycle. This energy loss can be interpreted as the viscoelastic energy absorbed by the specimen.

As example, the evolution of energy loss obtained from the fatigue tests of a specimen before and after the healing process is shown in Fig. 6.4. It can be seen that the curve increases constantly until a sudden change of behaviour related to the total failure of the specimen (ca. 8000 cycles). Further, a peak is found in the curve during the first loading cycles after the healing. The curve evolves to the previous trend (before healing) after a number of cycles. The peak effect appeared in most of the curves analysed but, sometimes the energy loss values after healing were lower than those before the process. Taking into account that the healing is based on the flowing of the bitumen into the cracks formed by the damaged, this peak could be related to the new bonds created after healing. These changes are explained by the requirement of more or less energy to continue with the accumulation of damage.

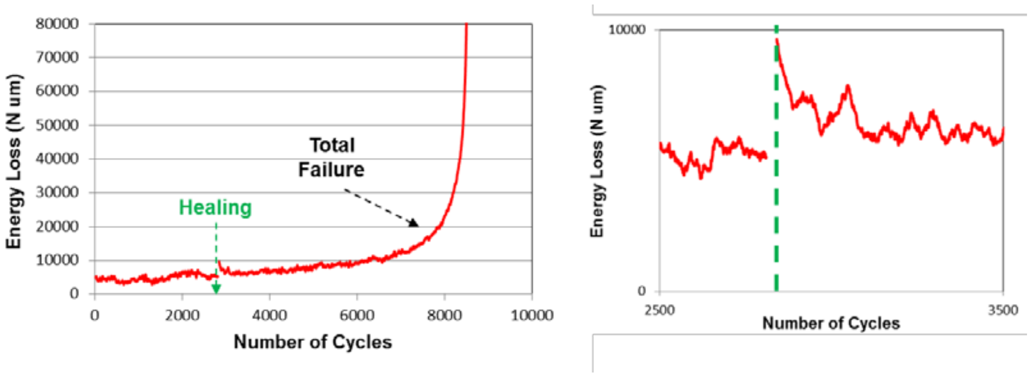

(a) (b)

Fig. 6.4 *Energy loss evolution with number of loading cycles in asphalt mixture test specimens before and after healing (a). Detail of the peak after healing (b).*

Moreover, in order to observe the self-healing of asphalt mixtures, X-ray tomography on different specimens was employed. For that, two representative damaged Marshall test specimens subject to 2826 cycles, before and after 10 s induction-heating were selected. The X-ray source was operated with an acceleration voltage of 450 kV and a current of 1.55 mA. The specimen was mounted on a rotational table in 11.8 mm distance from the X-ray source at a 0.4 mm nominal focal spot size. The distance between the X-ray source and the detector was 1499.75 mm. The pixel size obtained was 101.1 μm.

Finally, reconstructions of the microstructure were prepared by segmenting the materials found in a specific volume, based on simple threshold. With this method, aggregates, bitumen and air voids could be readily separated. The CT Scan images of asphalt mixture test specimens before and after healing are shown in Fig. 6.5. To represent the healing process, the air voids with a volume above 3 mm^3 have been highlighted. It was observed that before healing, these air voids account for 3755.36 mm^3 in the mixture being reduced to 1882.11 mm^3 after the healing process. This reduction in the porosity of the test specimens could be associated to an additional flow phenomenon where the bitumen closes some air voids. As it can be seen in the images, this fact could change the internal structure of the specimen.

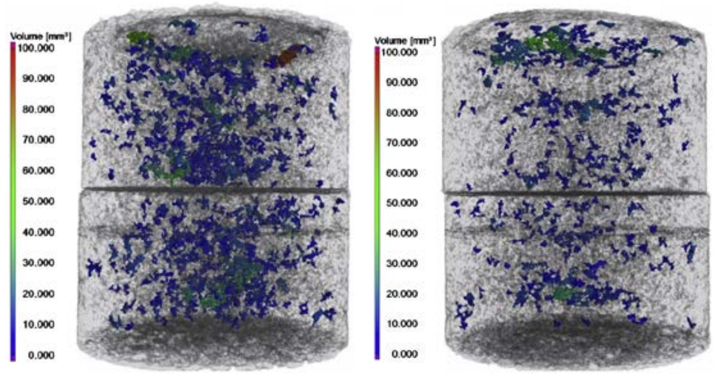

(a) (b)

Fig. 6.5 *Air voids in asphalt mixture test specimens before (a) and after healing (b).*

As main conclusion of this study, it can be remarked that induction healing can only heal cracks of a certain width. If fatigue damage is too high, cracks are too wide to be repaired via induction heating: hence, there is an optimum moment for healing cracks in asphalt mixture depending on the properties of the asphalt mixture.

6.2 Inductive healing of propagated cracks by double torsion test

In order to check the limits of the induction heating concept for healing purposes and for defining the maximum size of a crack that can be sealed without affecting the internal structure of the pavement, a special experimental study was carried out. This information could help to define future treatments in conventional roads for designing prevention plans where the application of this innovative technique should be carried out before cracks cannot be healed.

The double-torsion test was applied in order to simulate a realistic performance of an asphalt pavement considering the longitudinal cracking by repeated traffic wheel loads [66]. In this case, different series of tests were carried out to analyse the mechanical properties of different designs of asphalt mixtures with cast iron particles (before and after the healing treatment) controlling also the creation and propagation of a longitudinal cracks. To get the specimen geometry for double-torsion fracture tests, specimens were cut from asphalt slabs compacted by French roller compactor. The thickness of 20 mm was chosen because the double-torsion fracture test concept was based on the thin plat theory where specimens should have enough thickness, more than three times the maximum aggregate size (in this case 4 mm), to reduce the aggregate dependency on test results. Beam length of 300 mm, twice the width (150 mm) and more than six times the thickness, was chosen to produce reasonable bending conditions within the size limitation of the temperature chamber. Moreover, a notch 30 mm length and 3 mm width were used as stress concentration point for the crack initiation and a rectangular guide groove was made on the bottom surface of the specimen in order to control the propagation path of the crack. Asphalt specimens were placed on simple supported bars inside a temperature chamber under the mechanical loading frame and two round-shaped point loading pins with 10 mm diameters applied on the top of specimens with 1 mm/min monotonic loading speed. Mechanical loading was applied and monitored at low temperature using a 10 kN load cell. The loading was controlled by the crosshead movement.

As in previous studies, to analyse the influence of the healing treatment via induction heating, double torsion tests before and after damaging and healing were accomplished. This kind of double torsion test allows controlling the creation of a longitudinal crack in order to simulate a more realistic fracture distress. The initiation and propagation of the crack can be controlled by applying a constant load displacement over a notched specimen of defined dimensions at low temperature (Fig. 6.6). After some preliminary tests, the development of the crack can be monitored by the strength-displacement curve. In this way, the damage level of the specimen can be defined for a posterior healing treatment. The analysis of performances for different crack sizes after the healing process (up to healing temperature of the bitumen) allows describing the effect of the crack on the recovering level. At this point, it is also important to remark the influence of the natural healing on recovering to avoid any confusion in the interpretation of the induction heating effect.

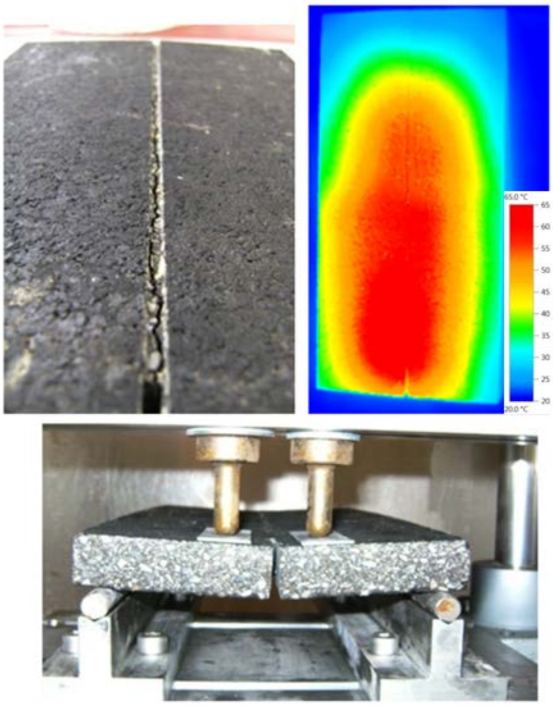

***Fig. 6.6** Details of the double torsion test (bottom) and the crack propagation (left) and thermographic images of the healing process (right) (see dimensions in Fig. 2.2).*

For this analysis the healing level was defined as the relation between the maximum forces reached before ($F_{max}(before)$) and after ($F_{max}(after)$) healing:

$$Healinglevel = \frac{F_{\max}(after)}{F_{\max}(before)} \cdot 100 \tag{6.2}$$

In addition, different characteristic parameters can be calculated from the strength-displacement curve (Fig. 6.7). Initial stiffness as well as deformation and work carried out until maximum force could define the mechanical behaviour before and after the healing process.

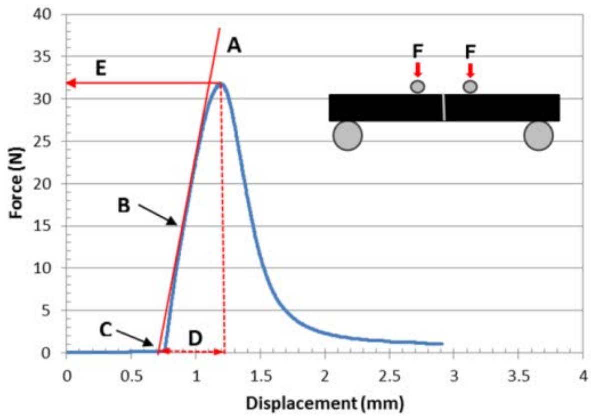

Fig. 6.7 *Displacement curve from a double torsion test. (A) Tangent at the (B) inflection point of the force versus displacement curve, (C) zero point and (D) displacement at (E) maximum force.*

Two set of specimens were evaluated during this study. Dense asphalt mixtures AC4 with 8% bitumen 70/100 (set A) and with 6% bitumen 35/50 (set B) were modified with 20 % wt. of cast iron particles (0.6-1.0 mm). Healing levels obtained after assessing the recovered performance are shown in Fig. 6.8. Some of the specimens were not subjected to induction healing but were kept at room temperature in order to analyse the effect of the natural healing in the mechanical properties. It can be seen that healing levels over 85% were reached by both kinds of mixtures. This means that part of the strength could be recovered after the formation of a crack by tension from bending. Moreover, the influence of the type and percentage of bitumen is clearly seen by comparing the results from the natural healing treatment. Specimens from set A got similar healing levels because the softness of the bitumen 70/100 which has an effect on the type of originated crack as well as eases the natural healing. However, analysing the results from Set B with less amount of harder bitumen, it can be seen that the healing by induction heating improved the performance after damaging.

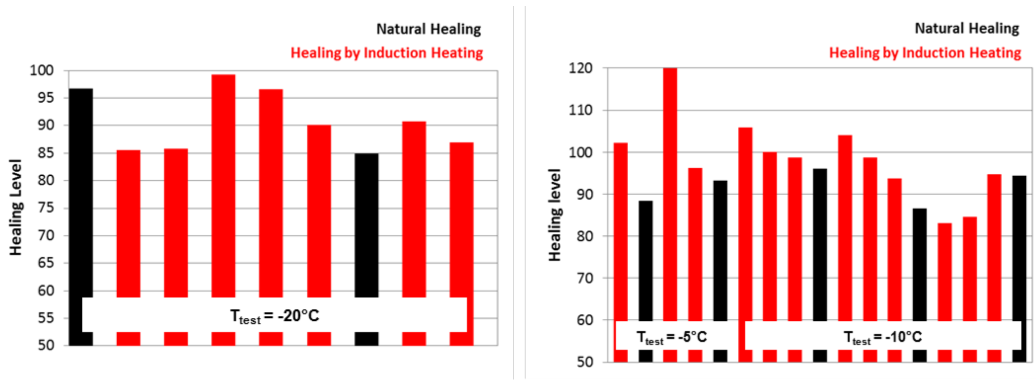

(a) (b)

Fig. 6.8 *Healing levels obtained for test specimens from set A (a) and from set B (b).*

The influence of the bitumen on deformation at maximum force before and after the healing process is shown in Fig. 6.9. Similar displacements were obtained for specimens from Set A with a slight reduction during the second evaluation after healing. However, a different behaviour could be observed in the Set B, where the deformations are larger after the healing process. This effect would be related to any change in the properties of the harder bitumen after the thermal treatment.

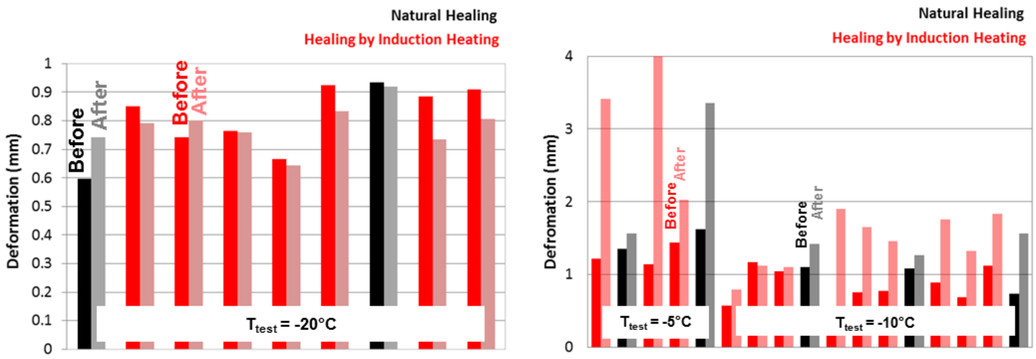

(a) (b)

Fig. 6.9 *Deformation after maximum load during the test obtained for test specimens from set A (a) and from set B (b) before (dark colour) and after (light colour) healing process.*

In addition, the initial stiffness at test temperature is presented in Fig. 6.10. It seems clear that the initial is lower at higher test temperature and that this parameter usually decreased after the natural and induction healing.

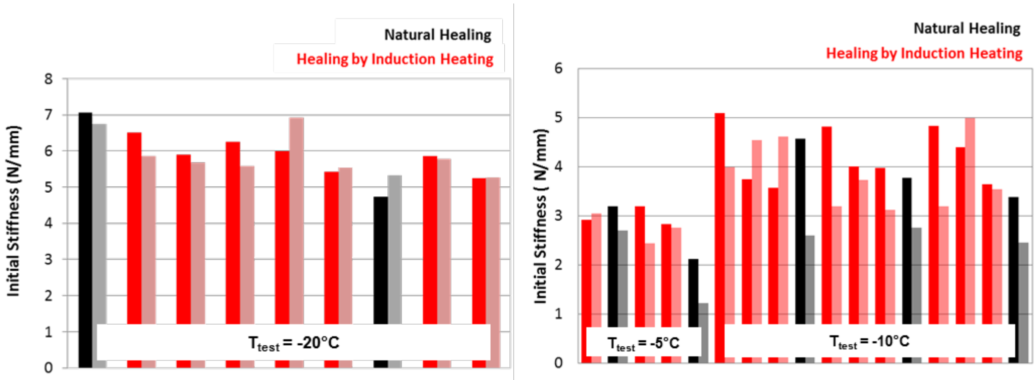

(a) (b)

Fig. 6.10 *Initial stiffness obtained for test specimens from set A (a) and from set B (b) before (dark colour) and after (light colour) healing process.*

In Fig. 6.11, other characteristic parameter such as the work carried out to reach the maximum force, can be analysed. Similar to the tendency observed with the deformation, it was found that the work kept constant or decreased after the healing process for the specimens within the Set A whereas this parameter used to increase for the specimens from the Set B.

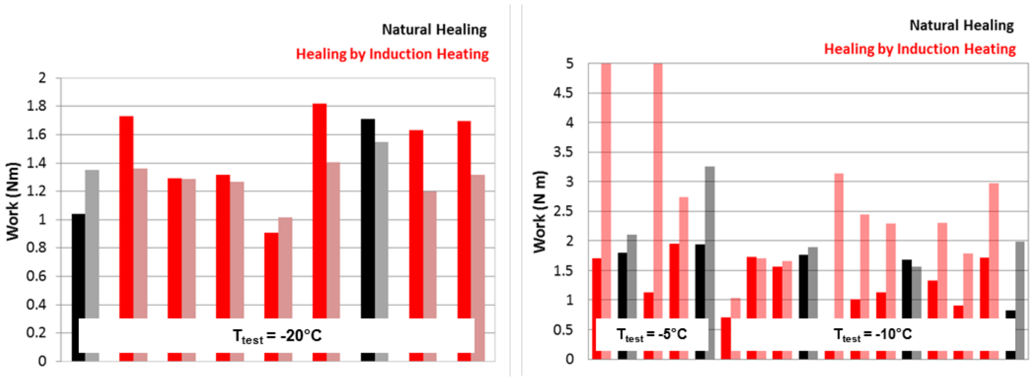

(a) (b)

Fig. 6.11 *Work until maximum load during the test obtained for test specimens from set A (a) and from set B (b) before (dark colour) and after (light colour) healing process.*

From this analysis it could be concluded that it is possible to heal a cracking damage by induction heating before its propagation. However, it was not clear how the natural healing influenced the recovery of the mechanical properties in asphalt mixtures with soft bitumen (Set A).

6.3 Mechanical performance recovering by induction healing in asphalt slabs

The last phase of the research project was used to evaluate the practical limits of the experimental concept in a larger scale. This study involved a series of experiments focused on the recovering of the mechanical performance of asphalt slabs after controlled damage with the Model Mobile Load Simulator (MMLS3) using healing with induction heating.

Four slabs (1800 mm x 435 mm x 40 mm) were compacted from a reference AC8 dense asphalt mixture with 5.9%wt. of bitumen 50/70 (softening point: 65°C) and a maximum mineral aggregate size of 8 mm. Moreover, cast iron particles (7400 kg/m^3) of 0.6-1 mm diameter were added (14% wt.) to the mixture in order to ease the heating process via induced electromagnetic fields. In addition, two rectangular grooves of 10 mm deep by 5 mm wide were cut along the bottom surface of each slab. These grooves were used as stress concentration points for crack initiation during the test and in order to control the propagation path of the cracks. Details of the specimen geometry can be found in Fig. 2.3

The healing capacity of the asphalt slabs was evaluated following a three-phase test procedure, which involved the mechanical loading of the slabs and the healing phase followed by a new loading phase. More precisely, the three phases were:

- **Pre-damaging phase**: Mechanical loading tests with the Model Mobile Load Simulator (MMLS3) were carried out on asphalt specimens until partial damage.
- **Healing phase**: The damaged specimens were healed by means of induction heating.
- **Validating phase**: A second set of mechanical loading was applied on healed specimens in order to validate the strength recovery after the healing process

The aim of the test was to induce the formation and propagation of fatigue cracks in the slabs due to repetitive loading of rolling tires, which simulate the effect of real traffic on the deterioration of a pavement. This step presents an upscaling of the laboratory tests carried out on small specimens. On the one hand, the fabrication of slabs is closer to reality than the production of specimens with Marshall procedures. On the other hand, the effect of rolling tires on the slabs produces stresses and strains that are similar to those produced in real pavements. In order to upscale the healing concept to a real scenario, the model mobile load simulator MMLS3 was used as a so-called third-scale load accelerated pavement testing system (Fig. 6.12) [67].

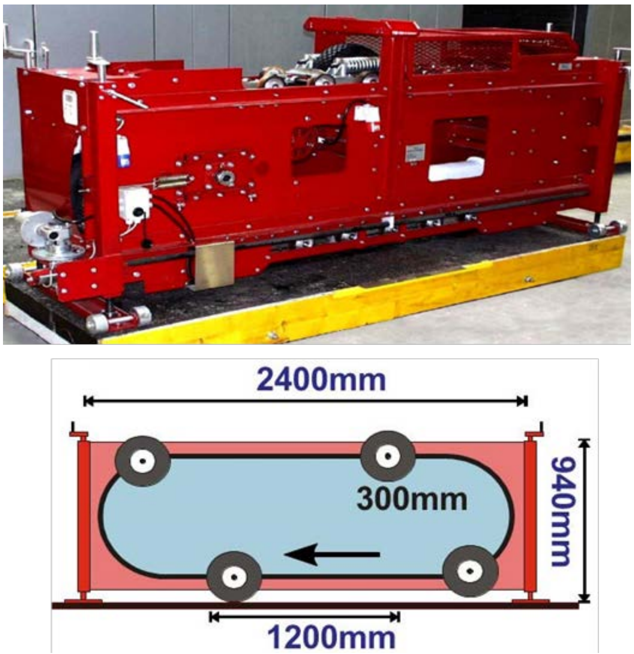

Fig. 6.12 *Model Mobile Load Simulator MMLS3.*

The MMLS3 is a valuable trafficking tool for studies of rutting and pavement surface distress. The system applies a downscaled load with four single pneumatic tires which are smaller than standard automobile tires, having a diameter of 0.3 m and a width of 0.11 m. The machine is 2.4m long by 0.6 m wide and 1.2 m high. Each tire loads the pavement width over a path length of 1.2 m up to 2.1 kN through a spring suspension system. At a maximum speed of 9 km/h, the MMLS3 allows approximately 7200 load applications per hour, corresponding to approximately a 2 Hz loading frequency.

The 1.8 m long asphalt slabs were placed such that the loading direction was perpendicular to the grooves. The slabs were positioned under the MMLS3 on two transversal supports, so that the rolling tires can produce bending stresses on the bottom. The distance between the supports was 1450 mm. In order to simulate the supportive effect of the subgrade produced on the asphalt layers and to buffer the total bending of the slabs when loaded, a 14 mm thick rubber mat was placed bellow the slab. The whole system was placed on top of a rigid wood plate. Details of this experimental setup can be observed in Fig. 6.13.

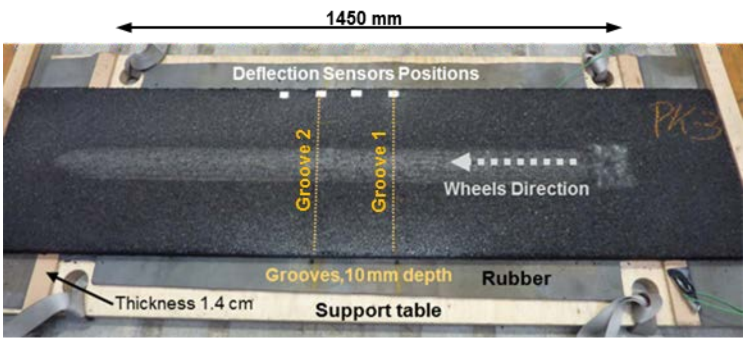

Fig. 6.13 *Detail of the asphalt slab (after loading) in the experimental setup.*

It was expected that the strength resistance of the slabs would decrease due to the progression of the damage (micro-cracking) caused by the MMLS3 loading. This strength reduction usually leads to an increase on the vertical bending deformation. Therefore, a number of deflection sensors were installed in four different positions over the surface in order to monitor the development of the damaging (Fig. 6.14). Measurements of the deflection of the slab were recorded every 30 seconds. Then, the average deflection during 10 seconds was calculated and associated to the number of wheel passing at which the file was recorded.

Fig. 6.14 *Detail of the vertical deformation sensors.*

The temperature evolution in the surface of the test specimens was measured with a 640 x 480 pixels, full colour infrared camera. Besides, different thermocouples were used to monitor the air temperature as well as the temperatures inside (20 mm depth) and on the bottom side of the specimen. The pre-damage and validation phase were carried out under temperature controlled operation inside a climate chamber. The air temperature during the damage and validation process was kept between 18-20 °C.

The induction heating experiments were performed with the 30 kW induction heating generator at a maximum frequency of 80 kHz. Healing temperature was also controlled using the infrared camera. This temperature depends on the bitumen type. In this case, the temperature needed for achieving the healing was 80°C. The heating area was only focused around the grooves where the concentration of the damage and initiation of microcracks were expected.

Four experimental tests were conducted in order to assess the healing performance for the asphalt slabs. As explained in the previous section, the healing treatment must be applied during the first phase of the loading when the stress is concentrated for the initiation of microcracks. Then, the healing treatment allows these microcracks to be promptly closed avoiding their propagation. However, repetitive loading can lead to the formation of larger cracks which cannot be healed. In this later case, the efficiency of the healing process would not be optimal and the recovering of the mechanical performance would not be significant. In this work, the number of cycles of wheel passings during the pre-damage phase was previously set for a conservative criterion (15000 cycles for Slab A) or based on the variation of the initial stiffness as a benchmark of the presence of damage while running the test (Slab B, Slab C and Slab D). Fig. 6.15 shows an example of the evolution of the vertical deformation and the temperature inside the slab during the different experimental phases. For the sake of simplicity, only the information related to the deflection sensor over the groove number one is presented because it is where the damage starts earlier during the loading phase. In this case, the healing treatment was carried out after approximately 40000 loading cycles. During the testing, the temperature in the slabs increased by about 5°C due to the continuous friction induced by the wheel over the surface. It can also be observed that the amplitude deformation increase with the number of loading cycles what means a reduction of the strength resistance.

In the Fig. 6.15 the analysis of the effect of the healing process in the performance shows that the vertical deformation after this heating treatment was similar to that obtained when the asphalt slab was still new and unloaded, at the beginning of the test. As in the study of the energy loss during the fatigue tests shown in the previous analysis (Fig. 6.4), this fact could be taken as a proof of the recovering of the initial stiffness of the slab. However, it is possible that the effect of the temperature on the deformation influences significantly and the deformation is related to the softening process of bitumen at higher temperature. For this reason, the evaluation of the capacity of the healing process was focused on the variation of the slope of the curve throughout the different phases. Following this criteria, different phases could be clearly distinguished. During the first phase, the vertical amplitude increases constantly with the number of loading cycles until the accumulated damage leads to a crack initiation which is linked to a sudden increase on the slope (ca. 35000 cycles). After the healing process, the slope decreased compared to the previous phase and showed a value similar to the first damage phase. This performance recovery can be taken as a clear indication of the healing effect. After approximately 12000 loading cycles more (at total ca. 52000 cycles), the slope increased again leading to a new phase where the cracks were initiated and propagated until total failure occurred (at ca. 65000 cycles). From these results, one can say that the induction healing increased the life-time by the order of magnitude of about 30%. This analysis indicates how the asphalt slab which is close to a irreversibly damage after a number of loading cycles can recover its initial behaviour and increase its life-span as a consequence of the healing process.

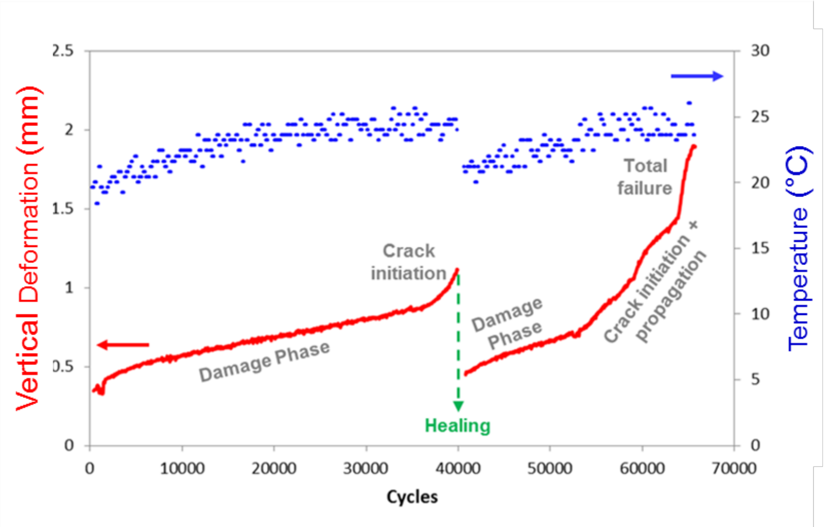

Fig. 6.15 *Evolution of the vertical deformation during the loading cycles before and after healing process.*

Table 6.1 shows a summary of the results obtained from three asphalt slabs tested in this part of the research study. An enhancement of the life of the slabs due to the healing process can clearly be noticed. It is also confirmed that the initial performance is almost recovered after the healing process.

Table 6.1 *Summary of the experimental results from the healing procedure.*

	Before Healing			After Healing			
	Slope (*m*)			Slope (*m*)			
Reference	Damage	Crack Initiation	Loading Cycles	Damage	Crack Initiation	Total Failure	Loading Cycles
A	1.5	--	15000	1.7	9.6	16.0	30000
B	1.9	7.8	38000	3.1	7.1	23.0	15000
C	2.9	9.8	28000	3.5	7.1	40.0	14000

Moreover, it is important to remark that the number of cycles until total failure is longer when the healing process is carried out before damage starts. This result can be observed by analysing the effect of multiple heating processes on the healing capacity. The last asphalt slab (D) was subjected to three different healing treatments by induction heating each one after a number of loading cycles. Fig. 6.16 shows the evolution of the vertical deformation and the internal temperature of the asphalt slab during MMLS3 loading and after multiple healing processes.

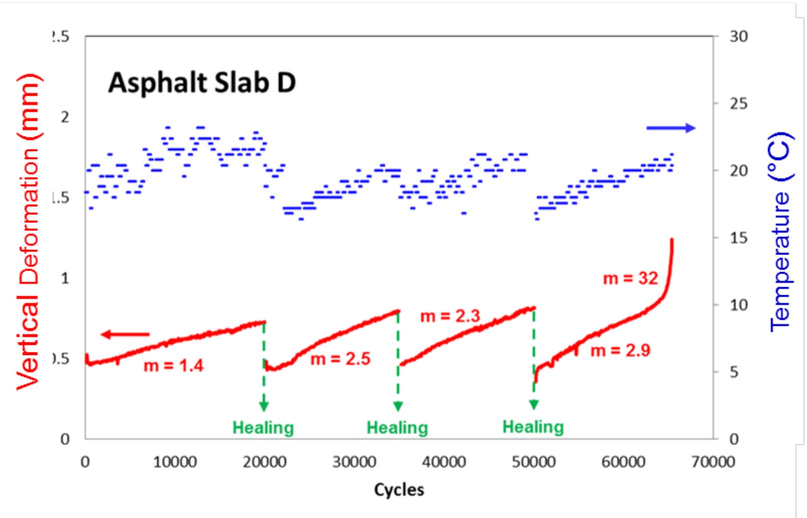

Fig. 6.16 *Multiple healing effect on the mechanical performance of an asphalt slab.*

The procedure consisted in four loading phases: 20000 initial cycles, 2 phases of 15000 cycles each and 12000 cycles until total failure. It can be confirmed that the cracks initiation and propagation phase is delayed as a consequence of the healing process. The range of deformation (slope curve) presented similar values (m < 2.5) during the initial phase and the different damage phases after each induction heating. The life-span of this asphalt slab was increased until 65000 loading cycles following this procedure. Crack initiation started after 64000 cycles, i.e. almost two times later than without heating (average of B and C) which means a double amount of life time in this case. These results confirmed that healing by induction heating can be a feasible alternative to extend the life-span of the asphalt pavements when is applied as maintenance technique before the structure has been irreversibly damaged.

7 Conclusions

In this research, the most critical parameters influenced by the incorporation of electrically conductive additives into dense asphalt mixture have been studied and quantified. During the first experimental phase, modified mixtures with different amounts, diameters and original lengths of steel wool fibers were analysed. It was found that it is important to control certain parameters to obtain good dispersion of fibers in the mixture, such as the amount of fibers, their diameter and length. Otherwise, steel wool fibers mixed with asphalt mixtures can form significant clusters. Moreover, the effect of steel wool fibers on physical and mechanical properties of dense asphalt mixtures was also quantified in this phase. The measured properties could be classified into five main groups: 1) characteristics of the fibers, 2) volumetric properties of the mixtures, 3) mechanical properties of the mixtures, including particle loss as well as the semi-circular load and deformation at 20ºC, 4) induction heating properties of the mixtures and 5) healing properties of asphalt concrete. The particle loss resistance of dense asphalt mixtures with steel wool fibers was analysed after subjecting the mixtures to three different types of environmental damage: water, salt water and ageing. Moreover, the semi-circular flexural strength of dense asphalt mixtures with steel wool fibers has been tested at different temperatures, from -20ºC to 20ºC. In addition, the healing properties of test samples from a self-healing road built in the Netherlands were compared to the healing properties of the mixtures made in the laboratory.

In the second experimental phase, cast iron particles were used as conductive additives in order to improve their distribution in the mixture and thus, to avoid cluster formation. The practical limits of the healing process were analysed by means of different studies involving controlled damage of the modified asphalt mixtures. Fatigue tests were carried out to evaluate the maximum number of load cycles that lead to a damage which cannot be healed by induction heating. Besides, double torsion tests on prismatic specimens allowed controlling the initiation and propagation of a longitudinal crack in order to assess the effect of the healing treatment locally on modified mixtures with different bitumen properties. Finally, an upscaling study was accomplished where long slabs were damaged by using the Model Mobile Load Simulator (MMLS3) in order to simulate the effect of real traffic on the deterioration of a pavement and to demonstrate the concept of induction heating for practical application.

The main conclusions obtained from the different studies related to this project are as follows:

- **Steel wool fiber distribution into dense asphalt mixture**

During this study, it could be observed that the final length of fibers after mixing and compacting the asphalt mixture is independent of their original length when added to the mixture. This can be explained by the observation that the fibers suffer shear and tensile stresses and impacts during the mixing process. As a result, they degrade and cut into pieces. Therefore, the total amount of damage of the fiber from mixing and compaction depends only on the total length of fibers that was originally added into the mixture. This was a matter for researching and had also important implication for the practical optimization of the production and compaction methods of such mixtures.

Additionally, it was found that many clusters of fibers appear during the first moments of mixing, probably affecting the mechanical properties of the mixtures. Moreover, it was found that the amount of clusters grows with the amount of fibers in the mixture and with reducing the diameter of the fibers. Finally, it could be observed that the original length of the fibers has a high impact on the amount of clusters in the mixture. This happens especially in the case of the thin fibers, but the influence of fiber length reduces with increasing fiber diameter. Furthermore, the air void content in the asphalt mixture increased with the number of fibers in the mixture and, consequently, when the area percentage of clusters was higher.

As main conclusion, it can be said that steel wool fibers can be mixed in asphalt mixtures for induction healing purposes. In order to achieve a good distribution, it was observed that short fibers with larger diameters should be used. As a recommendation, they should be below 2 mm length and their diameter should be at least 0.15498 mm or larger. For this reason, it appears clear that a good alternative would be the use of particle-shaped material as conductive additives. Finally, as these fibers are meant to be used for induction heating purposes and, as it is well known that a higher amount of fibers produces an increased heating rate, it is recommended that their content in the mixture must be 6% or higher.

- **Mechanical behaviour of dense asphalt mixture with steel wool fibers**

It was expected that the addition of steel wool fibers would improve the mechanical properties of the dense asphalt mixtures. However, during this study for the investigated materials and temperatures, it was found that the particle loss increased exponentially with the increase of the air void content such that beneficial effects could be lost. Additionally, it has been found that the amount, diameter or length of fibers do not have any influence on the semi-circular flexural strength of dense asphalt mixtures independently of the test temperature.

This study also demonstrated that different pre-treatments, such as ageing or submerging the test specimens in water and salt water, cause different types of damage on dense asphalt mixtures with steel wool fibers. It has been found that water is the factor that damages most dense asphalt mixtures, followed by salt water and ageing. Besides, it has been concluded that steel wool fibers do not improve or worsen particle loss resistance of dense asphalt mixture to water, water with salt and ageing.

Summarizing, it has been found that the mechanical properties of the asphalt mixtures evaluated under the specific conditions of this study were not improved by the addition of steel wool fibers. Indeed, steel wool fibers can change the air void distribution of the mixture and form clusters, which may even harm its particle loss resistance. However, to maintain the induction heating properties required for the healing process, the use of conductive material is essential, albeit their amount into the mixture has to be limited.

- **Physical properties of dense asphalt mixture with steel wool fibers**

It was observed that the thermal conductivity of dense asphalt concrete reduces with the increase of the air void content in the mixtures. It has also been found that the thermal conductivity can be improved to some extend by the presence of steel wool fibers in the mixture. This happens because the thermal conductivity of steel is much higher than the thermal conductivity of asphalt concrete. On the one hand, it has also been observed that the effect of the steel wool fibers is limited, because their amount inside the mixture is very small. Moreover, an increase in the volume of fibers in the mixture would imply also an increase in the air void content. In addition, it has been found that the thermal conductivity of asphalt concrete has a very low correlation with the length and diameter of the steel wool fibers.

Furthermore, as expected, the electrical resistivity is reduced with increasing the amount of steel fibers. However, the change of this physical property could be related mainly to the variation of air void content caused by the addition of the fibers.

- **Healing properties of dense asphalt mixture with steel fibers**

During this part of the study, the effect of induction heating on the recovery of damaged test samples of dense asphalt concrete tested under three point bending was shown. From the results followed that the healing rates of dense asphalt concrete increase with the increase of temperature. In this research, the mechanical resistance of the test samples could be recovered up to 60% when the material was damaged. This happened at around 100ºC. This recovery value was relatively low because the test samples deformed during induction heating. To reach a certain healing level, it is necessary to heat the test samples above a certain temperature. This coincides with the temperature where bitumen behaves as a near-newtonian fluid. If the heating time is short, damage will not be fully recovered.

Moreover, it was shown that healing recovery of the evaluated dense and porous asphalt specimens happened at different temperatures, which corresponds to the temperature of near-Newtonian behaviour of each bitumen. In this research, 50°C was the healing temperature found for the bitumen recovered from the dense asphalt mixture prepared in the laboratory and 23°C for the bitumen recovered from the porous asphalt mixture in the Netherlands. It can be concluded that, regardless the type of bitumen, healing recovery will not depend on the composition of the asphalt concrete mixture but on the temperature reached by the binder. For this reason, it is suggested that for getting a good healing performance, the bitumen temperature must be increased above the Newtonian transition and maintained for a certain amount of time. Hence, asphalt concrete was a very low thermal conductivity, which means that the energy is not easily transferred to the environment.

The same conclusions were also drawn from the model deducted from the Lucas-Washburn equation which corroborates the experimental results for the same bitumen and aggregates in a crack with constant width, which show that healing recovery will depend only on the average temperature on the asphalt concrete specimens. It is important to mention that the developed theoretical models are limited since they do not consider the cases where the total amount of energy introduced in the asphalt concrete is too high, i.e. at a level where the structure of asphalt concrete can be destroyed. Moreover, the exact amount of heat necessary for healing a crack in asphalt concrete is still unclear, since with induction heating, the whole asphalt concrete volume, including the undamaged volumes are being heated.

- **Effect of induction heating on the properties of bitumen**

This point of the research investigated the effect of the electromagnetic field generated in the induction process on the bitumen properties. First, bitumen test samples on steel plates were exposed to induction heating and to various temperature treatments in a forced air convection oven. Additionally, Marshall test specimens containing steel particles, were exposed to the electromagnetic field of an induction heating machine, the eddy currents generated in the steel particles, the high temperature in the steel particles and the high temperatures in the oven. The parameters analysed in the recovered bitumen for evaluating the ageing level were the flow behaviour index measured though rheological characterization and the increase in the concentration of carbonyl (C=0) and sulfoxide functional (S=0) bonds analysing the spectra obtained from chemical evaluation.

It was found that the electromagnetic field generated by the induction heating process, had not affected the rheological and chemical properties of bitumen. Nevertheless, for samples treated by induction heating, it could be observed that there was an energetic level from which the flow behaviour index of bitumen decreased. This effect was not observed in samples exposed to high temperatures in the air forced oven. By analysing this phenomenon locally, it was concluded that bitumen around the metallic particles aged due to the extreme temperatures (> 200 °C) reached by the metallic particles as a consequence of induction heating.

An important recommendation to avoid damage in asphalt concrete heated by induction would be to control the maximum temperature reached by the metallic particles embedded in the mixture in order to minimize the overheating of the bitumen. In future research, it would be convenient to analyse the effect of different sizes of metallic particles on the maximum temperature reached by the particles as well as on the heating rate of asphalt concrete.

- **Induction healing after fatigue damage of asphalt mixtures modified with cast steel particles**

The optimum moment and temperature needed to repair asphalt mixture under fatigue damage was experimentally determined. With this purpose, Marshall test specimens compacted from asphalt concrete with cast steel particles were damaged through indirect tensile fatigue tests and healed via induction heating. In addition, damage and healing were quantified through computed tomography scan tests. It was observed that the lifetime of test specimens subjected to fatigue damage could be extended up to 31% by means of induction heating. Nevertheless, it was found that this process could only heal cracks of a certain width. Hence, if fatigue damage was too high, cracks were too wide to be repaired via induction heating. It was seen that there was an optimum moment in time for healing cracks in asphalt mixtures. Besides, it was confirmed that the total lifetime of asphalt mixtures under fatigue can be increased only if their temperature during induction heating is above a certain threshold; for the asphalt mixture used in this study, approximately 55 °C. It was observed that with higher healing temperatures, improvements of lifetime were smaller.

As an important conclusion, it was found that induction heating cannot repair permanent deformations. Besides, an excess of temperature during induction heating might degrade the bitumen locally, which may affect its capacity for healing the mixture.

- **Induction healing after longitudinal cracking of asphalt mixtures modified with cast iron particles**

Double torsion tests were used to create controlled longitudinal cracks on prismatic specimens specially designed for this purpose. During this study, two set of asphalt concrete mixtures were evaluated to analyse the effect of the bitumen on the healing process. It was observed that natural healing had a significant importance in the healing process of asphalt mixtures with high percentage of soft bitumen. However, for mixtures with low amount of hard bitumen, the induction heating leaded to a better healing performance. Moreover, it was found that for asphalt mixture with hard bitumen, bending deformations were higher after healing. Finally, the initial stiffness obtained after heating was reduced compared to that before the cracking phase. This fact could be related to the variation of the properties of the modified mixture due to the healing treatments.

As conclusion, the influence of the natural healing should be considered in the general analysis of the healing behaviour mainly when soft bitumen is used.

- **Evaluation of the induction healing at a larger scale**

This stage of the research project was focused on finding the practical limits of this innovative healing technique. A new method for assessing the healing of asphalt slabs (up-scaled) by induction heating was developed and validated. This evaluation was accomplished by upscaling the healing concept to dimensions close to a real road by using the model mobile load simulator MMLS3. A number of asphalt slabs modified with cast iron particles were subjected to damage processes after different loading cycles. Afterwards, it was confirmed that a healing treatment carried out by induction heating allowed specimens to recover its initial performance. In addition, it was checked that the number of cycles until total failure was longer when the healing process was carried out before damage starts. It was concluded that this last part of the research proved in a larger scale the enhancement of the life of the pavement due to the healing process. It was also revealed that healing treatment can be reasonable as maintenance technique to prevent early deterioration of asphalt roads.

8 Recommendations for the future

The different conclusions reached during the experimental studies have defined the benefits of the healing process by induction heating as well as the limits of this innovative method to be applied in a feasible way. Nevertheless, an important knowledge has been gained that will allow us to optimize the technique and to be able to design enhanced asphalt mixtures modified with conductive particles. For this objective, a number of proposals are specified in order to remark the important issues to be addressed:

- **Electrically conductive particles**. Once it has been shown that steel wool fibers do not improve the mechanical performance but also the formation of cluster can have a negative influence by varying the internal structure, new designs of modified asphalt mixtures with conductive particles must be taken into account.
- **Parametric study on the influence of the new additives**. Electromagnetic properties of the additives (e.g. steel or iron) must be considered. A complete study on the influence of particle size and amount of material on the mechanical performance should be accomplished. The replacement of part of the mineral aggregates by these metallic additives should also be tested.
- **Effect of the bitumen.** Bituminous binders with low softening points ease the natural and the inductive healing processes. Moreover, a more detailed analysis of the influence of the properties of bitumen (including polymer modified bitumen) will help to understand the physical mechanisms.
- **Influence of the internal structure.** Different types of asphalt mixtures must be evaluated regarding their healing capacities. It has been observed that porosity might be significant for the thermal properties of the mixtures due to its effect on the cooling phase. Besides, the application of this technique to porous asphalt mixtures seems to be a practical alternative to enhance the adhesive characteristics and their resistance against ravelling. In this study, the effect of the moisture on the healing behaviour should be analysed.
- **Evaluation method for healing performance characterisation**. It has been found that the evaluation of the healing performance was closely linked to the characteristics of the mechanical test carried out. For this reason, a reliable and practical method has to be clearly defined for the quantification of the healing level. Besides, the influence of natural healing should be assessed and included in the analysis of the empirical data.
- **Test track construction in the field**. A final validation of the final designs must be done under real conditions. For this purpose, the Mobile Load Simulator (MLS10) should be used in order to reproduce traffic loading. Besides, a movable induction heating device with the suitable characteristics must be used. Afterwards, the healing behaviour and life extension of the modified asphalt mixtures should be evaluated.
- **Optimization of the induction heating system**. The optimization of this innovative solution should be carried out in parallel to the design of a portable induction heating device with the adequate characteristics. The control parameters for the generation of the electromagnetic field such as the generator power level, electrical current through the inductor coil, its working frequency (as a product of the complete setup of the oscillating circuit) or the coupling distance are operating parameters that have an effect on the heating performance and thus, they should be regarded in the design of heating applications. Furthermore, the coil design is other important factor to be taken into account for achieving fast and homogeneous particle-based induction heating.
- **Optimization of the healing procedure**. The induction healing procedure as maintenance technique must be proposed by defining the heating conditions and how often to accomplish healing treatments in order to avoid any irreversible damage.

Furthermore, the experience obtained from this research project can allow us to apply this approach to new and more specified applications, such as:

- the development of new systems of asphalt joints with better adhesion properties and healing capacity;
- the use of a metallic grid or an asphalt mixture modified with conductive additives as interlayer alternative to minimize the reflective cracking effect by healing via induction heating;
- as alternative/supporting process for the heating of the mineral aggregates during the construction of cold and warm asphalt mixtures (e.g. foaming techniques).

References

[1] Bonnaure F. P., Huibers A. H. and Boonders A., "**A laboratory investigation of the influence of rest periods on the fatigue characteristics of bituminous mixes**", Journal of the Association of Asphalt Paving Technologists, 51. 1982

[2] Daniel J. S. and Kim Y. R., "**Laboratory evaluation of fatigue damage and healing of asphalt mixtures**", Journal of Materials in Civil Engineering, 13. 2001

[3] Raithby K. D. and Sterling A. B., "**The effect of rest periods on the fatigue performance of a hot-rolled asphalt under reversed axial loading**", Journal of the Association of Asphalt Paving Technologists, 39. 1970

[4] Williams D., Little D.N., Lytton R.L., Kim Y.R. and Kim Y., "**Microdamage healing in asphalt and asphalt concrete, volume II: Laboratory and field testing to assess and evaluate microdamage and microdamage healing**". Publication No. FHWA-RD-98-142, Federal Highway Administration, Washington, D.C. 2001

[5] Kim Y.R., Little D.N. and Lytton R.L., "**Fatigue and healing characterization of asphalt mixtures**". Journal of Materials in Civil Engineering, 15,(1), 75–83. 2003

[6] Song I., Little D., Masad E. and Lytton R., "**Comprehensive evaluation of damage in asphalt mastics using X-ray CT, continuum mechanics, and micromechanics**". Journal of the Association of Asphalt Paving Technologist; 74, 885–920. 2005

[7] Little D.N. and Bhasin A., "**Exploring mechanisms of healing in asphalt mixtures and quantifying its impact. Self Healing Materials an Alternative Approach to 20 Centuries of Materials Science"**, Springer Series in Materials Science, 100, 205-218. 2007

[8] Lytton R.L., "**Characterizing asphalt pavements for performance**", Transportation Research Record, 1723, 5-16. 2000

[9] García A., "**Self-healing of open cracks in asphalt mastic**", Fuel, 93, 264-272. 2012

[10] Liu Q., García A., Schlangen E. and van de Ven M., "**Induction healing of asphalt mastic and porous asphalt concrete**", Construction and Building Materials 25. 2011

[11] García A., Schlangen E. and van de Ven M., "**Closing cracks on conductive asphalt mortar by induction heating**", Second International Conference on Self-Healing Materials, Chicago. 2009

[12] García A., Schlangen E. and van de Ven M., "**Induction heating of mastic containing conductive fibers and fillers**", Materials and Structures, 44, 499-508. 2011

[13] Liu Q., Schlangen E., García A. and van de Ven M., "**Induction heating of electrically conductive porous asphalt concrete**", Construction and Building Materials 24, 7. 2009

[14] Garcia A., Schlangen E. and van de Ven M., "**Electrical conductivity of asphalt mortar containing conductive fibers and fillers**", Construction and Building Materials, 23. 2009

[15] García A., Schlangen E., van de Ven M. and Liu Q., "**A simple model to define induction heating in asphalt mastic**", Construction and Building Materials, 31, 38-46. 2012

[16] Brown S.F., Rowlett R.D. and Boucher J.L., "**Asphalt modification**". Proceedings of the conference on the United States strategic highway research program: sharing the benefits. London: Thomas Telford; 1990. p. 181-203. 1990

[17] Fitzgerald R.L. "**Novel applications of carbon fiber for hot mix asphalt reinforcement and car-bon–carbon pre-forms**". MSc Thesis, Department of Chemical Engineering, Michigan Techno-logical University; 2000

[18] Huang H. and White TD. "**Dynamic properties of fiber-modified overlay mixture**". Trans Res Rec; 1545:98-104. 1996

[19] Wu S., Ye Q., Li N. and Yue H., "**Effects of fibers on the dynamic properties of asphalt mixtures**". J Wuhan Univ Technol – Mater Sci Ed. 22:733-736. 2007

[20] Putman B.J. and Amirkhanian S.N. "**Utilization of waste fibers in stone matrix asphalt mixtures**", Res, Conserv Recycle, 42:265-274. 2004

[21] Chen H., Li N., Hu C. and Zhang Z., "**Mechanical performance of fibers-reinforced asphalt mixture**", J Chan Univ (Nat Sci Ed), 24(2):1-5. 2004

[22] Echols J., "**New mix method for fiber-reinforced asphalt**", Public Works, 119(8):72-73. 1989

[23] Maurer Dean A. and Gerald M., "**Field performance of fabrics and fibers to retard reflective cracking**", Trans Res Rec; 1248, 13-23. 1989

[24] Mahrez A., Karim M. and Katman H., "**Prospect of using glass fiber reinforced bituminous mixes**", J East Asia Soc Trans Studies, 5:794-807. 2003

[25] Goel A..and Das A., "**Emerging road materials and innovative**". National conference on materials and their application in civil engineering. Hamipur, India; August 2004

[26] Wu S.P., Mo L.T. and Shui Z.H., "**An improvement on electrical properties of asphalt**", J Wuhan Univ Tech (Mater. Sci. Ed), 17(4):63-65. 2002

[27] Wu S.P., Mo L.T., Shui Z.H. and Chen Z., "**Investigation of the conductivity of asphalt concrete with conductive fillers**", Carbon, 43(7):1358-1363. 2005

[28] Wu S., Liu X., Ye Q. and Li N., **"Self-monitoring electrically conductive asphalt-based composite with carbon fillers**", Trans Nonferrous Met Soc China, 16:512-516. 2006

[29] Wu S., Li B., Wang and, Qiu J., "**Numerical simulation of temperature distribution in conductive asphalt solar collector due to pavement material parameters**", Mat Sci Forum, 575-578: 1314-1319. 2008

[30] García A., Norambuena-Contreras J. and Partl M.N., "**Experimental evaluation of dense asphalt concrete properties for induction heating purposes**", Construction and Building Materials, 46, 48-54. 2013

[31] Chang C., Chang Y. and Chen J., "**Effect of mixture characteristics on cooling rate of asphalt pavements**", J Transp Eng, 135(5); 297-304. 2009

[32] Ukwuoma O. and Ademodi B., "**The effects of temperature and shear rate on the apparent viscosity of Nigerian oil sand bitumen**", Fuel Process Technol, 60: 95-101. 1999

[33] Zhao Y. and Machel H.G., "**Determination of the viscosities of Grosmong Reservoir Bitumen, Alberta, Canada**", CSP CSEG CWLS Convention. Calgary, Canada, 2009

[34] Sybilski D., "**Non-Newtonian viscosity of polymer-modified bitumens**", Mater Struct, 26: 15-23. 1993

[35] García A., "**Self-Healing of open cracks in asphalt mastic**". Fuel, 93:264-272. 2011

[36] Partl M.N., Flisch A. and Johnsson M., "**Comparison of different compaction methods using X-ray computer tomography**", Roads Mat Pav Des, 8(2):139-164.2007

[37] Garcia A., Schlangen E., van de Ven M. and van Bochove G., "**Optimization of composition and mixing process of a self-healing porous asphalt**", Const Build Mat, 30, 59-65. 2012

[38] García A., Norambuena-Contreras J., Partl M.N. and Schuetz P., "**Uniformity and mechanical properties of dense asphalt concrete with steel wool fibers**". Constr Build Mater, 43:107-117. 2013

[39] Foster G.C., "**Tensile and flexure strength of unidirectional fiber-reinforced composites: direct numerical simulations and analytic models**", MSc Thesis, Virginia Tech. 1998.

[40] Feldkamp L.A., Davis L.C. and Kress J.W. "**Practical Cone-Beam Algorithm**". Journal of the Optical Society of America A: Optics, Image Science, and Vision, 1, 612-619. 1984

[41] García A., Castro-Fresno D., Polanco J.A. and Thomas C., "**Abrasive wear evolution in concrete pavements**", Road Materials and Pavement Design, 13(3):534-548. 2012

[42] Nando G.B. and Gupta B.R., "**Short fiber thermoplastic elastomer composites in short fiber-polymer composites**", J.R. White and S.K. De (eds.), Woodhead Publishing, Cambridge. 1996

[43] Hamzah M.O., Hasan M.R.M., Ismail M.R. and Shahadan Z., "**Effects of temperature on abrasion loss of porous and dense asphalt mixes**". Eur J Sci Res,40(4):589-597. 2010

[44] García, A., Norambuena-Contreras, J. and Partl, M.N., "**A parametric study on the influence of the steel wool fibers in dense asphalt concrete**", Materials and Structures, 47, 1559–1571. 2014

[45] Dos Santos R.G., Mohamed R.S., Bannwart A.C. and Loh W., "**Contact angle measurements and wetting behaviour of inner surfaces of pipelines exposed to heavy crude oil and water**", J Petrol Sci Eng 51:6-9. 2006

[46] Herrington P., Reilly S. and Cook S.., "**Porous asphalt durability test**", Transfund New Zealand Research Report No. 265, 2005.

[47] Templeton C.C. and Rushing S.S., "**Oil-Water displacements in microscopic capillaries**", J Petrol Technol, 8(9):211-214.1956

[48] Aseada T. and Ca V.T., "**Characteristics of permeable pavement during hot summer weather and impact on the thermal environment**", Building and Environment, 13, 363-375. 2002

[49] Gui J., Phelan P.E., Kaloush K.E. and Golden J.S., "**Impact of pavement thermophysical properties on surface temperatures**", Journal of Materials in Civil Engineering, 19 683-690. 2007

[50] Luca J. and Mrawira P.E., "**New measurement of thermal properties of Superpave asphalt concrete**", J. Mater. Civ. Eng., 17(1), 72–79. 2005.

[51] Powell B.W., Ho C.Y. and Liley P.E., "**Thermal conductivity of selected materials**", NSRDS-NBS 8. National Standard Reference Data Series-National Bureau of Standards-8. 1966

[52] García A., Bueno, M., Norambuena-Contreras J. and Partl M.N., "**Induction healing of dense asphalt concrete**". Construction and Building Materials, 49:1-7. 2013

[53] Liu Q., Schlangen E. and van de Ven M., "**Characterization of the material from the induction healing porous asphalt concrete trial sectio**n", Materials and Structures, 46; 831-839. 2013

[54] García A., Norambuena-Contreras J., Bueno, M. and Partl M.N., "**Single and multiple healing of porous and dense asphalt concrete**", Journal of Intelligent Material Systems and Structures, 26(4), 425–433. 2015

[55] García-Morales, M., Partal, P., Navarro, F.J., Martínez-Boza, F., Gallegos, C., González, N., González, O. and Muñoz, M.E., "**Viscous properties and microstructure of recycled eva modified bitumen**". Fuel 83 (1), 31-38. 2004

[56] Lu, X. and Isacsson, U. "**Influence of styrene-butadiene-styrene polymer modification on bitumen viscosity**", Fuel 76 (14-15), 1353-1359. 1997

[57] Sung, Y.T., Kum, C.K., Lee, H.S., Kim, J.S., Yoon, H.G. and Kim, W.N., "**Effects of crystal-linity and crosslinking on the thermal and rheological properties of ethylene vinyl acetate copolymer**". Polymer 46 (25), 11844-11848. 2005

[58] Nahar S.N., Schmets A.J.M., Scarpas A. and Schitter G., "**Temperature and thermal history dependence of the microstructure in bituminous materials**", European Polymer Journal, 49, 1964-1074. 2013

[59] Edwards Y. and Redelius P., "**Rheological effects of waxes in bitumen**", Energy Fuels, 17(3):511-520. 2003

[60] Dave E.V., Buttlar W.G. and Paulino G.H., "**Asphalt pavement aging and temperature dependent properties through a functionally graded viscoelastic model, Part-II: Applications**", Materials Science Forum 2010, 631-632, 53-58. 2010

[61] Stangl K., Jäger A. and Lackner R., "**Microstructure-based identification of bitumen performance**", Road Mater Pavement Des, 7(sup 1): 111-42. 2006

[62] Gaskin J., "**On bitumen microstructure and the effects of crack healing**", PhD Thesis, University of Nottingham, 2013

[63] Menozzi, A., García, A., Partl, M.N., Tebaldi, G. and Schuetz, P., "**Induction healing of fatigue damage**", Construction and Building Materials, 74, 162-168, 2015

[64] Little D.N., Lytton R.L. and Williams D., "**Propagation and healing of microcracks in asphalt concrete and their contributions to fatigue**", Asphalt Science and Technology. New York, NY: Marcel Dekker Inc. pp. 149–195. 1997

[65] Ghaly A.M., "**A mechanistic analysis of static and repeated loading effects on rubberized asphalt**", Int J Pave Eng, 4:4. 2003

[66] Kim, H., and Part M.N., "**Development of a double-torsion fracture test to predict channelized crack behaviors of asphalt concrete**", Construction and Building Materials, 26, 694-700. 2012

[67] Arraigada, M., Pugliessi A., Partl M.N., and Martínez F., "**Effect of full-size and down-scale accelerated traffic loading on pavement behaviour**", Materials and Structures, 47, 1409-1424. 2014

Projektabschluss

Schweizerische Eidgenossenschaft
Confédération suisse
Confederazione Svizzera
Confederaziun svizra

Eidgenössisches Departement für
Umwelt, Verkehr, Energie und Kommunikation UVEK
Bundesamt für Strassen ASTRA

FORSCHUNG IM STRASSENWESEN DES UVEK

Version vom 09.10.2013

Formular Nr. 3: Projektabschluss

erstellt / geändert am: 18.11.2015

Grunddaten

Projekt-Nr.:	ASTRA 2011/012_OBF
Projekttitel:	Development of a self-healing asphalt road via induction heating
Enddatum:	November 2015

Texte

Zusammenfassung der Projektresultate:

The aim of this research project was to develop a self-healing asphalt road via induction heating. For that purpose, the influence of different conductive additives on the properties of the modified asphalt mixtures was analysed in order to know the advantages and/or limits of this innovative approach. Moreover, the healing performance was evaluated obtaining significant conclusions related to the importance of thermal, rheological and chemical properties of the bitumen. Finally, the feasibility of the healing concept for asphalt roads was analysed at large scale by simulating the effect of real traffic on the deterioration of a pavement.

From the beginning, experimental results showed the problems of using steel wool fibers as conductive additives. The incorporation of these fibers did not improve the mechanical properties of the modified asphalt mixtures as it was originally expected. In fact, clusters of fibers were formed during the mixing procedure. These clusters leaded to changes in the internal structure of the mixture by increasing the air void content. As a consequence, it could be observed that higher air void contents showed a negative effect on the mechanical properties of the modified asphalt mixtures, mainly on the particle loss resistance. Furthermore, the thermal conductivity was lower for asphalt mixture with higher air void contents due to the addition of steel wool fibers. After these results, the use of particle-shaped material as conductive additives was found as an important alternative to improve the mechanical performance of the modified asphalt mixtures by avoiding the formation of fibers clusters.

Concerning the healing capability, bitumen properties were found the key factor to control the process. It was observed that the bitumen must be able to flow as a near-Newtonian fluid in order to close the cracks. For this reason, the temperature of the material must be increased above certain limit (heating phase) and maintained during some time (cooling phase). The healing temperature depends on the type of bitumen and its rheological properties. It was also shown that natural healing had a significant role in the process when high percentage of soft bitumen is used in the mixture. In addition, it was found the electromagnetic field needed for the induction heating process had no effect on the chemical structure of the bitumen. Nevertheless, excess of temperature during induction heating might degrade the bitumen locally due to the extreme temperatures reached by the metallic particles. Thus, it is highly recommended to control the heating temperature in order to minimize the aging of the bitumen caused by overheating.

Last experimental studies concluded that permanent deformation cannot be repaired by induction heating. Moreover, it was experimentally checked that this healing technique can only close cracks of certain size (micrometre scale) and that the heating treatment must be carried out before irreversible damage starts. Finally, during the upscaling of the healing concept to dimensions close to reality by using the model mobile load simulator MMLS3 over 1.8 m long asphalt test slabs, it was showed that the number of loading cycles until total failure was longer when the healing process was accomplished earlier. Thus, it could be concluded that this method could be a reasonable maintenance option to prevent premature deterioration of asphalt roads.

Forschung im Strassenwesen des UVEK: Formular 3 Seite 1 / 3

Schweizerische Eidgenossenschaft
Confédération suisse
Confederazione Svizzera
Confederaziun svizra

Eidgenössisches Departement für
Umwelt, Verkehr, Energie und Kommunikation UVEK
Bundesamt für Strassen ASTRA

Zielerreichung:

The experimental studies developed during the research project have confirmed the potential of the induction healing as technique to extend the life-span of the asphalt roads. Besides, the experience obtained after the analysis of the main factors affecting the mechanical and healing performance will allow us to know the limits of this innovative procedure. Finally, an important knowledge has been gained that will help us to optimize the technique and to be able to design enhanced and feasible asphalt mixtures modified with conductive particles for healing purpose.

Folgerungen und Empfehlungen:

- Steel wool fibers do not improve the mechanical performance and physical properties but also the formation of cluster can have a negative influence by varying the internal structure.
- The healing rates of dense asphalt concrete increase with the increase of temperature. The bitumen temperature must be increased above the Newtonian transition and maintained for a certain amount of time. The healing temperature is related to the properties of the bitumen.
- After a certain number of cycles (fatigue behaviour), there is no mechanical recover by induction heating. This process could only heals cracks of a certain width (micrometer scale).
- The evaluation of the induction healing at a larger scale showed that the number of cycles until total failure is longer when the healing process is carried out before damage. In this context, multiple healing process was found as reliable maintenance technique to prevent premature deterioration of asphalt roads.

Recommendations for further research:
- Modified asphalt mixtures with conductive particles must be taken into account. Moreover, a more detailed analysis of the influence of the properties of bitumen (including polymer modified bitumen) will help to understand the physical mechanisms. Furthermore, different types of asphalt mixtures must be evaluated regarding their healing capacities.
- A reliable and practical method has to be clearly defined for the quantification of the healing level. Besides, the influence of natural healing should be assessed and included in the analysis of the empirical data.
- A final validation of the final designs must be done under real conditions. For this purpose, the Mobile Load Simulator (MLS10) should be used in order to reproduce traffic loading. Besides, a movable induction heating device with the suitable characteristics must be used

Publikationen:

- Uniformity and mechanical properties of dense asphalt concrete with steel wool fibers. García A., Norambuena-Contreras J., Partl M.N., P. Schuetz. Construction and Building Materials, vol. 43, pp. 107-117
- A Parametric study of the influence of steel wool fibers in dense asphalt concrete. García A., Norambuena-Contreras J., Part M.N. Materials and Structures, 46 (8), pp. 1-13
- Electrical, thermal and induction heating properties of dense asphalt concrete. García A., Norambuena-Contreras J., Partl M.N.Advanced Materials Research, 723, pp 301-311
- Experimental evaluation of dense asphalt concrete properties for induction healing purposes. García A., Norambuena-Contreras J., Partl M.N. Construction and Building Materials, vol. 46, pp 48-54
- Induction healing of dense asphalt concrete. García, A., Bueno, M., Norambuena, J., Partl, M.N. Construction and Building Materials, vol. 49, pp. 1-7
- Single and multiple healing of porous and dense asphalt concrete. García A., Norambuena-Contreras J., Bueno, M. Partl M.N.Journal of Intelligent Materials Systems and Structures vol. 26(4), pp. 425-433
- Influence of steel wool fibers on the mechanical, thermal and healing properties of dense asphalt concrete. Garcia, A., Bueno, M., Norambuena-Contreras, J., Partl, M.N. Journal of Testing and Evaluation, vol. 42 (5), pp. 1-12

Der Projektleiter/die Projektleiterin:

Name: Partl Vorname: Manfred N.

Amt, Firma, Institut: Empy, Road Engineering and Sealing Components Laboratory

Unterschrift des Projektleiters/der Projektleiterin:

Forschung im Strassenwesen des UVEK: Formular 3 Seite 2 / 3

Schweizerische Eidgenossenschaft
Confédération suisse
Confederazione Svizzera
Confederaziun svizra

Eidgenössisches Departement für
Umwelt, Verkehr, Energie und Kommunikation UVEK
Bundesamt für Strassen ASTRA

FORSCHUNG IM STRASSENWESEN DES UVEK

Formular Nr. 3: Projektabschluss

Beurteilung der Begleitkommission:

Beurteilung:

This experimental study has shown the advantages and disadvantages of this innovative healing technique for asphalt roads. The overall efficiency of the induction heating for healing pavements has been confirmed, but during the different research phases unexpected parameters, that were considered irrelevant at the beginning of the project, have been finally found to be significant for the final results. These factors caused that the objective defined in the original proposal was modified while new results were revealed. For example, the formation of fibers clusters and its effect on the properties of the asphalt mixtures required the use of alternative materials as electrically conductive additive (particles). As a direct consequence, the optimization of the healing performance of the asphalt mixes was replaced by the study of the limitations of the process (i.e. damage to be able to heal) during the last part of the project. Finally, the assessment of the induction healing technique at large scale with a traffic simulator provided a feasible proof of concept. In this sense, the goal of the project has been successfully accomplished. This study has helped to identify main directions of further research in the field.

Umsetzung:

The implementation of this solution into the current alternatives and methods for asphalt roads is not ready yet. Further analysis must be done in order to optimize new designs and protocols that meet the characteristics required for the roads administrations. Besides, the development of the adequate induction heating device for real road dimensions must be also done.

weitergehender Forschungsbedarf:

Further research should be focused on the adjustment of the key parameters for the final designs of asphalt roads with selfhealing capacity. For this purpose, additional analysis of bitumens with different properties and types of asphalt mixtures is recommended. The study showed that the next promising step would be to evaluate this application for the improvement of the resistance of porous asphalt mixtures against ravelling and crack formation. After that, the mechanical requirements and healing performance in a field test track must be evaluated. Finally, an analysis of the economical feasibility of this experimental approach is recommended.

Einfluss auf Normenwerk:

A basis for designing asphalt mixtures with healing capabilities as well as of the evaluation methods and working protocols for a future standardization has been established.

Der Präsident/die Präsidentin der Begleitkommission:

Name: Dünner Vorname: Sandra

Amt, Firma, Institut: Walo Bertschinger AG

Unterschrift des Präsidenten/der Präsidentin der Begleitkommission:

Forschung im Strassenwesen des UVEK: Formular 3 Seite 3 / 3

Verzeichnis der Berichte der Forschung im Strassenwesen

Bericht-Nr.	Projekt Nr.	Titel	Jahr
1522	VSS 2011/106	Normierte gesamtverkehrliche Erschliessungsqualitäten - Grundlagenbericht	2015
1520	ASTRA 2008/013_OBF	Nächtliche Immissionsprognosen von Strassenlärm (Hochleistungsstrassen)	2015
1519	VSS 2009/201	Lärmimmissionen bei Knoten und Kreiseln	2015
1518	SVI 2011/024	Langsamverkehrsfreundliche Lichtsignalanlagen	2015
1517	VSS 2011/103	Bemessungsverkehrsstärken: Ein neuer Ansatz	2015
1516	VSS 2011/711	Forschungspaket Nutzensteigerung für die Anwender des SIS: EP1: Zeitaspekte und Historisierung	2015
1514	VSS 2006/513_OBF	Forschungspaket Brückenabdichtungen: EP3 - Langzeitverhalten des Verbundes	2015
1513	VSS 2005/403	Fliesskoeffizienten von feinen Gesteinskörnungen aus der Schweiz	2015
1512	SVI 2004/069	Veloverkehr in den Agglomerationen - Einflussfaktoren, Massnahmen und Potenziale	2015
1511	VSS 2012/601	Die Physik zwischen Salz, Schnee und Reifen	2015
1510	VSS 2005/453	Forschungspaket Recycling von Ausbauasphalt in Heissmischgut: EP2: Mehrfachrecycling von Strassenbelägen	2015
1509	ASTRA 2010/022	Markt- und Nutzermonitoring Elektromobilität (MANUEL)	2015
1508	VSS 2011/716	Forschungspaket Nutzensteigerung für die Anwender des SIS: EP6: Schnittstellen aus den Auswertungssystemen SIS (SIS-DWH)	2015
1507	FGU 2007/004	TBM Tunneling in Faulted and Folded Rocks	2015
1506	VSS 2006/512_OBF	Forschungspaket Brückenabdichtungen: EP2 - Flüssigkunststoff-Abdichtungen, Erfassen der Verbundproblematik	2015
1505	VSS 2006/509	Abdichtungssysteme und bitumenhaltige Schichten auf Betonbrücken - Initialprojekt	2014
1504	VSS 2005/504	Druckschwellversuch zur Beurteilung des Verformungsverhaltens von Belägen	2014
1503	VSS 2006/515_OBF	Research Package on Bridge Deck Waterproofing Systems: EP5-Mechanisms of Blister Formation	2014
1502	VSS 2010/502	Road – landside interaction : Applications	2014
1501	VSS 2011/705	Grundlagen zur Anwendung von Lebenszykluskosten im Erhaltungsmanagement von Strassenverkehrsanlagen	2014
1500	ASTRA 2010/007	SURPRICE (Sustainable mobility through road user charging) - Swiss contribution: Equity effects of congestion charges and intra-individual variation in preferences	2015
1499	ASTRA 2011/010	Stauprognoseverfahren und -systeme	2014
1498	VSS 2011/914	Coordinated Ramp Metering Control with Variable Speed Limits for Swiss Freeways	2014
1497	VSS 2009/705	Verfahren zur Bildung von homogenen Abschnitten der Strassenverkehrsanlage für das Erhaltungsmanagement Fahrbahnen	2014
1496	VSS 2010/601	Einfluss von Lärmschutzwänden auf das Raumnutzungsverhalten von Reptilien	2014
1495	VSS 2009/703	Zusammenhang Textur und Griffigkeit von Fahrbahnen und Einflüsse auf die Lärmemission	2014
1494	VSS 2010/704	Erhaltungsmanagement der Strassen - Erarbeiten der Grundlagen und Schadenkataloge zur systematischen Zustandserhebung und -bewertung von zusätzlichen Objekten der Strassen	2014
1493	VSS 2006/001	Neue Methoden zur Beurteilung der Tieftemperatureigenschaften von bitumenhaltigen Bindemitteln	2014
1492	SVI 2004/029	Kombiniertes Verkehrsmittel- und Routenwahlmodell	2014
1491	VSS 2007/704	Gesamtbewertung von Kunstbauten	2014
1490	FGU 2004/002	Langzeit-Beständigkeit von Tunnel-Abdichtungssystemen aus Kunststoffen (Best TASK)	2014
1489	VSS 2006/516_OBF	Forschungspaket Brückenabdichtungen: EP6 - Anschlüsse von Brückenabdichtungen	2014
1488	SVI 2007/020	Methodik zur Nutzenermittlung von Verkehrsdosierungen	2014
1487	SVI 2008/001	Erfahrungsbericht Forschungsbündel	2014
1486	SVI 2004/005	Partizipation in Verkehrsprojekten	2014

Bericht-Nr.	Projekt Nr.	Titel	Jahr
1485	VSS 2007/401	Anforderungen an Anschlussfugensysteme in Asphaltdecken - Teil 1: Praxiserfahrung	2014
1484	FGU 2010/003	Misestimating time of collision in the tunnel entrance due to a disturbed adaptation	2014
1483	VSS 2005/452	Forschungspaket Recycling von Ausbauasphalt in Heissmischgut: EP1: Optimaler Anteil an Ausbauasphalt	2014
1482	ASTRA 2010/018	SURPRICE: Sustainable mobility through road user charges Swiss contribution: Comprehensive road user charging (RUC)	2015
1481	VSS 2001/702	Application des méthodes de représentation aux données routières	2014
1480	ASTRA 2008/004	Prozess- und wirkungsorientiertes Management im betrieblichen Strassenunterhalt Modell eines siedlungsübergreifenden Unterhalts	2014
1479	ASTRA 2005/004	Entscheidungsgrundlagen & Empfehlungen für ein nachhaltiges Baustoffmanagement	2014
1478	VSS 2005/455	Research Package on Recycling of Reclaimed Asphalt in Hot Mixes - EP4: Evaluation of Durability	2014
1477	VSS 2008/503	Feldversuch mit verschiedenen Pflästerungen und Plattendecken	2014
1476	VSS 2011/202	Projet initial pour la conception multi-usagers des carrefours	2014
1475	VSS 1999/125	Ringversuch "Eindringtiefe eines ebenen Stempels, statische Prüfung an Gussasphalt"	2014
1474	VSS 2009/704	Wechselwirkung zwischen Aufgrabungen, Zustand und Alterungsverhalten im kommunalen Strassennetz-Entwicklung eines nachhaltigen Aufgrabungsmanagement	2014
1473	VSS 2011/401	Forschungspaket "POLIGRIP - Einfluss der Polierbarkeit von Gesteinskörnungen auf die Griffigkeit von Deckschichten - Initialprojekt"	2014
1472	SVI 2010/003	Einfluss der Verlässlichkeit der Verkehrssysteme auf das Verkehrsverhalten	2014
1471	ASTRA 2008/011	Strategien zum wesensgerechten Einsatz der Verkehrsmittel im Güterverkehr Forschungspaket UVEK/ASTRA - Synthese	2014
1470	VSS 2011/907	Initialprojekt für ein Forschungspaket "Kooperative Systeme für Fahrzeug und Strasse"	2014
1469	VSS 2008/902	Untersuchungen zum Einsatz von Bewegungssensoren für fahrzeitbezogene Verkehrstelematik-Anwendungen	2014
1468	VSS 2010/503	Utilisation des géostructures énergétiques pour la régulation thermique et l'optimisation énergétique des infrastructures routières et ouvrages d'art	2014
1467	ASTRA 2010/021	Sekundärer Feinstaub vom Verkehr	2014
1466	VSS 2010/701	Grundlagen zur Revision der Normen über die visuelle Erhebung des Oberflächenzustands	2014
1465	ASTRA 2000/417	Erfahrungen mit der Sanierung und Erhaltung von Betonoberflächen	2014
1462	ASTRA 2011/004	Ermittlung der Versagensgrenze eines T2 Norm-Belages mit der mobiles Grossversuchsanlage MLS10	2014
1460	SVI 2007/017	Nutzen der Verkehrsinformation für die Verkehrssicherheit	2014
1459	VSS 2002/501	Leichtes Fallgewichtsgerät für die Verdichtungskontrolle von Fundationsschichten	2014
1458	VSS 2010/703	Umsetzung Erhaltungsmanagement für Strassen in Gemeinden - Arbeitshilfen als Anhang zur Norm 640 980	2014
1457	SVI 2012/006	Forschungspaket VeSPA Teilprojekt 5: Medizinische Folgen des Strassenunfallgeschehens	2014
1456	SVI 2012/005	Fotschungspaket VeSPA Teilprojekt 4: Einflüsse des Wetters auf das Strassenunfallgeschehen	2014
1455	SVI 2012/004	Forschungspaket VeSPA Teilprojekt 3: Einflüsse von Fahrzeugeigenschaften auf das Strassenunfallgeschehen	2014
1454	SVI 2012/003	Forschungspaket VeSPA Teilprojekt 2: Einflüsse von Situation und Infrastruktur auf das Strassenunfallgeschehen: Phase 1	2014
1453	SVI 2012/002	Forschungspaket VeSPA Teilprojekt 1: Einflüsse von Mensch und Gesellschaft auf das Strassenunfallgeschehen: Phase 1	2014
1452	SVI 2012/001	Forschungspaket VeSPA: Synthesebericht Phase 1	2014
1451	FGU 2010/006	Gasanalytik zur frühzeitigen Branddetektion in Tunneln	2013
1450	VSS 2002/401	Kaltrecycling von Ausbauasphalt mit bituminösen Bindemitteln	2014
1449	ASTRA 2010/024	E-Scooter - Sozial- und naturwissenschaftliche Beiträge zur Förderung leichter Elektrofahrzeuge in der Schweiz	2013

Bericht-Nr.	Projekt Nr.	Titel	Jahr
1448	SVI 2009/008	Anforderungen der Güterlogistik an die Netzinfrastruktur und die langfristige Netzentwicklung in der Schweiz. Forschungspaket UVEK/ASTRA "Strategien zum wesensgerechten Einsatz der Verkehrsmittel im Güterverkehr der Schweiz", Teilprojekt C	2014
1447	SVI 2009/005	Informationstechnologien in der zukünftigen Gütertransportwirtschaft Forschungspaket UVEK/ASTRA "Strategien zum wesensgerechten Einsatz der Verkehrsmittel im Güterverkehr der Schweiz", Teilprojekt E	2013
1446	VSS 2005/454	Forschungspaket Recycling von Ausbauasphalt in Heissmischgut: EP3: Stofffluss- und Nachhaltigkeitsbeurteilung	2013
1445	VSS 2009/301	Öffnung der Busstreifen für weitere Verkehrsteilnehmende	2013
1444	VSS 2007/306	Verkehrsqualität und Leistungsfähigkeit von Anlagen des leichten Zweirad- und des Fussgängerverkehrs	2013
1443	VSS 2007/305	Verkehrsqualität und Leistungsfähigkeit des strassengebundenen ÖV	2013
1442	SVI 2010/004	Messen des Nutzens von Massnahmen mit Auswirkungen auf den Langsamverkehr - Vorstudie	2013
1441_2	SVI 2009/010	Zielsystem im Güterverkehr. Forschungspaket UVEK/ASTRA Strategien zum wesensgerechten Einsatz der Verkehrsmittel im Güterverkehr der Schweiz - Teilprojekt G	2013
1441_1	SVI 2009/010	Effizienzsteigerungspotenziale in der Transportwirtschaft durch integrierte Bewirtschaftungsinstrumente aus Sicht der Infrastrukturbetreiber Synthese der Teilprojekte B3, C, D, E und F des Forschungspakets Güterverkehr anhand eines Zielsystems für den Güterverkehr	2013
1440	SVI 2009/006	Benchmarking-Ansätze im Verkehrswesen	2013
1439	SVI 2009/002	Konzept zur effizienten Erfassung und Analyse der Güterverkehrsdaten Forschungspaket UVEK/ASTRA Strategien zum wesensgerechten Einsatz von Verkehrsmitteln im Güterverkehr der Schweiz TP A	2013
1438_2	SVI 2009/011	Ortsbezogene Massnahmen zur Reduktion der Auswirkungen des Güterverkehrs - Teil 2. Forschungspaket UVEK/ASTRA Strategien zum wesensgerechten Einsatz der Verkehrsmittel im Güterverkehr der Schweiz TP H	2013
1438_1	SVI 2009/011	Ortsbezogene Massnahmen zur Reduktion der Auswirkungen des Güterverkehrs - Teil 1. Forschungspaket UVEK/ASTRA Strategien zum wesensgerechten Einsatz der Verkehrsmittel im Güterverkehr der Schweiz TP H	2013
1437	VSS 2008/203	Trottoirüberfahrten und punktuelle Querungen ohne Vortritt für den Langsamverkehr	2013
1436	VSS 2010/401	Auswirkungen verschiedener Recyclinganteile in ungebundenen Gemischen	2013
1435	FGU 2008/007_OBF	Schadstoff- und Rauchkurzschlüsse bei Strassentunneln	2013
1434	VSS 2006/503	Performance Oriented Requirements for Bitumainous Mixtures	2013
1433	ASTRA 2010/001	Güterverkehr mit Lieferwagen: Entwicklungen und Massnahmen Forschungspaket UVEK/ASTRA Strategien zum wesensgerechten Einsatz der Verkehrsmittel im Güterverkehr der Schweiz TP B3	2013
1432	ASTRA 2007/011	Praxis-Kalibrierung der neuen mobilen Grossversuchanlage MLS10 für beschleunigte Verkehrslastsimulation auf Strassenbelägen in der Schweiz	2013
1431	ASTRA 2011/015	TeVeNOx - Testing of SCR-Systems on HD-Vehicles	2013
1430	ASTRA 2009/004	Impact des conditions météorologiques extrêmes sur la chaussée	2013
1429	SVI 2009/009	Einschätzungen der Infrastrukturnutzer zur Weiterentwicklung des Regulativs Forschungspaket UVEK/ASTRA Strategien zum wesensgerechten Einsatz der Verkehrsmittel im Güterverkehr der Schweiz TP F	2013
1428	SVI 2010/005	Branchenspezifische Logistikkonzepte und Güterverkehrsaufkommen sowie deren Trends Forschungspaket UVEK/ASTRA Strategien zum wesensgerechten Einsatz der Verkehrsmittel im Güterverkehr der Schweiz TP B2	2013
1427	SVI 2006/002	Begegnungszonen - eine Werkschau mit Empfehlungen für die Realisierung	2013
1426	ASTRA 2010/025_OBF	Luftströmungsmessung in Strassentunneln	2013
1425	VSS 2005/401	Résistance à l'altération des granulats et des roches	2013

Bericht-Nr.	Projekt Nr.	Titel	Jahr
1424	ASTRA 2006/007	Optimierung der Baustellenplanung an Autobahnen	2013
1423	ASTRA 2010/012	Forschungspaket: Lärmarme Beläge innerorts EP3: Betrieb und Unterhalt lärmarmer Beläge	2013
1422	ASTRA 2011/006_OBF	Fracture processes and in-situ fracture observations in Gipskeuper	2013
1421	VSS 2009/901	Experimenteller Nachweis des vorgeschlagenen Raum- und Topologiemodells für die VM-Anwendungen in der Schweiz (MDATrafo)	2013
1420	SVI 2008/003	Projektierungsfreiräume bei Strassen und Plätzen	2013
1419	VSS 2001/452	Stabilität der Polymere beim Heisseinbau von PmB-haltigen Strassenbelägen	2013
1418	VSS 2008/402	Anforderungen an hydraulische Eigenschaften von Geokunststoffen	2012
1417	FGU 2009/002	Heat Exchanger Anchors for Thermo-active Tunnels	2013
1416	FGU 2010/001	Sulfatwiderstand von Beton: verbessertes Verfahren basierend auf der Prüfung nach SIA 262/1, Anhang D	2013
1415	VSS 2010/A01	Wissenslücken im Infrastrukturmanagementprozess "Strasse" im Siedlungsgebiet	2013
1414	VSS 2010/201	Passive Sicherheit von Tragkonstruktionen der Strassenausstattung	2013
1413	SVI 2009/003	Güterverkehrsintensive Branchen und Güterverkehrsströme in der Schweiz Forschungspaket UVEK/ASTRA Strategien zum wesensgerechten Einsatz der Verkehrsmittel im Güterverkehr der Schweiz Teilprojekt B1	2013
1412	ASTRA 2010/020	Werkzeug zur aktuellen Ganglinienнorm	2013
1411	VSS 2009/902	Verkehrstelematik für die Unterstützung des Verkehrsmanagements in ausserordentlichen Lagen	2013
1410	VSS 2010/202_OBF	Reduktion von Unfallfolgen bei Bränden in Strassentunneln durch Abschnittsbildung	2013
1409	ASTRA 2010/017_OBF	Regelung der Luftströmung in Strassentunneln im Brandfall	2013
1408	VSS 2000/434	Vieillissement thermique des enrobés bitumineux en laboratoire	2012
1407	ASTRA 2006/014	Fusion des indicateurs de sécurité routière : FUSAIN	2012
1406	ASTRA 2004/015	Amélioration du modèle de comportement individuell du Conducteur pour évaluer la sécurité d'un flux de trafic par simulation	2012
1405	ASTRA 2010/009	Potential von Photovoltaik an Schallschutzmassnahmen entlang der Nationalstrassen	2012
1404	VSS 2009/707	Validierung der Kosten-Nutzen-Bewertung von Fahrbahn-Erhaltungsmassnahmen	2012
1403	SVI 2007/018	Vernetzung von HLS- und HVS-Steuerungen	2012
1402	VSS 2008/403	Witterungsbeständigkeit und Durchdrückverhalten von Geokunststoffen	2012
1401	SVI 2006/003	Akzeptanz von Verkehrsmanagementmassnahmen-Vorstudie	2012
1400	VSS 2009/601	Begrünte Stützgitterböschungssysteme	2012
1399	VSS 2011/901	Erhöhung der Verkehrssicherheit durch Incentivierung	2012
1398	ASTRA 2010/019	Environmental Footprint of Heavy Vehicles Phase III: Comparison of Footprint and Heavy Vehicle Fee (LSVA) Criteria	2012
1397	FGU 2008/003_OBF	Brandschutz im Tunnel: Schutzziele und Brandbemessung Phase 1: Stand der Technik	2012
1396	VSS 1999/128	Einfluss des Umhüllungsgrades der Mineralstoffe auf die mechanischen Eigenschaften von Mischgut	2012
1395	FGU 2009/003	KarstALEA: Wegleitung zur Prognose von karstspezifischen Gefahren im Untertagbau	2012
1394	VSS 2010/102	Grundlagen Betriebskonzepte	2012
1393	VSS 2010/702	Aktualisierung SN 640 907, Kostengrundlage im Erhaltungsmanagement	2012
1392	ASTRA 2008/008_009	FEHRL Institutes WIM Initiative (Fiwi)	2012
1391	ASTRA 2011/003	Leitbild ITS-CH Landverkehr 2025/30	2012
1390	FGU 2008/004_OBF	Einfluss der Grundwasserströmung auf das Quellverhalten des Gipskeupers im Belchentunnel	2012
1389	FGU 2003/002	Long Term Behaviour of the Swiss National Road Tunnels	2012
1388	SVI 2007/022	Möglichkeiten und Grenzen von elektronischen Busspuren	2012
1387	VSS 2010/205_OBF	Ablage der Prozessdaten bei Tunnel-Prozessleitsystemen	2012

Bericht-Nr.	Projekt Nr.	Titel	Jahr
1386	VSS 2006/204	Schallreflexionen an Kunstbauten im Strassenbereich	2012
1385	VSS 2004/703	Bases pour la révision des normes sur la mesure et l'évaluation de la planéité des chaussées	2012
1384	VSS 1999/249	Konzeptuelle Schnittstellen zwischen der Basisdatenbank und EMF-, EMK- und EMT-DB	2012
1383	FGU 2008/005	Einfluss der Grundwasserströmung auf das Quellverhalten des Gipskeupers im Chienbergtunnel	2012
1382	VSS 2001/504	Optimierung der statischen Eindringtiefe zur Beurteilung von harten Gussasphaltsorten	2012
1381	SVI 2004/055	Nutzen von Reisezeiteinsparungen im Personenverkehr	2012
1380	ASTRA 2007/009	Wirkungsweise und Potential von kombinierter Mobilität	2012
1379	VSS 2010/206_OBF	Harmonisierung der Abläufe und Benutzeroberflächen bei Tunnel-Prozessleitsystemen	2012
1378	SVI 2004/053	Mehr Sicherheit dank Kernfahrbahnen?	2012
1377	VSS 2009/302	Verkehrssicherheitsbeurteilung bestehender Verkehrsanlagen (Road Safety Inspection)	2012
1376	ASTRA 2011/008_004	Erfahrungen im Schweizer Betonbrückenbau	2012
1375	VSS 2008/304	Dynamische Signalisierungen auf Hauptverkehrsstrassen	2012
1374	FGU 2004/003	Entwicklung eines zerstörungsfreien Prüfverfahrens für Schweissnähte von KDB	2012
1373	VSS 2008/204	Vereinheitlichung der Tunnelbeleuchtung	2012
1372	SVI 2011/001	Verkehrssicherheitsgewinne aus Erkenntnissen aus Datapooling und strukturierten Datenanalysen	2012
1371	ASTRA 2008/017	Potenzial von Fahrgemeinschaften	2011
1370	VSS 2008/404	Dauerhaftigkeit von Betonfahrbahnen aus Betongranulat	2011
1369	VSS 2003/204	Rétention et traitement des eaux de chaussée	2012
1368	FGU 2008/002	Soll sich der Mensch dem Tunnel anpassen oder der Tunnel dem Menschen?	2011
1367	VSS 2005/801	Grundlagen betreffend Projektierung, Bau und Nachhaltigkeit von Anschlussgleisen	2011
1366	VSS 2005/702	Überprüfung des Bewertungshintergrundes zur Beurteilung der Strassengriffigkeit	2010
1365	SVI 2004/014	Neue Erkenntnisse zum Mobilitätsverhalten dank Data Mining?	2011
1364	SVI 2009/004	Regulierung des Güterverkehrs Auswirkungen auf die Transportwirtschaft Forschungspaket UVEK/ASTRA Strategien zum wesensgerechten Einsatz der Verkehrsmittel im Güterverkehr der Schweiz TP D	2012
1363	VSS 2007/905	Verkehrsprognosen mit Online -Daten	2011
1362	SVI 2004/012	Aktivitätenorientierte Analyse des Neuverkehrs	2012
1361	SVI 2004/043	Innovative Ansätze der Parkraumbewirtschaftung	2012
1360	VSS 2010/203	Akustische Führung im Strassentunnel	2012
1359	SVI 2004/003	Wissens- und Technologientransfer im Verkehrsbereich	2012
1358	SVI 2004/079	Verkehrsanbindung von Freizeitanlagen	2012
1357	SVI 2007/007	Unaufmerksamkeit und Ablenkung: Was macht der Mensch am Steuer?	2012
1356	SVI 2007/014	Kooperation an Bahnhöfen und Haltestellen	2011
1355	FGU 2007/002	Prüfung des Sulfatwiderstandes von Beton nach SIA 262/1, Anhang D: Anwendbarkeit und Relevanz für die Praxis	2011
1354	VSS 2003/203	Anordnung, Gestaltung und Ausführung von Treppen, Rampen und Treppenwegen	2011
1353	VSS 2000/368	Grundlagen für den Fussverkehr	2011
1352	VSS 2008/302	Fussgängerstreifen (Grundlagen)	2011
1351	ASTRA 2009/001	Development of a best practice methodology for risk assessment in road tunnels	2011
1350	VSS 2007/904	IT-Security im Bereich Verkehrstelematik	2011
1349	VSS 2003/205	In-Situ-Abflussversuche zur Untersuchung der Entwässerung von Autobahnen	2011
1348	VSS 2008/801	Sicherheit bei Parallelführung und Zusammentreffen von Strassen mit der Schiene	2011
1347	VSS 2000/455	Leistungsfähigkeit von Parkierungsanlagen	2010
1346	ASTRA 2007/004	Quantifizierung von Leckagen in Abluftkanälen bei Strassentunneln mit konzentrierter Rauchabsaugung	2010

Bericht-Nr.	Projekt Nr.	Titel	Jahr
1345	SVI 2004/039	Einsatzbereiche verschiedener Verkehrsmittel in Agglomerationen	2011
1344	VSS 2009/709	Initialprojekt für das Forschungspaket "Nutzensteigerung für die Anwender des SIS"	2011
1343	VSS 2009/903	Basistechnologien für die intermodale Nutzungserfassung im Personenverkehr	2011
1342	FGU 2005/003	Untersuchungen zur Frostkörperbildung und Frosthebung beim Gefrierverfahren	2010
1341	FGU 2007/005	Design aids for the planning of TBM drives in squeezing ground	2011
1340	SVI 2004/051	Aggressionen im Verkehr	2011
1339	SVI 2005/001	Widerstandsfunktionen für Innerorts-Strassenabschnitte ausserhalb des Einflussbereiches von Knoten	2010
1338	VSS 2006/902	Wirkungsmodelle für fahrzeugseitige Einrichtungen zur Steigerung der Verkehrssicherheit	2009
1337	ASTRA 2006/015	Development of urban network travel time estimation methodology	2011
1336	ASTRA 2007/006	SPIN-ALP: Scanning the Potential of Intermodal Transport on Alpine Corridors	2010
1335	VSS 2007/502	Stripping bei lärmmindernden Deckschichten unter Überrollbeanspruchung im Labormassstab	2011
1334	ASTRA 2009/009	Was treibt uns an? Antriebe und Treibstoffe für die Mobilität von Morgen	2011
1333	SVI 2007/001	Standards für die Mobilitätsversorgung im peripheren Raum	2011
1332	VSS 2006/905	Standardisierte Verkehrsdaten für das verkehrsträgerübergreifende Verkehrsmanagement	2011
1331	VSS 2005/501	Rückrechnung im Strassenbau	2011
1330	FGU 2008/006	Energiegewinnung aus städtischen Tunneln: Systemeevaluation	2010
1329	SVI 2004/073	Alternativen zu Fussgängerstreifen in Tempo-30-Zonen	2010
1328	VSS 2005/302	Grundlagen zur Quantifizierung der Auswirkungen von Sicherheitsdefiziten	2011
1327	VSS 2006/601	Vorhersage von Frost und Nebel für Strassen	2010
1326	VSS 2006/207	Erfolgskontrolle Fahrzeugrückhaltesysteme	2011
1325	SVI 2000/557	Indices caractéristiques d'une cité-vélo. Méthode d'évaluation des politiques cyclables en 8 indices pour les petites et moyennes communes.	2010
1324	VSS 2004/702	Eigenheiten und Konsequenzen für die Erhaltung der Strassenverkehrsanlagen im überbauten Gebiet	2009
1323	VSS 2008/205	Ereignisdetektion im Strassentunnel	2011
1322	SVI 2005/007	Zeitwerte im Personenverkehr: Wahrnehmungs- und Distanzabhängigkeit	2008
1321	VSS 2008/501	Validation de l'oedomètre CRS sur des échantillons intacts	2010
1320	VSS 2007/303	Funktionale Anforderungen an Verkehrserfassungssysteme im Zusammenhang mit Lichtsignalanlagen	2010
1319	VSS 2000/467	Auswirkungen von Verkehrsberuhigungsmassnahmen auf die Lärmimmissionen	2010
1318	FGU 2006/001	Langzeitquellversuche an anhydritführenden Gesteinen	2010
1317	VSS 2000/469	Geometrisches Normalprofil für alle Fahrzeugtypen	2010
1316	VSS 2001/701	Objektorientierte Modellierung von Strasseninformationen	2010
1315	VSS 2006/904	Abstimmung zwischen individueller Verkehrsinformation und Verkehrsmanagement	2010
1314	VSS 2005/203	Datenbank für Verkehrsaufkommensraten	2008
1313	VSS 2001/201	Kosten-/Nutzenbetrachtung von Strassenentwässerungssystemen, Ökobilanzierung	2010
1312	SVI 2004/006	Der Verkehr aus Sicht der Kinder: Schulwege von Primarschulkindern in der Schweiz	2010
1311	VSS 2000/543	VIABILITE DES PROJETS ET DES INSTALLATIONS ANNEXES	2010
1310	ASTRA 2007/002	Beeinflussung der Luftströmung in Strassentunneln im Brandfall	2010
1309	VSS 2008/303	Verkehrsregelungssysteme - Modernisierung von Lichtsignalanlagen	2010
1308	VSS 2008/201	Hindernisfreier Verkehrsraum - Anforderungen aus Sicht von Menschen mit Behinderung	2010
1307	ASTRA 2006/002	Entwicklung optimaler Mischgüter und Auswahl geeigneter Bindemittel; D-A-CH - Initialprojekt	2008
1306	ASTRA 2008/002	Strassenglätte-Prognosesystem (SGPS)	2010
1305	VSS 2000/457	Verkehrserzeugung durch Parkierungsanlagen	2009

Bericht-Nr.	Projekt Nr.	Titel	Jahr
1304	VSS 2004/716	Massnahmenplanung im Erhaltungsmanagement von Fahrbahnen	2008
1303	ASTRA 2009/010	Geschwindigkeiten in Steigungen und Gefällen; Überprüfung	2010
1302	VSS 1999/131	Zusammenhang zwischen Bindemitteleigenschaften und Schadensbildern des Belages?	2010
1301	SVI 2007/006	Optimierung der Strassenverkehrsunfallstatistik durch Berücksichtigung von Daten aus dem Gesundheitswesen	2009
1300	VSS 2003/903	SATELROU Perspectives et applications des méthodes de navigation pour la télématique des transports routiers et pour le système d'information de la route	2010
1299	VSS 2008/502	Projet initial - Enrobés bitumineux à faibles impacts énergétiques et écologiques	2009
1298	ASTRA 2007/012	Griffigkeit auf winterlichen Fahrbahnen	2010
1297	VSS 2007/702	Einsatz von Asphaltbewehrungen (Asphalteinlagen) im Erhaltungsmanagement	2009
1296	ASTRA 2007/008	Swiss contribution to the Heavy-Duty Particle Measurement Programme (HD-PMP)	2010
1295	VSS 2005/305	Entwurfsgrundlagen für Lichtsignalanlagen und Leitfaden	2010
1294	VSS 2007/405	Wiederhol- und Vergleichspräzision der Druckfestigkeit von Gesteinskörnungen am Haufwerk	2010
1293	VSS 2005/402	Détermination de la présence et de l'efficacité de dope dans les bétons bitumineux	2010
1292	ASTRA 2006/004	Entwicklung eines Pflanzenöl-Blockheizkraftwerkes mit eigener Ölmühle	2010
1291	ASTRA 2009/005	Fahrmuster auf überlasteten Autobahnen Simultanes Berechnungsmodell für das Fahrverhalten auf Autobahnen als Grundlage für die Berechnung von Schadstoffemissionen und Fahrzeitgewinnen	2010
1290	VSS 1999/209	Conception et aménagement de passages inférieurs et supérieurs pour piétons et deux-roues légers	2008
1289	VSS 2005/505	Affinität von Gesteinskörnungen und Bitumen, nationale Umsetzung der EN	2010
1288	ASTRA 2006/020	Footprint II - Long Term Pavement Performance and Environmental Monitoring on A1	2010
1287	VSS 2008/301	Verkehrsqualität und Leistungsfähigkeit von komplexen ungesteuerten Knoten: Analytisches Schätzverfahren	2009
1286	VSS 2000/338	Verkehrsqualität und Leistungsfähigkeit auf Strassen ohne Richtungstrennung	2010
1285	VSS 2002/202	In-situ Messung der akustischen Leistungsfähigkeit von Schallschirmen	2009
1284	VSS 2004/203	Evacuation des eaux de chaussée par les bas-cotés	2010
1283	VSS 2000/339	Grundlagen für eine differenzierte Bemessung von Verkehrsanlagen	2008
1282	VSS 2004/715	Massnahmenplanung im Erhaltungsmanagement von Fahrbahnen: Zusatzkosten infolge Vor- und Aufschub von Erhaltungsmassnahmen	2010
1281	SVI 2004/002	Systematische Wirkungsanalysen von kleinen und mittleren Verkehrsvorhaben	2009
1280	ASTRA 2004/016	Auswirkungen von fahrzeuginternen Informationssystemen auf das Fahrverhalten und die Verkehrssicherheit Verkehrspsychologischer Teilbericht	2010
1279	VSS 2005/301	Leistungsfähigkeit zweistreifiger Kreisel	2009
1278	ASTRA 2004/016	Auswirkungen von fahrzeuginternen Informationssystemen auf das Fahrverhalten und die Verkehrssicherheit - Verkehrstechnischer Teilbericht	2009
1277	SVI 2007/005	Multimodale Verkehrsqualitätsstufen für den Strassenverkehr - Vorstudie	2010
1276	VSS 2006/201	Überprüfung der schweizerischen Ganglinien	2008
1275	ASTRA 2006/016	Dynamic Urban Origin - Destination Matrix - Estimation Methodology	2009
1274	SVI 2004/088	Einsatz von Simulationswerkzeugen in der Güterverkehrs- und Transportplanung	2009

Bericht-Nr.	Projekt Nr.	Titel	Jahr
1273	ASTRA 2008/006	UNTERHALT 2000 - Massnahme M17, FORSCHUNG: Dauerhafte Materialien und Verfahren SYNTHESE - BERICHT zum Gesamtprojekt "Dauerhafte Beläge" mit den Einzelnen Forschungsprojekten: - ASTRA 200/419: Verhaltensbilanz der Beläge auf Nationalstrassen - ASTRA 2000/420: Dauerhafte Komponenten auf der Basis erfolgreicher Strecken - ASTRA 2000/421: Durabilité des enrobés - ASTRA 2000/422: Dauerhafte Beläge, Rundlaufversuch - ASTRA 2000/423: Griffigkeit der Beläge auf Autobahnen, Vergleich zwischen den Messergebnissen von SRM und SCRIM - ASTRA 2008/005: Vergleichsstrecken mit unterschiedlichen oberen Tragschichten auf einer Nationalstrasse	2008
1272	VSS 2007/304	Verkehrsregelungssysteme - behinderte und ältere Menschen an Lichtsignalanlagen	2010
1271	VSS 2004/201	Unterhalt von Lärmschirmen	2009
1270	VSS 2005/502	Interaktion Strasse Hangstabilität: Monitoring und Rückwärtsrechnung	2009
1269	VSS 2005/201	Evaluation von Fahrzeugrückhaltesystemen im Mittelstreifen von Autobahnen	2009
1268	ASTRA 2005/007	PM10-Emissionsfaktoren von Abriebspartikeln des Strassenverkehrs (APART)	2009
1267	VSS 2007/902	MDAinSVT Einsatz modellbasierter Datentransfernormen (INTERLIS) in der Strassenverkehrstelematik	2009
1266	VSS 2000/343	Unfall- und Unfallkostenraten im Strassenverkehr	2009
1265	VSS 2005/701	Zusammenhang zwischen dielektrischen Eigenschaften und Zustandsmerkmalen von bitumenhaltigen Fahrbahnbelägen (Pilotuntersuchung)	2009
1264	SVI 2004/004	Verkehrspolitische Entscheidfindung in der Verkehrsplanung	2009
1263	VSS 2001/503	Phénomène du dégel des sols gélifs dans les infrastructures des voies de communication et les pergélisols alpins	2006
1262	VSS 2003/503	Lärmverhalten von Deckschichten im Vergleich zu Gussasphalt mit strukturierter Oberfläche	2009
1261	ASTRA 2004/018	Pilotstudie zur Evaluation einer mobilen Grossversuchsanlage für beschleunigte Verkehrslastsimulation auf Strassenbelägen	2009
1260	FGU 2005/001	Testeinsatz der Methodik "Indirekte Vorauserkundung von wasserführenden Zonen mittels Temperaturdaten anhand der Messdaten des Lötschberg-Basistunnels	2009
1259	VSS 2004/710	Massnahmenplanung im Erhaltungsmanagement von Fahrbahnen - Synthesebericht	2008
1258	VSS 2005/802	Kaphaltestellen Anforderungen und Auswirkungen	2009
1257	SVI 2004/057	Wie Strassenraumbilder den Verkehr beeinflussen Der Durchfahrtswiderstand als Arbeitsinstrument bei der städtebaulichen Gestaltung von Strassenräumen	2009
1256	VSS 2006/903	Qualitätsanforderungen an die digitale Videobild-Bearbeitung zur Verkehrsüberwachung	2009
1255	VSS 2006/901	Neue Methoden zur Erkennung und Durchsetzung der zulässigen Höchstgeschwindigkeit	2009
1254	VSS 2006/502	Drains verticaux préfabriqués thermiques pour la consolidation in-situ des sols	2009
1253	VSS 2001/203	Rétention des polluants des eaux de chausées selon le système "infiltrations sur les talus". Vérification in situ et optimisation	2009
1252	SVI 2003/001	Nettoverkehr von verkehrsintensiven Einrichtungen (VE)	2009
1251	ASTRA 2002/405	Incidence des granulats arrondis ou partiellement arrondis sur les propriétés d'ahérence des bétons bitumineux	2008
1250	VSS 2005/202	Strassenabwasser Filterschacht	2007
1249	FGU 2003/004	Einflussfaktoren auf den Brandwiderstand von Betonkonstruktionen	2009
1248	VSS 2000/433	Dynamische Eindringtiefe zur Beurteilung von Gussasphalt	2008
1247	VSS 2000/348	Anforderungen an die strassenseitige Ausrüstung bei der Umwidmung von Standstreifen	2009

Bericht-Nr.	Projekt Nr.	Titel	Jahr
1246	VSS 2004/713	Massnahmenplanung im Erhaltungsmanagement von Fahrbahnen: Bedeutung Oberflächenzustand und Tragfähigkeit sowie gegenseitige Beziehung für Gebrauchs- und Substanzwert	2009
1245	VSS 2004/701	Verfahren zur Bestimmung des Erhaltungsbedarfs in kommunalen Strassennetzen	2009
1244	VSS 2004/714	Massnahmenplanung im Erhaltungsmanagement von Fahrbahnen - Gesamtnutzen und Nutzen-Kosten-Verhältnis von standardisierten Erhaltungsmassnahmen	2008
1243	VSS 2000/463	Kosten des betrieblichen Unterhalts von Strassenanlagen	2008
1242	VSS 2005/451	Recycling von Ausbauasphalt in Heissmischgut	2007
1241	ASTRA 2001/052	Erhöhung der Aussagekraft des LCPC Spurbildungstests	2009
1240	ASTRA 2002/010	L'acceptabilité du péage de congestion : Résultats et analyse de l'enquête en Suisse	2009
1239	VSS 2000/450	Bemessungsgrundlagen für das Bewehren mit Geokunststoffen	2009
1238	VSS 2005/303	Verkehrssicherheit an Tagesbaustellen und bei Anschlüssen im Baustellenbereich von Hochleistungsstrassen	2008
1237	VSS 2007/903	Grundlagen für eCall in der Schweiz	2009
1236	ASTRA 2008/008_07	Analytische Gegenüberstellung der Strategie- und Tätigkeitsschwerpunkte ASTRA-AIPCR	2008
1235	VSS 2004/711	Forschungspaket Massnahmenplanung im EM von Fahrbahnen - Standardisierte Erhaltungsmassnahmen	2008
1234	VSS 2006/504	Expérimentation in situ du nouveau drainomètre européen	2008
1233	ASTRA 2000/420	Unterhalt 2000 Forschungsprojekt FP2 Dauerhafte Komponenten bitumenhaltiger Belagsschichten	2009
667	AGB 2008/004	Résistance au déversement des poutres métalliques de pont	2015
666	AGB 2012/015	Structural Identification for Condition Assessment of Swiss Bridges	2015
665	AGB 2011/001	Wirksamkeit und Prüfung der Nachbehandlungsmethoden von Beton	2014
664	AGB 2009/005	Charges de trafic actualisées pour les dalles de roulement en béton des ponts existants	2014
663	AGB 2003/014	Seismic Safety of Existing Bridges	2014
662	AGB 2008/001	Seismic Safety of Existing Bridges - Cyclic Inelastic Behaviour of Bridge Piers	2014
661	AGB 2010/002	Fatigue limit state of shear studs in steel-concrete composite road bridges	2014
660	AGB 2008/002	Indirekt gelagerte Betonbrücken - Sachstandsbericht	2014
659	AGB 2009/014	Suizidprävention bei Brücken: Follow-Up	2014
658	AGB 2006/015_OBF	Querkraftwiderstand vorgespannter Brücken mit ungenügender Querkraftbewehrung	2014
657	AGB 2003/012	Brücken in Holz: Möglichkeiten und Grenzen	2013
656	AGB 2009/015	Experimental verification oif integral bridge abutments	2013
655	AGB 2007/004	Fatigue Life Assessment of Roadway Bridges Based on Actual Traffic Loads	2013
654	AGB 2005-008	Thermophysical and Thermomechanical Behavior of Cold-Curing Structural Adhesives in Bridge Construction	2013
653	AGB 2007/002	Poinçonnement des pontsdalles précontraints	2013
652	AGB 2009/006	Detektion von Betonstahlbrüchen mit der magnetischen Streufeldmethode	2013
651	AGB 2006/006_OBF	Instandsetzung und Monitoring von AAR-geschädigten Stützmauern und Brücken	2013
650	AGB 2005/010	Korrosionsbeständigkeit von nichtrostenden Betonstählen	2012
649	AGB 2008/012	Anforderungen an den Karbonatisierungswiderstand von Betonen	2012
648	AGB 2005/023 + AGB 2006/003	Validierung der AAR-Prüfungen für Neubau und Instandsetzung	2011
647	AGB 2004/010	Quality Control and Monitoring of electrically isolated post- tensioning tendons in bridges	2011
646	AGB 2005/018	Interactin sol-structure : ponts à culées intégrales	2010
645	AGB 2005/021	Grundlagen für die Verwendung von Recyclingbeton aus Betongranulat	2010
644	AGB 2005/004	Hochleistungsfähiger Faserfeinkornbeton zur Effizienzsteigerung bei der Erhaltung von Kunstbauten aus Stahlbeton	2010

Bericht-Nr.	Projekt Nr.	Titel	Jahr
643	AGB 2005/014	Akustische Überwachung einer stark geschädigten Spannbetonbrücke und Zustandserfassung beim Abbruch	2010
642	AGB 2002/006	Verbund von Spanngliedern	2009
641	AGB 2007/007	Empfehlungen zur Qualitätskontrolle von Beton mit Luftpermeabilitätsmessungen	2009
640	AGB 2003/011	Nouvelle méthode de vérification des ponts mixtes à âme pleine	2010
639	AGB 2008/003	RiskNow-Falling Rocks Excel-basiertes Werkzeug zur Risikoermittlung bei Steinschlagschutzgalerien	2010
638	AGB2003/003	Ursachen der Rissbildung in Stahlbetonbauwerken aus Hochleistungsbeton und neue Wege zu deren Vermeidung	2008
637	AGB 2005/009	Détermination de la présence de chlorures à l'aide du Géoradar	2009
636	AGB 2002/028	Dimensionnement et vérification des dalles de roulement de ponts routiers	2009
635	AGB 2004/002	Applicabilité de l'enrobé drainant sur les ouvrages d'art du réseau des routes nationales	2008
634	AGB 2002/007	Untersuchungen zur Potenzialfeldmessung an Stahlbetonbauten	2008
633	AGB 2002/014	Oberflächenschutzsysteme für Betontragwerke	2008
632	AGB 2008/201	Sicherheit des Verkehrssystem Strasse und dessen Kunstbauten Testregion - Methoden zur Risikobeurteilung Schlussbericht	2010
631	AGB 2000/555	Applications structurales du Béton Fibré à Ultra-hautes Performances aux ponts	2008
630	AGB 2002/016	Korrosionsinhibitoren für die Instandsetzung chloridverseuchter Stahlbetonbauten	2010
629	AGB 2003/001 + AGB 2005/019	Integrale Brücken - Sachstandsbericht	2008
628	AGB 2005/026	Massnahmen gegen chlorid-induzierte Korrosion und zur Erhöhung der Dauerhaftigkeit	2008
627	AGB 2002/002	Eigenschaften von normalbreiten und überbreiten Fahrbahnübergängen aus Polymerbitumen nach starker Verkehrsbelastung	2008
626	AGB 2005/110	Sicherheit des Verkehrssystems Strasse und dessen Kunstbauten: Baustellensicherheit bei Kunstbauten	2009
625	AGB 2005/109	Sicherheit des Verkehrssystems Strasse und dessen Kunstbauten: Effektivität und Effizienz von Massnahmen bei Kunstbauten	2009
624	AGB 2005/108	Sicherheit des Verkehrssystems / Strasse und dessen Kunstbauten / Risikobeurteilung für Kunstbauten	2010
623	AGB 2005/107	Sicherheit des Verkehrssystems Strasse und dessen Kunstbauten: Tragsicherheit der bestehenden Kunstbauten	2009
622	AGB 2005/106	Rechtliche Aspekte eines risiko- und effizienzbasierten Sicherheitskonzepts	2009
621	AGB 2005/105	Sicherheit des Verkehrssystems Strasse und dessen Kunstbauten Szenarien der Gefahrenentwicklung	2009
620	AGB 2005/104	Sicherheit des Verkehrssystems Strasse und dessen Kunstbauten: Effektivität und Effizienz von Massnahmen	2009
619	AGB 2005/103	Sicherheit des Verkehrssystems / Strasse und dessen Kunstbauten / Ermittlung des Netzrisikos	2010
618	AGB 2005/102	Sicherheit des Verkehrssystems Strasse und dessen Kunstbauten: Methodik zur vergleichenden Risikobeurteilung	2009
617	AGB 2005/100	Sicherheit des Verkehrssystems Strasse und dessen Kunstbauten Synthesebericht	2010
616	AGB 2002/020	Beurteilung von Risiken und Kriterien zur Festlegung akzeptierter Risiken in Folge aussergewöhnlicher Einwirkungen bei Kunstbauten	2009